

Systematics of the *Osteocephalus buckleyi* species complex (Anura, Hylidae) from Ecuador and Peru

Santiago R. Ron^{1,†}, Pablo J. Venegas^{2,‡}, Eduardo Toral^{1,3,§}, Morley Read^{1,1},
Diego A. Ortiz^{1,¶}, Andrea L. Manzano^{1,4,#}

1 Museo de Zoología, Escuela de Biología, Pontificia Universidad Católica del Ecuador, Av. 12 de Octubre y Roca, Aptdo. 17-01-2184, Quito, Ecuador **2** División de Herpetología-Centro de Ornitología y Biodiversidad (CORBIDI), Santa Rita N°105 Of. 202, Urb. Huertos de San Antonio, Surco, Lima, Perú **3** Current address: Facultad de Ciencias Ambientales, Universidad Internacional SEK, Quito, Ecuador **4** Current address: Biology Department, HH227, San Francisco State University, 1600 Holloway Avenue, San Francisco, CA 94132, USA

† [urn:lsid:zoobank.org:author:ACF9C463-F771-459C-B22B-AF6B9902DF57](https://zoobank.org/urn:lsid:zoobank.org:author:ACF9C463-F771-459C-B22B-AF6B9902DF57)

‡ [urn:lsid:zoobank.org:author:15AD03E1-9ACF-4F38-AA96-09A5A56A3DC4](https://zoobank.org/urn:lsid:zoobank.org:author:15AD03E1-9ACF-4F38-AA96-09A5A56A3DC4)

§ [urn:lsid:zoobank.org:author:1A4F31AF-5629-4EE5-83DD-1EBB93139A5B](https://zoobank.org/urn:lsid:zoobank.org:author:1A4F31AF-5629-4EE5-83DD-1EBB93139A5B)

| [urn:lsid:zoobank.org:author:10D75453-75A0-49C7-B577-A7687398CEF0](https://zoobank.org/urn:lsid:zoobank.org:author:10D75453-75A0-49C7-B577-A7687398CEF0)

¶ [urn:lsid:zoobank.org:author:51147772-F315-412E-BA89-B8990CA49544](https://zoobank.org/urn:lsid:zoobank.org:author:51147772-F315-412E-BA89-B8990CA49544)

[urn:lsid:zoobank.org:author:7C29ADA6-00FB-45DC-9A5B-7B9A217B71F6](https://zoobank.org/urn:lsid:zoobank.org:author:7C29ADA6-00FB-45DC-9A5B-7B9A217B71F6)

Corresponding author: Santiago R. Ron (santiago.r.ron@gmail.com)

Academic editor: F. Andreone | Received 24 June 2012 | Accepted 5 October 2012 | Published 18 October 2012

[urn:lsid:zoobank.org:pub:163872F0-BE66-436C-9663-EE2226C358AB](https://zoobank.org/pub:163872F0-BE66-436C-9663-EE2226C358AB)

Citation: Ron SR, Venegas PJ, Toral E, Read M, Ortiz DA, Manzano AL (2012) Systematics of the *Osteocephalus buckleyi* species complex (Anura, Hylidae) from Ecuador and Peru. ZooKeys 229: 1–52. doi: 10.3897/zookeys.229.3580

Abstract

We present a new phylogeny, based on DNA sequences of mitochondrial and nuclear genes, for frogs of the genus *Osteocephalus* with emphasis in the *Osteocephalus buckleyi* species complex. Genetic, morphologic, and advertisement call data are combined to define species boundaries and describe new species. The phylogeny shows strong support for: (1) a basal position of *O. taurinus* + *O. oophagus*, (2) a clade containing phytotelmata breeding species, and (3) a clade that corresponds to the *O. buckleyi* species complex. Our results document a large proportion of hidden diversity within a set of populations that were previously treated as a single, widely distributed species, *O. buckleyi*. Individuals assignable to *O. buckleyi* formed a paraphyletic group relative to *O. verruciger* and *O. cabrerai* and contained four species, one of which is *O. buckleyi sensu stricto* and three are new. Two of the new species are shared between Ecuador and Peru (*O. vilmae* **sp. n.** and *O. cannatellai* **sp. n.**) and one is distributed in the Amazon region of southern Peru (*O. germani* **sp. n.**). We discuss the difficulties of using morphological characters to define species boundaries and propose a hypothesis to explain them.

Resumen

Presentamos una nueva filogenia, basada en secuencias de ADN de genes nucleares y mitocondriales, para ranas del género *Osteocephalus* con énfasis en el complejo de especies *Osteocephalus buckleyi*. Datos genéticos, morfológicos, y de cantos de anuncio se combinan para definir límites de especies y describir nuevas especies. La filogenia muestra un soporte fuerte para: (1) una posición basal de *O. taurinus* + *O. oophagus*, (2) un clado que contiene especies con reproducción en fitotelmatas, y (3) un clado que corresponde el complejo de especies *O. buckleyi*. Nuestros resultados documentan una gran proporción de diversidad escondida dentro de un grupo de poblaciones que previamente habían sido tratadas como una sola especie ampliamente distribuida, *O. buckleyi*. Los individuos asignables a *O. buckleyi* formaron un grupo parafilético en relación a *O. verruciger* y *O. cabrerai* y contuvieron cuatro especies, una de las cuales es *O. buckleyi sensu scripto* y tres son nuevas. Dos de las nuevas especies están compartidas entre Ecuador y Perú (*O. vilmae* sp. n. y *O. cannatellai* sp. n.) y una está en el sur de Perú (*O. germani* sp. n.) Discutimos las dificultades de usar caracteres morfológicos para definir límites de especies y proponemos una hipótesis para explicarla.

Keywords

Advertisement calls, Amazon, Anura, Cryptic species, Morphology, *Osteocephalus buckleyi*, Phylogeny

Introduction

The Upper Amazon region has the highest alpha diversity of amphibians in the World with several sites exceeding 100 species in less than 10 km² (Bass et al. 2010). Remarkably, these figures may vastly underestimate the total diversity as shown by the discovery of large numbers of cryptic species with the use of genetic markers (e.g., Fouquet et al. 2007; Funk et al. 2011; Padial and De la Riva 2009; Ron et al. 2006). These preliminary efforts suggest that the use of genetic characters is crucial to attain a complete understanding of the diversity and evolutionary history of Amazonian amphibians. This necessity is particularly pressing in widespread taxa with pervasive taxonomic problems.

One such group is *Osteocephalus*, a genus of hylid frogs widely distributed in the Amazon Basin, Guianas and upper drainages of the Magdalena and Orinoco rivers (Frost 2010). *Osteocephalus* are arboreal and nocturnal frogs with reproduction modes varying from deposition of eggs in lentic water and exotrophic tadpoles to deposition of eggs in bromeliads and oophagus tadpoles and biparental care (Crump 1974; Jungfer and Weygoldt 1999). There are 24 described species and reports of undescribed species are frequent (e.g., Jungfer 2010; Moravec et al. 2009; Ron et al. 2010). There is only one formally defined species group within *Osteocephalus*, the *O. buckleyi* complex. It was first proposed by Cochran and Goin (1970) to allocate *O. buckleyi* (Boulenger 1882), *O. pearsoni* (Gauge 1929), and *O. cabrerai* (Cochran and Goin 1970). Its first large scale review was carried out by Trueb and Duellman (1971) who examined the morphology of specimens from seven countries and concluded that the *O. buckleyi* complex (excluding *O. verruciger* Werner 1901) consisted of a single, morphologi-

cally variable and widely distributed species. They synonymized *O. cabrerai*, *O. carri* (Cochran and Goin 1970), and *O. festae* (Peracca 1904) under *O. buckleyi*. The three species have been subsequently resurrected (Duellman and Mendelson 1995; Jungfer 2010; Lynch 2006). Recent reviews (Jungfer 2010; 2011; Moravec et al. 2009; Ron et al. 2010) imply that the *O. buckleyi* species complex consists of nine species: *O. buckleyi*, *O. cabrerai*, *O. carri*, *O. duellmani* Jungfer 2011, *O. festae*, *O. inframaculatus* (Boulenger 1882), *O. mutabor* Jungfer and Hödl 2002, *O. verruciger* and an undescribed species sister to *O. verruciger*. A phylogeny based on mitochondrial DNA revealed strong support for the *O. buckleyi* complex as well as paraphyly in *O. verruciger* and *O. buckleyi* (Ron et al. 2010).

Despite recent contributions to the taxonomy of the group (e.g., Jungfer 2010; 2011) the *O. buckleyi* species complex still contains undescribed species as well as alpha taxonomic problems (Jungfer 2010; Ron et al. 2010) which attest the difficulties of correctly identifying species boundaries on the basis of morphological evidence alone. Herein we integrate genetic, morphological and advertisement call data to assess the phylogenetic relationships and species boundaries among populations of the *O. buckleyi* complex from Ecuador and Peru. The results demonstrate the existence of three new species, which are formally described here.

Methods

For ease of comparison, we generally follow the format of Trueb and Duellman (1971) for diagnosis and description. Morphological terminology and abbreviations follow Lynch and Duellman (1997). Notation for hand and foot webbing is based on Myers and Duellman (1982). Sex was determined by the texture of dorsal skin, the presence of nuptial pads or vocal sac folds, and by gonadal inspection. Specimens were fixed in 10% formalin and preserved in 70% ethanol. Snout-vent length is abbreviated as SVL. Examined specimens (listed in the type-series and Appendix I) are housed at the collection of the División de Herpetología, Centro de Ornitología y Biodiversidad (CORBIDI), Herpetology Collection at Escuela Politécnica Nacional (EPN-H), Museo de Historia Natural at Universidad San Marcos (MUSM), Museo de Zoología at Pontificia Universidad Católica del Ecuador (QCAZ), and Natural History Museum (BMNH). The pencil drawing of the holotype of *O. cannatella* sp. n. was made using a Wild Heerbrugg M3B 10×/21 stereo microscope equipped with a camera lucida.

Principal Components Analysis (PCA) and Discriminant Function Analysis (DFA) were used to assess the degree of morphometric differentiation between species. Only well preserved specimens (Simmons 2002) were measured for the following eight morphological variables, following Duellman (1970): (1) SVL; (2) head length; (3) head width; (4) tympanum diameter; (5) femur length; (6) tibia length; (7) foot length; and (8) eye diameter. All variables were log-transformed. To remove the effect of co-

variation with SVL, the PCA was applied to the residuals from the linear regressions between the seven measured variables and SVL. We applied a multivariate analysis of variance (MANOVA) to tests for morphometric differences between sexes. Because we found significant differences in *O. buckleyi*, the PCA and DFA were applied on each sex separately. For the PCA, only components with eigenvalues > 1 were retained. The DFA was applied to the measured variables without size correction because we wanted to assess discriminability among species based on all the variables, including SVL. Sample sizes are: *O. buckleyi* 24 males, 3 females; *O. cabrerai* 7 males; *O. cannatellai* sp. n. 33 males, 3 females; *O. festae* 7 males, 18 females; *O. germani* sp. n. 2 males, 5 females; *O. verruciger* 22 males, 5 females; and *O. vilmae* sp. n. 4 males. Both PCA and DFA were conducted in JMP® 8.01 (SAS Institute 2008). Measurements were made using digital calipers (to the nearest 0.01 mm).

Advertisement calls recordings were made with a Sennheiser™ ME-67 directional microphone with digital recorder Olympus™ LS10. Calls were analyzed using software Raven 1.2.1 (Charif et al. 2004) at a sampling frequency of 22.1 kHz and a frequency resolution of 21.5 Hz. Calls consist of two components, the first is a rattle note and the second is a quack note. Measured call variables are: (1) call rate: number of calls per second, (2) dominant frequency: frequency with the most energy, measured along all the call, (3) duration of first component note: time from the beginning to the end of note, (4) duration of second component: time from beginning of first quack to the end of the last, (5) first component interval: time from the end of last note of the first component to the beginning of the first note of the second component, (6) number of pulses: number of pulses in a first component note, (7) pulse rate: number of pulses/duration of first component note, (8) duration of second component note: duration from beginning to end of a single quack, (9) quack rate: number of quacks/duration of second component. If available, several calls or notes were analyzed per individual to calculate an individual average. Original recordings are deposited in the audio archive of the QCAZ and are available through the AmphibiaWebEcuador website (<http://zoologia.puce.edu.ec/vertebrados/anfibios/>).

DNA extraction, amplification, and sequencing

Total DNA was extracted from muscle or liver tissue preserved in 95% ethanol or tissue storage buffer using standard phenol–chloroform extraction protocols (Sambrook et al. 1989). Polymerase chain reaction (PCR) was used to amplify the mitochondrial genes 12S rRNA, 16S rRNA, ND1 (with flanking tRNA genes), CO1, and control region. We amplified one DNA fragment for 12S, CO1, and the control region and one or two overlapping fragments for the last ~320 bp of 16S and the adjacent ND1 using primers listed in Goebel et al. (1999) and Moen and Wiens (2009). We also amplified the nuclear gene *POMC* as a single fragment using primers listed by Wiens et al. (2005). PCR amplification was carried under standard protocols. Amplified products were sequenced by the MacroGen Sequencing Team (MacroGen Inc., Seoul, Korea).

Phylogenetic analyses

We estimated phylogenetic relations between species of *Osteocephalus* based on newly generated sequence data for five mitochondrial (*12S* RNA, *CO1*, *16S*, *ND1*, control region) and one nuclear gene (*POMC*) for a total of up to 4170 bp. To expand the species sampling, we also included sequences from GenBank. All samples are listed in Table 1. For the outgroup, we included one sample of *Trachycephalus jordani* and one of *T. typhoni* (based on Faivovich et al. 2005 and Wiens et al. 2010). The completeness of the sequences varied considerably among individuals (specially for samples from GenBank which typically lacked three or more loci). Nevertheless, we included samples with missing data because analyses of both empirical and simulated matrices have shown that taxa with missing sequences can be accurately placed in model-based phylogenetic analyses if the number of characters is large, as in our matrix (for a review see Wiens and Morrill 2011).

Preliminary sequence alignment was done with MAFFT 6.814b software with the L-INS-i algorithm (Katoh et al. 2002). The sequence matrix was imported to Mesquite (version 2.72; Maddison and Maddison 2009) and the ambiguously aligned regions were adjusted manually to produce a parsimonious alignment (i.e., informative sites minimized). In protein coding loci, DNA sequences were translated to amino acids with Mesquite to aid the manual alignment. Phylogenetic trees were obtained using Bayesian inference.

Because our dataset includes several loci, it is unlikely that it fits a single model of nucleotide substitution. Thus, we partitioned the data to analyze each partition under a separate model. The best model for each partition was chosen with JModelTest version 0.1.1 (Posada 2008) using the Akaike Information Criterion with sample size correction as optimality measure. We also evaluated three different partition strategies: (i) a single partition, (ii) six partitions (one per loci), and (iii) twelve partitions (one for each codon position in protein coding loci plus one for each non protein coding loci). The best partition strategy was chosen by estimating Bayes factors using a threshold of 10 as evidence in favor of the more complex partition (Brandley et al. 2005).

Each Bayesian analysis consisted of two parallel runs of the Metropolis coupled Monte Carlo Markov chain for 5×10^6 generations. Each run had four chains with a temperature of 0.05. The prior for the rate matrix was a uniform dirichlet and all topologies were equally probable a priori. Convergence into a stationary distribution was determined by reaching average standard deviation split frequencies < 0.05 between runs. We also used software Tracer ver. 1.5 (Rambaut and Drummond 2007) to visually inspect convergence and stationarity of the runs. The first 50% of the sampled generations were discarded as burn-in and the remaining were used to estimate the Bayesian tree, posterior probabilities and other model parameters. Phylogenetic analyses were carried out in MrBayes 3.2.1 (Ronquist et al. 2012).

Because the only nuclear gene analyzed had low variability and few informative sites, it was concatenated to the mitochondrial genes into a single matrix. We recognize the advantages of species-tree methods (e.g., Edwards et al. 2007) but could not use them given the insufficient number of nuclear genes sampled. We encourage the application of those methodologies in future phylogenetic inferences in *Osteocephalus*.

Table 1. Genbank accession numbers for DNA sequences used in the phylogenetic analysis.

Museum No.	Species	Genbank Accession No.						Reference
		16S-ND1	12S	COI	Control Region	POMC		
KU 143119	<i>Ostecephalus alboguttatus</i>	EU034081	--	--	--	--	Moen and Wiens 2009	
QCAZ 15981	<i>O. alboguttatus</i>	HQ600596	HQ600629	--	JX875680	JX875744	Ron et al. 2010; This study	
LAC 2216	<i>O. buckleyi</i>	EU034082	DQ380378	--	--	EU034116	Moen and Wiens 2009; Wiens et al. 2006	
CORBIDI 7458	<i>O. buckleyi</i>	JX875606	JX847067	JX875806	--	JX875734	This study	
CORBIDI 7459	<i>O. buckleyi</i>	JX875607	JX847068	JX875807	--	JX875735	This study	
CORBIDI 7462	<i>O. buckleyi</i>	JX875608	JX847069	JX875808	JX875657	JX875736	This study	
CORBIDI 7516	<i>O. buckleyi</i>	--	JX847070	--	--	JX875737	This study	
LAC 2216	<i>O. buckleyi</i>	EU034082	DQ380378	--	--	--	Moen and Wiens 2009	
QCAZ 14948	<i>O. buckleyi</i>	JX875611	JX847081	JX875812	JX875718	JX875742	This study	
QCAZ 24446	<i>O. buckleyi</i>	HQ600600	HQ600633	JX875821	JX875708	JX875753	Ron et al. 2010; This study	
QCAZ 24447	<i>O. buckleyi</i>	HQ600601	HQ600634	JX875822	JX875686	JX875754	Ron et al. 2010; This study	
QCAZ 28277	<i>O. buckleyi</i>	HQ600606	HQ600639	JX875831	JX875720	JX875763	Ron et al. 2010; This study	
QCAZ 28395	<i>O. buckleyi</i>	HQ600607	HQ600640	JX875832	JX875677	JX875764	Ron et al. 2010; This study	
QCAZ 28427	<i>O. buckleyi</i>	JX875618	JX847087	JX875833	JX875689	JX875765	This study	
QCAZ 36703	<i>O. buckleyi</i>	JX875625	JX847092	JX875845	JX875722	JX875778	This study	
QCAZ 39073	<i>O. buckleyi</i>	JX875627	JX847094	JX875848	JX875714	JX875782	This study	
QCAZ 39074	<i>O. buckleyi</i>	JX875628	JX847095	JX875849	JX875672	JX875783	This study	
QCAZ 39285	<i>O. buckleyi</i>	JX875629	--	JX875850	JX875694	JX875784	This study	
QCAZ 43071	<i>O. buckleyi</i>	JX875633	JX847099	JX875858	JX875724	JX875793	This study	
QCAZ 48093	<i>O. buckleyi</i>	JX875639	JX847105	JX875864	JX875702	JX875798	This study	
QCAZ 48827	<i>O. buckleyi</i>	JX875640	JX847106	JX875865	JX875703	JX875799	This study	
AJC 2566	<i>O. cabrerai</i>	JX875598	JX847062	JX875801	JX875650	JX875725	This study	
AJC 2567	<i>O. cabrerai</i>	JX875599	JX847063	JX875802	JX875707	JX875726	This study	

Museum No.	Species	Genbank Accession No.						Reference
		<i>16S-ND1</i>	<i>12S</i>	<i>COI</i>	Control Region	<i>POMC</i>		
CORBIDI 120	<i>O. cabrerai</i>	JX875600	--	--	JX875651	JX875727	This study	
CORBIDI 5819	<i>O. cabrerai</i>	JX875604	JX847066	JX875804	JX875655	JX875731	This study	
CORBIDI 5821	<i>O. cabrerai</i>	JX875605	--	JX875805	JX875656	JX875732	This study	
LSUMZ H-13720	<i>O. cabrerai</i>	--	AY843705	--	--	--	Fairovich et al. 2005	
QCAZ 27923	<i>O. cabrerai</i>	JX875617	JX847086	JX875827	JX875709	JX875760	This study	
QCAZ 28231	<i>O. cabrerai</i>	HQ600621	HQ600654	JX875830	JX875710	JX875762	Ron et al. 2010; This study	
CORBIDI 9368	<i>O. cannatellai</i>	--	JX847072	--	JX875658	--	This study	
CORBIDI 9370	<i>O. cannatellai</i>	JX875643	JX847074	--	JX875660	--	This study	
CORBIDI 9394	<i>O. cannatellai</i>	JX875644	JX847075	--	JX875661	--	This study	
CORBIDI 9507	<i>O. cannatellai</i>	JX875645	JX847077	--	JX875662	--	This study	
QCAZ 25469	<i>O. cannatellai</i>	HQ600617	HQ600650	JX875823	JX875687	JX875755	Ron et al. 2010; This study	
QCAZ 31016	<i>O. cannatellai</i>	JX875621	JX847089	JX875839	JX875712	JX875771	This study	
QCAZ 31032	<i>O. cannatellai</i>	JX875622	JX847090	JX875840	JX875691	JX875772	This study	
QCAZ 31033	<i>O. cannatellai</i>	JX875623	--	JX875841	JX875668	JX875773	This study	
QCAZ 32506	<i>O. cannatellai</i>	HQ600618	HQ600651	JX875843	JX875692	JX875775	Ron et al. 2010; This study	
QCAZ 32508	<i>O. cannatellai</i>	HQ600619	HQ600652	JX875844	JX875693	JX875776	Ron et al. 2010; This study	
QCAZ 37175	<i>O. cannatellai</i>	HQ600620	HQ600653	JX875846	JX875713	JX875779	Ron et al. 2010; This study	
QCAZ 39633	<i>O. cannatellai</i>	JX875630	JX847096	JX875852	JX875678	JX875786	This study	
QCAZ 40258	<i>O. cannatellai</i>	JX875631	JX847097	JX875854	JX875696	JX875788	This study	
QCAZ 45909	<i>O. cannatellai</i>	JX875635	JX847101	JX875860	JX875701	JX875795	This study	
QCAZ 46472	<i>O. cannatellai</i>	JX875638	JX847104	JX875863	JX875717	JX875797	This study	
QCAZ 49572	<i>O. cannatellai</i>	JX875641	JX847107	JX875866	JX875674	JX875800	This study	
CBF 6051	<i>O. castaneicola</i>	--	FJ965300	--	--	--	Moravec et al. 2009	
NMP6d 28/2009	<i>O. castaneicola</i>	--	FJ965302	--	--	--	Moravec et al. 2009	
NMP6V 73810/3	<i>O. castaneicola</i>	--	FJ965301	--	--	--	Moravec et al. 2009	
NMP6V 73820	<i>O. castaneicola</i>	--	FJ965303	--	--	--	Moravec et al. 2009	

Museum No.	Species	Genbank Accession No.						Reference
		<i>16S-ND1</i>	<i>12S</i>	<i>COI</i>	Control Region	<i>POMC</i>		
QCAZ 20711	<i>O. deridens</i>	JX875613	JX847083	JX875817	JX875699	JX875749	This study	
NMP6V 71262/2	<i>O. deridens</i>	--	FJ965304	--	--	--	Motravec et al. 2009	
CORBIDI 623	<i>O. festae</i>	HQ600616	HQ600649	JX875810	JX875705	JX875733	Ron et al. 2010	
CORBIDI 760	<i>O. festae</i>	--	--	JX875809	--	JX875738	This study	
CORBIDI 10461	<i>O. festae</i>	JX875649	JX847071	--	--	--	This study	
CORBIDI 1965	<i>O. festae</i>	--	JX847064	JX875803	--	JX875728	This study	
CORBIDI 9585	<i>O. festae</i>	JX875647	JX847079	--	--	--	This study	
CORBIDI 9587	<i>O. festae</i>	JX875648	JX847080	--	--	--	This study	
QCAZ 38420	<i>O. festae</i>	HQ600613	HQ600646	JX875847	--	JX875781	Ron et al. 2010; This study	
QCAZ 39364	<i>O. festae</i>	HQ600615	HQ600648	JX875851	JX875715	JX875785	Ron et al. 2010; This study	
QCAZ 41039	<i>O. festae</i>	HQ600614	HQ600647	JX875855	JX875716	JX875790	Ron et al. 2010; This study	
QCAZ 20785	<i>O. fuscifacies</i>	HQ600598	HQ600631	JX875818	JX875685	JX875750	Ron et al. 2010; This study	
CORBIDI 5505	<i>O. germani</i>	JX875603	--	--	JX875654	--	This study	
CORBIDI 8267	<i>O. germani</i>	JX875609	--	--	--	JX875739	This study	
CORBIDI 8284	<i>O. germani</i>	JX875610	--	--	--	JX875740	This study	
141 MC	<i>O. lepricarii</i>	--	EF376031	--	--	--	Salducci et al. 2005	
AMNH-A 131254	<i>O. lepricarii</i>	--	AY843707	--	--	--	Faivovich et al. 2005	
CORBIDI 4645	<i>O. mutabor</i>	JX875601	--	--	JX875652	JX875729	This study	
CORBIDI 19369	<i>O. mutabor</i>	JX875642	JX847073	--	JX875659	--	This study	
KU 221930	<i>O. mutabor</i>	--	DQ380379	--	--	--	Wiens et al. 2006	
QCAZ 25603	<i>O. mutabor</i>	HQ600598	HQ600631	JX875824	JX875676	JX875756	Ron et al. 2010; This study	
QCAZ 25684	<i>O. mutabor</i>	JX875615	JX847085	JX875825	JX875700	JX875757	This study	
QCAZ 28223	<i>O. mutabor</i>	HQ600605	HQ600638	JX875829	JX875682	--	Ron et al. 2010; This study	
QCAZ 28646	<i>O. mutabor</i>	HQ600608	HQ600641	JX875834	JX875721	JX875766	Ron et al. 2010; This study	
QCAZ 28647	<i>O. mutabor</i>	HQ600609	HQ600642	JX875835	JX875675	JX875767	Ron et al. 2010; This study	
QCAZ 29430	<i>O. mutabor</i>	JX875619	JX847088	JX875836	JX875704	JX875768	This study	

Museum No.	Species	Genbank Accession No.						Reference
		<i>16S-ND1</i>	<i>12S</i>	<i>COI</i>	Control Region	<i>POMC</i>		
QCAZ 30925	<i>O. mutabor</i>	JX875620	--	JX875837	JX875690	JX875769	This study	
QCAZ 30926	<i>O. mutabor</i>	HQ600610	HQ600643	JX875838	JX875711	JX875770	Ron et al. 2010; This study	
QCAZ 40253	<i>O. mutabor</i>	HQ600611	HQ600644	JX875853	JX875695	JX875787	Ron et al. 2010; This study	
QCAZ 41030	<i>O. mutabor</i>	JX875632	JX847098	--	JX875673	JX875789	This study	
QCAZ 42999	<i>O. mutabor</i>	HQ600612	HQ600645	JX875857	JX875723	JX875792	Ron et al. 2010; This study	
QCAZ 46470	<i>O. mutabor</i>	JX875636	JX847102	JX875861	JX875697	--	This study	
QCAZ 46471	<i>O. mutabor</i>	JX875637	JX847103	JX875862	JX875698	JX875796	This study	
14 MC	<i>O. oophagus</i>	--	EF376030	--	--	--	Salducci et al. 2005	
MNHN 2001.0828	<i>O. oophagus</i>	--	AY843708	--	--	--	Faivovich et al. 2005	
KU 221933	<i>O. planiceps</i>	--	DQ380380	--	--	--	Wiens et al. 2006	
NMP6V 71174/1	<i>O. planiceps</i>	--	FJ965305	--	--	--	Moravec et al. 2009	
NMP6V 71264/1	<i>O. planiceps</i>	--	FJ965306	--	--	--	Moravec et al. 2009	
NMP6V 71264/2	<i>O. planiceps</i>	--	FJ965307	--	--	--	Moravec et al. 2009	
QCAZ 20797	<i>O. planiceps</i>	HQ600599	HQ600632	JX875819	JX875665	JX875751	Ron et al. 2010; This study	
214 MC	<i>O. taurinus</i>	--	EF376032	--	--	--	Salducci et al. 2005	
JM 2007/60	<i>O. taurinus</i>	--	FJ965296	--	--	--	Moravec et al. 2009	
KU 221941	<i>O. taurinus</i>	AY819512	AY819380	--	--	--	Wiens et al. 2005	
QCAZ 18230	<i>O. taurinus</i>	HQ600597	HQ600630	JX875815	JX875719	JX875747	Ron et al. 2010; This study	
KU 205406	<i>O. taurinus</i>	--	AY326041	--	--	--	Darst and Cannatella 2004	
CORBIDI 19477	<i>O. verruciger</i>	--	JX847076	--	--	--	This study	
CORBIDI 19525	<i>O. verruciger</i>	JX875646	JX847078	--	--	--	This study	
KU 217751	<i>O. verruciger</i>	--	DQ380381	--	--	--	Wiens et al. 2006	
QCAZ 15942	<i>O. verruciger</i>	HQ600626	HQ600659	JX875813	JX875679	JX875743	Ron et al. 2010; This study	
QCAZ 15991	<i>O. verruciger</i>	HQ600623	HQ600656	JX875814	JX875681	JX875745	Ron et al. 2010; This study	
QCAZ 17285	<i>O. verruciger</i>	JX875612	JX847082	--	JX875706	JX875746	This study	
QCAZ 20544	<i>O. verruciger</i>	HQ600622	HQ600655	JX875816	JX875664	JX875748	Ron et al. 2010; This study	

Museum No.	Species	Genbank Accession No.						Reference
		16S-ND1	12S	COI	Control Region	POMC		
QCAZ 22201	<i>O. verruciger</i>	JX875614	JX847084	JX875820	JX875666	JX875752	This study	
QCAZ 26304	<i>O. verruciger</i>	JX875616	--	--	--	JX875758	This study	
QCAZ 32032	<i>O. verruciger</i>	HQ600625	HQ600658	JX875842	JX875669	JX875774	Ron et al. 2010; This study	
QCAZ 41108	<i>O. verruciger</i>	HQ600627	HQ600660	JX875856	JX875683	JX875791	Ron et al. 2010; This study	
QCAZ 45344	<i>O. verruciger</i>	JX875634	JX847100	JX875859	JX875684	JX875794	This study	
CORBIDI 4773	<i>O. vilmae</i>	JX875602	JX847065	--	JX875653	JX875730	This study	
QCAZ 14947	<i>O. vilmae</i>	HQ600595	HQ600628	JX875811	JX875663	JX875741	Ron et al. 2010; This study	
QCAZ 27816	<i>O. yasuni</i>	HQ600603	HQ600636	JX875826	JX875688	JX875759	Ron et al. 2010; This study	
QCAZ 27998	<i>O. yasuni</i>	HQ600604	HQ600637	JX875828	JX875667	JX875761	Ron et al. 2010; This study	
NMP6d 41/2009	<i>Osteocephalus</i> sp.	--	FJ965297	--	--	--	Moravec et al. 2009	
NMP6V 72173/1	<i>Osteocephalus</i> sp.	--	FJ965299	--	--	--	Moravec et al. 2009	
NMP6V 72173/3	<i>Osteocephalus</i> sp.	--	FJ965308	--	--	--	Moravec et al. 2009	
NMP6V 73105	<i>Osteocephalus</i> sp.	--	FJ965298	--	--	--	Moravec et al. 2009	
QCAZ 35405	<i>Trachycephalus jordani</i>	JX875624	JX847091	--	JX875670	JX875777	This study	
QCAZ 38075	<i>Trachycephalus typhonius</i>	JX875626	JX847093	--	JX875671	JX875780	This study	

Results

Phylogenetic analyses

Throughout this section, genetic distances are uncorrected *p*-distances for gene *12S*. The complete data set consists of up to six gene fragments (956 bp of *12S*, 325 bp of *16S*, 693 pb of *COI*, 579 bp of control region, 1079 bp of *NDI*, and 539 bp of POMC) from 113 individuals representing 20 species. The models with the best fit and the estimated parameters for each partition for the Bayesian analyses are shown in Table 2. Comparisons of partition strategies based on Bayes factors favored the 12-partition analysis (factors values > 200).

The topology (Fig. 1) is generally well supported and agrees with Salerno et al. (2012) phylogeny in showing a basal divergence between (*O. taurinus* + *O. oophagus*) and the other *Osteocephalus* species. Within the later, *O. alboguttatus* diverges basally while the remaining species are divided in two clades. One clade (posterior probability, PP, = 1.0) corresponds to the *O. buckleyi* species group. The other clade has weaker support (PP = 0.91) and consists of the phytotelmata breeding species (*O. planiceps*, *O. fuscifacies*, *O. deridens*, *O. castaneicola*; PP = 1.0) and *O. lepriurii*, *O. yasuni* and *O. sp. B* (*sensu* Moravec et al. 2009; PP = 1.0). The “*O. lepriurii*” sample in the clade with phytotelmata breeding is likely misidentified as suggested by Moravec et al. (2009).

Table 2. Post burn-in averages for parameters of Bayesian analyses. Abbreviations are: I = proportion of invariant sites, G = shape parameter of the gamma distribution of rate variation.

Partition	Best-fit model	I	G	Rate Matrix						Base Frequency			
				AC	AG	AT	CG	CT	GT	A	C	G	T
<i>12S</i>	GTR+G	–	0.201	0.049	0.347	0.071	0.028	0.494	0.009	0.330	0.249	0.182	0.238
<i>16S</i>	SYM+I+G	0.592	1.229	0.079	0.209	0.123	0.022	0.547	0.019	–	–	–	–
<i>COI</i> , 1 st position	K80+I	–	–	–	–	–	–	–	–	–	–	–	–
<i>COI</i> , 2 nd position	F81	–	–	–	–	–	–	–	–	0.168	0.269	0.155	0.408
<i>COI</i> , 3 rd position	GTR+G	–	2.972	0.024	0.651	0.027	0.027	0.236	0.035	0.272	0.324	0.093	0.310
Control region	HKY+G	–	0.367	–	–	–	–	–	–	0.399	0.183	0.085	0.333
<i>NDI</i> , 1 st position	HKY+G	–	0.198	–	–	–	–	–	–	0.319	0.254	0.180	0.247
<i>NDI</i> , 2 nd position	HKY+I+G	0.716	0.043	–	–	–	–	–	–	0.177	0.290	0.126	0.407
<i>NDI</i> , 3 rd position	GTR+G	–	1.780	0.032	0.601	0.036	0.018	0.295	0.019	0.353	0.273	0.098	0.275
POMC, 1 st position	F81+G	–	0.128	–	–	–	–	–	–	0.412	0.169	0.259	0.160
POMC, 2 nd position	F81	–	–	–	–	–	–	–	–	0.419	0.183	0.199	0.199
POMC, 3 rd position	HKY+I+G	0.485	0.761	–	–	–	–	–	–	0.318	0.319	0.164	0.199

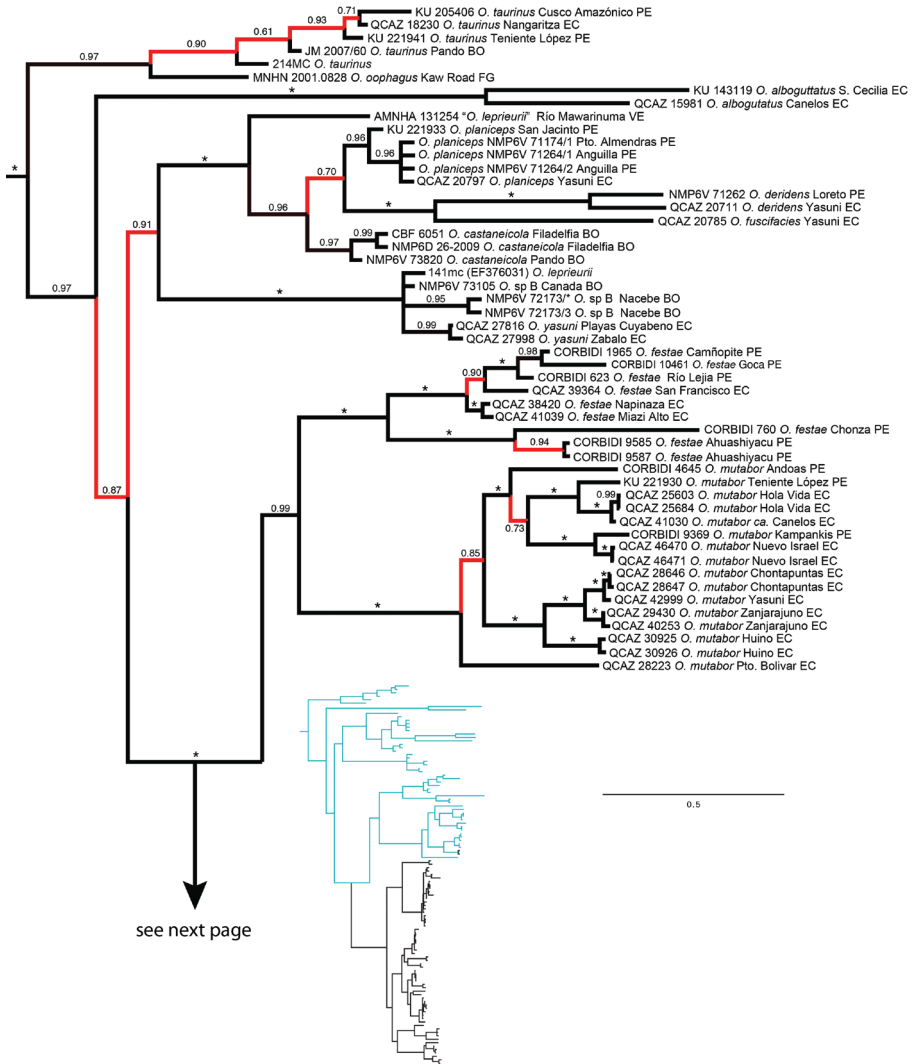


Figure 1. Bayesian consensus phylogram depicting relationships within *Osteocephalus*. Phylogram derived from analysis of 4170 bp of mitochondrial (gene fragments *12S*, *16S*, *ND1*, *CO1*, control region) and nuclear DNA (*POM-C*). Museum catalog no. (or, if unavailable, GenBank accession no.) and locality are shown for each sample. Posterior probabilities resulting from Bayesian Markov chain Monte Carlo searches appear above branches. An asterisk represents a value of 1 and red branches represent values < 0.95. Outgroup species (*Trachycephalus jordani* and *T. typhonius*) are not shown. Abbreviations are: **BO** Bolivia, **BR** Brazil, **CO** Colombia, **EC** Ecuador, **FG** French Guiana, **PE** Peru, **VE** Venezuela.

All species within the *O. buckleyi* species complex, except *O. buckleyi*, are monophyletic. Individuals assignable to *O. buckleyi* are paraphyletic relative to *O. verruciger* and *O. cabrerai* and are separated in four clades (named A–D in Fig. 1).

Populations of *O. mutabor* segregate latitudinally: the most divergent population (Puerto Bolívar) is the only north of the Napo and Aguarico rivers; the remaining

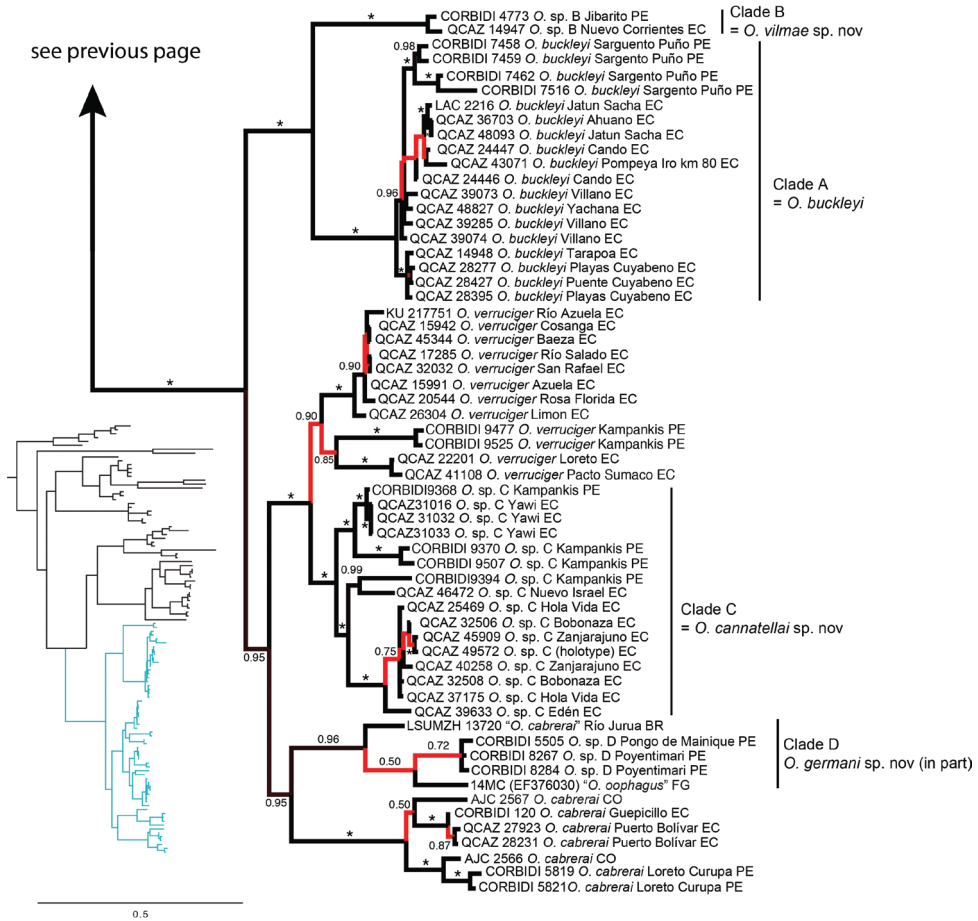


Figure 1. Continued.

populations are separated in one central and one southern clade, both with strong support. Pairwise genetic distances between populations are below 2% in all comparisons.

The phylogeny recovers a monophyletic *O. verruciger* (in contrast to Ron et al. 2010) divided in two clades with an unexpected geographic pattern. Loreto and Pacto Sumaco are at a distance of 20–50 km from Cosanga, Río Salado and other nearby localities in central Ecuador (Fig. 2). Yet, in they phylogeny the two samples are sister to samples from Cordillera Kampankis in Peru, at a distance of 370 km. Cordillera Kampankis is an isolated mountain range separated from the rest of the Andes by areas below 500 m above sea level. The records from Cordillera Kampankis are the first confirmed occurrences of *O. verruciger* in Peru. Genetic distances among *O. verruciger* samples range between 0 and 1.5%.

Osteocephalus festae samples were collected on both sides of the dry valley of the Marañón River. This valley, with elevations as low as 600 m, is part of the Huanabamba depression, a well-known biogeographic barrier in the Andes. Nevertheless, populations on both sides do not form reciprocally monophyletic groups. In some

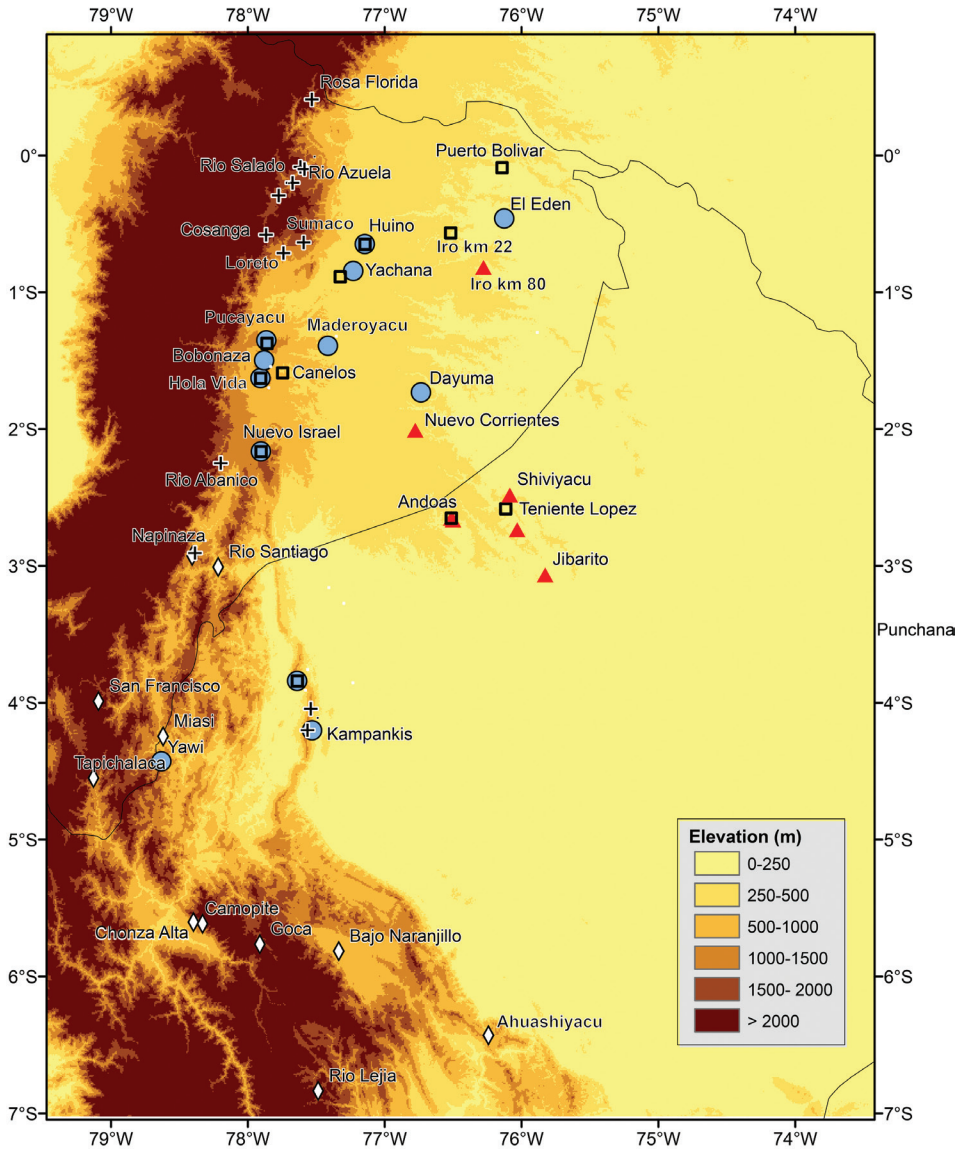


Figure 2. Records of *Osteocephalus cannatellai*, *O. festae*, *O. mutabor*, *O. verruciger*, and *O. vilmae*. *Osteocephalus cannatellai*, circles; *O. festae*, diamonds; *O. mutabor*, squares; *O. verruciger*, crosses; and *O. vilmae*, triangles. Locality data from the literature (Duellman and Mendelson 1995; Jungfer 2010; Peracca 1904; Ron et al. 2010) and specimens deposited at Museo de Zoología of Pontificia Universidad Católica del Ecuador, the Herpetology Collection, Escuela Politécnica Nacional, and Centro de Ornitología y Biodiversidad CORBIDI.

cases, low genetic distances (e.g., San Francisco-Camñoopite p -distance 0.3%) separate populations across the valley indicating recent gene flow. Relatively high genetic distances separate populations south of the Marañón (up to 2.8% between Catarata Ahuashiyacu and Camñoopite).



Figure 3. Variation in dorsal coloration of preserved specimens of adult *Osteocephalus buckleyi*. Left to right, upper row: BMNH 1947.2.13.44 (Lectotype), QCAZ 38704, EPN-H 6374, 11718 (males), QCAZ 2876, 14948 (females); lower row: QCAZ 39799, 26552 (females), 26488, 26561, 39364 (males). Provincia Napo, Orellana, Pastaza and Sucumbíos, Ecuador (See Appendix I for locality data). All specimens are shown at the same scale.



Figure 4. Variation in ventral coloration of preserved specimens of adult *Osteocephalus buckleyi*. Specimen identity and arrangement is the same as in Figure 3. All specimens are shown at the same scale.

Osteocephalus buckleyi-like individuals are grouped in four clades (A, B, C, and D in Fig. 1). Each clade has unique morphological features (see species descriptions) indicating that each represents a species. The external morphology of the lectotype of *O. buckleyi* (BMNH 1947.2.13.44, an adult male with nuptial excrescences, Figs 3–4) shows that it belongs to clade A because: (1) its body size (37.90 mm; Fig. 5) is within the range for adult males of Clade A (37.32–45.25 mm, $n = 24$) but below the range of clades B (48.23–51.85, $n = 4$) and C (38.47–57.21 mm, $n = 24$), (2) its relative tympanum size (tympanum diameter/SVL = 0.093; Fig. 5) falls outside the range of Clade C (0.056–0.084, $n = 24$ males) but within the range of clade A (0.072–0.095, $n = 24$ males), (3) it has conspicuous tarsal tubercles (absent in clade D), and (4) clade D have a geographic range that, according to the available specimens, does not overlap with the type locality (Canelos, Provincia de Pastaza, Ecuador, 650 m; Figs 2 and 6). Thus, we attach the binomial *O. buckleyi* to clade A. Clades B, C, and D cannot be assigned to any described species of

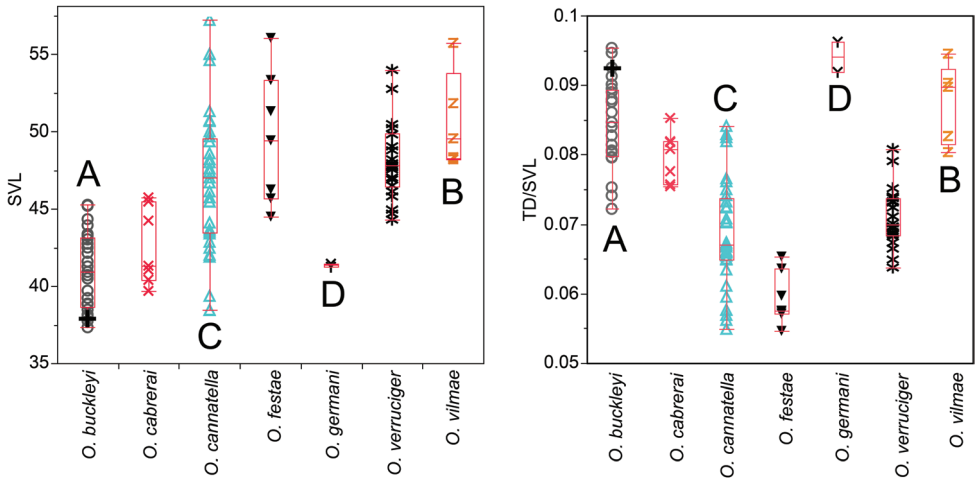


Figure 5. Boxplots for snout-vent length (SVL; left) and the ratio tympanum diameter/snout-vent length (TD/SVL; right). The line in the middle of the box represents the median, and the lower and upper ends of the box are the 25% and 75% quartiles respectively. Each individual is shown with a symbol; the cross in *O. buckleyi* represents the lectotype. Letters correspond to those of clades on Figure 1.

Osteocephalus and thus represent new species that we describe herein as *O. cannatellai* sp. n. (Clade C), *O. germani* sp. n. (part of Clade D), and *O. vilmae* sp. n. (Clade B).

Samples of *O. buckleyi sensu stricto* (clade A) have low genetic differentiation (uncorrected *p* from 0 to 0.7%) despite including localities separated by up to 450 km. As in *O. mutabor*, the most divergent populations in the phylogeny were those north of the Napo and Aguatico rivers (Cuyabeno and Tarapoa).

Osteocephalus cannatellai sp. nov. comprises eight populations with genetic distances ranging from 0 to 1.7%. Populations group latitudinally forming a central and a southern clade. However, one of three samples (CORBIDI 9394) from the southern locality Pongo de Chinim (Kampankis) groups with the central localities.

Clade D comprises five samples from four populations. For two individuals (from Brazil and French Guyana) only GenBank sequences were available and thus we cannot determine if they belong to *O. germani* sp. n. The three remaining samples (from Peru) are assigned to *O. germani*.

Species accounts

Osteocephalus cannatellai sp. n.

urn:lsid:zoobank.org:act:EDEC6BF4-F11C-4812-A06E-065C9035999D

http://species-id.net/wiki/Osteocephalus_cannatellai

Holotype. (Figs 7–10) QCAZ 49572 (field no. PUCE 18835), adult male from Ecuador, Provincia Pastaza, Cantón Santa Clara, Río Pucayacu, in the vicinities of the

Zanjarajuno Reserve (1.3578°S, 77.8477°W), 940 m above sea level, collected by P. Peña-Loyola, N. Peñafiel, and R. Tarvin on 3 July 2010.

Paratopotypes. 20 adult males, 1 adult female. QCAZ 33256, adult male, collected by I. G. Tapia, D. Almeida-Reinoso and M. Páez on 30 March 2007; QCAZ 39579, 39586–87, adult males, collected by D. Salazar-Valenzuela and G. Diaz between 12 and 14 December 2008; QCAZ 40909–10, adult males, collected by I. G. Tapia, L. A. Coloma, and S. R. Ron on 31 March 2008; QCAZ 40252, 40258, adult males, collected by D. Salazar-Valenzuela, D. Acosta-López and C. Korfel between 23 February and 1 March 2009; QCAZ 45271–72, 45277, 45281, adult males, collected by D. Acosta-López between 30 July and 2 August 2009; QCAZ 45907, 45909, adult males, collected by P. Peña-Loyola on 16 October 2009; QCAZ 49569–71, adult males, collected by N. Peñafiel between 26 June and 3 July 2010; QCAZ 49021–22, adult males, collected by R. Tarvin, and L. Bustamante on 3 August 2010; QCAZ 49439, adult female, collected by R. Tarvin and P. Aguilar on September 2010; QCAZ 48744 adult male, collected by S. R. Ron, L. Bustamante, I. G. Tapia, P. Peña-Loyola and R. Tarvin on 3 July 2010.

Paratypes. 42 adult males, 2 adult females. Ecuador: Provincia Morona Santiago: Bobonaza (1.4980°S, 77.8793°W), 660 m above sea level, QCAZ 32506, 32508, 32512, adult males, collected by L. A. Coloma and I. G. Tapia on 18 August 2008; Nuevo Israel (2.165°S, 77.902919°W), 1289 m above sea level, QCAZ 46472, adult male, collected by J. Brito-Molina on 2 January 2010; Provincia Napo: Reserva Yachana (0.8458°S, 77.2287°W), 300–350 m above sea level, QCAZ 48790, 48797, 48803–04, 48811, 48814, adult males, collected by S. North, S. Topp and G. Estevez between 4 June and 18 August 2008; Huino, QCAZ 50198, adult female, collected by W. C. Funk on February 2003; Provincia Orellana: El Edén (0.46147°S, 76.1252°W), 228 m above sea level, QCAZ 39633, adult male, collected by S. Aldás-Alarcón, Dayuma, Pozo Sunka (1.7333°S, 76.7333°W), 279 m above sea level, EPN-H 2752, 2755–56, 6372; Provincia Pastaza: Fundación Hola Vida (1.6285°S, 77.9072°W), 845 m above sea level, QCAZ 25607, 25469, adult males, collected by K. Elmer and I. G. Tapia on 27 June 2003, QCAZ 37175, adult male collected by I. G. Tapia, L. A. Coloma, P. Peña-Loyola and M. Páez on July 2007; Río Maderoyacu (1.3917°S, 77.4139°W), 500–600 m above sea level, EPN-H 6373, 6385, adult males, collected by A. Almendáriz; Provincia Zamora Chinchipe: Centro Shuar Yawi (4.4300°S, 78.6316°W), 945 m above sea level, QCAZ 31016, 31032–33, 31047, 31053, adult males, QCAZ 31051, adult female, collected by D. Almeida-Reinoso and A. Armijos between 13 and 19 September 2003. Peru: Región Loreto: Provincia Datem del Marañón: Cordillera de Kampankis: Pongo de Chinim (3.1130°S, 77.7762°W), 365 m above sea level, CORBIDI 09368, 09370, 09394, 9396, 10534, 10537, MUSM 28050, adult males collected by P. J. Venegas and A. Catenazzi on 3 August 2011; Quebrada Kampankis (4.0431°S, 77.5412°W), 325 m above sea level, CORBIDI 09507, 10535, adult males collected by P. J. Venegas and A. Catenazzi on 13 August 2011; Quebrada Wee (4.2041°S, 77.5298°W), 310 m above sea level, CORBIDI 09545–46, 09553, 09569, 10532–33, 10535–36, MUSM 28051, adult males, collected by P. J. Venegas and A. Catenazzi on 18 August 2011.

Diagnosis. Throughout this section, coloration refers to preserved specimens unless otherwise noted. *Osteocephalus cannatellai* is a medium-sized species of *Osteocephalus*

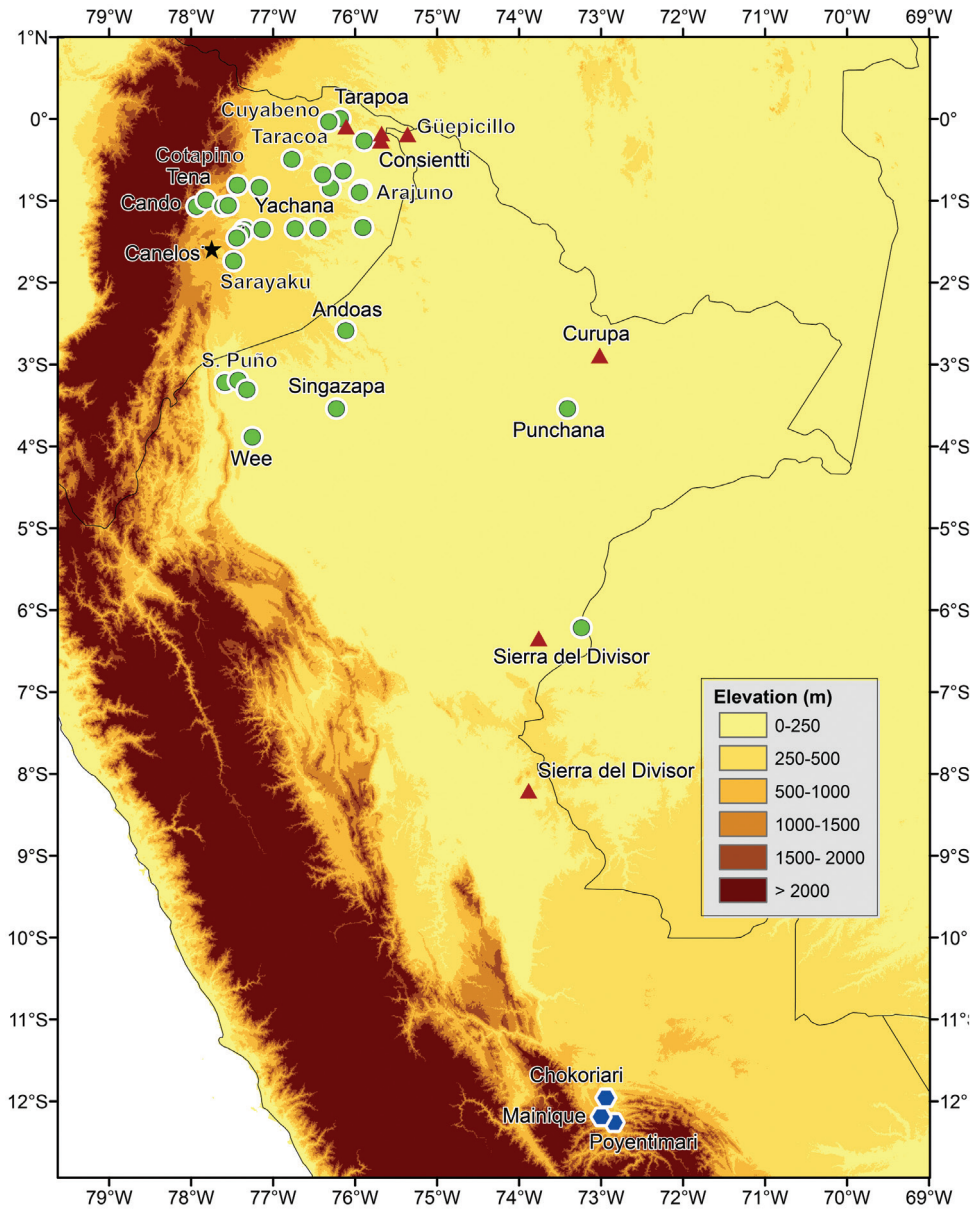


Figure 6. Records of *Osteocephalus buckleyi*, *O. cabrerai*, and *O. germani*. *Osteocephalus buckleyi*, circles; *O. cabrerai*, triangles, and *O. germani*, hexagons. The type locality of *O. buckleyi* is shown with a star. Locality data from the literature (Duellman and Mendelson 1995; Jungfer 2010; Peracca 1904; Ron et al. 2010) and specimens deposited at Museo de Zoología of Pontificia Universidad Católica del Ecuador, the Herpetology Collection, Escuela Politécnica Nacional, and Centro de Ornitología y Biodiversidad CORBIDI.

lus having the following combination of characters: (1) size sexually dimorphic; maximum SVL in males 57.21 mm ($n = 33$), in females 70.88 ($n = 3$); (2) skin on dorsum bearing scattered tubercles in males, smooth in females; (3) skin on flanks areolate; (4)

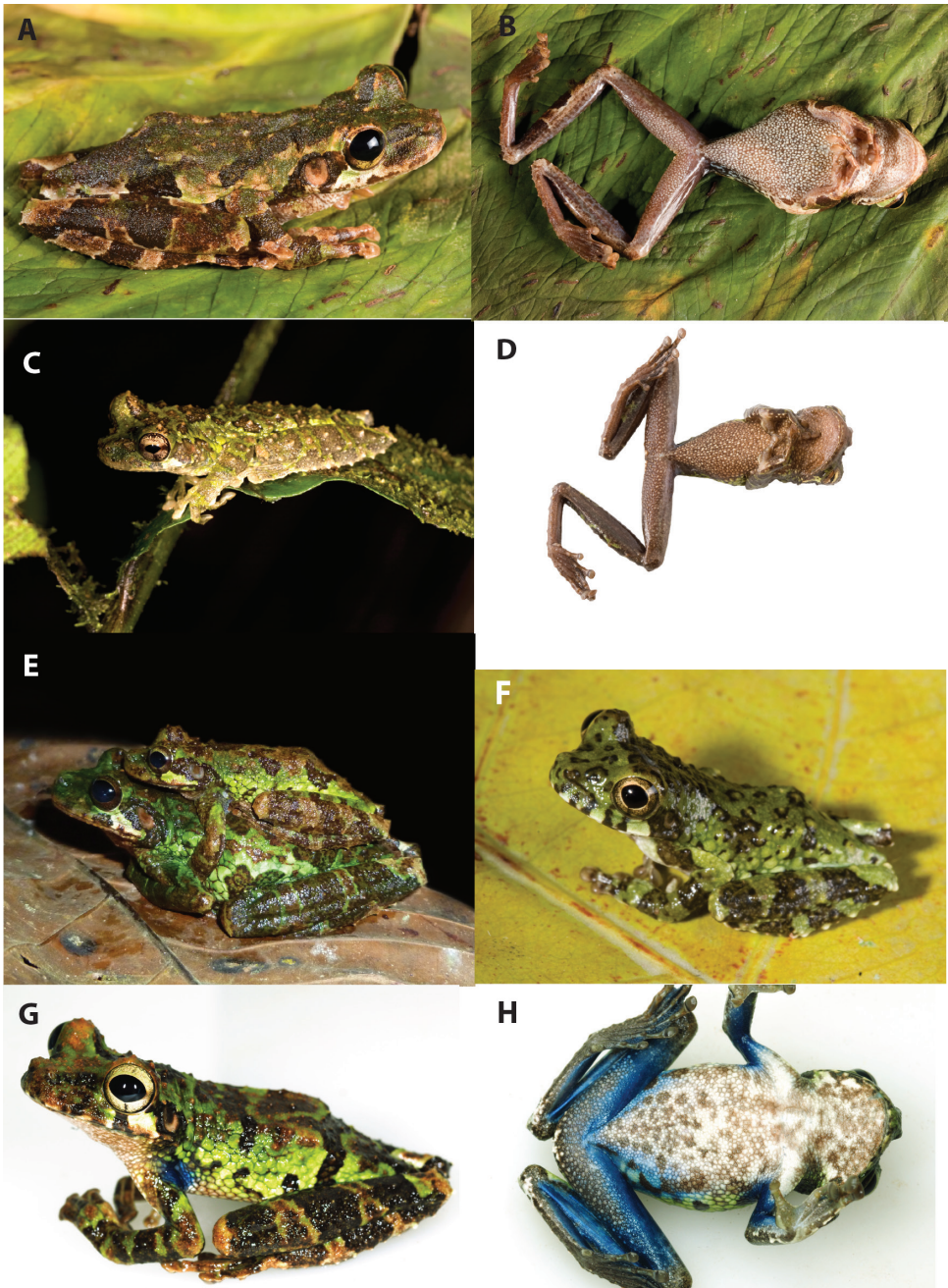


Figure 7. Dorsolateral and ventral views of *Osteocephalus*. **A–B** *Osteocephalus buckleyi*, QCAZ 43071, adult female, SVL = 50.95 mm, Jatun Sacha, Ecuador **C–D** *O. cannatellai* QCAZ 48744, adult male, SVL = 51.96 mm, Reserva Zanjarajuno, Río Pucayacu, Ecuador **E** *O. cannatellai*, amplexant pair QCAZ 49572 (holotype) adult male, SVL = 52.85 mm, from Río Pucayacu, Provincia Pastaza, Ecuador **F** *O. cannatellai* QCAZ 40859, juvenile, SVL = 26.7 mm (type locality) **G–H** *Osteocephalus cannatellai* (COR-BIDI 10534) from Cordillera Kampankis, Peru. Photographs E by R. Tarvin and **G–H** by A. Catenazzi.

hand webbing formula varying from I basal II1½ —2¹/₃ III2⁺—2IV to I basal II2⁻—3⁻ III2²/₃—2½IV; foot webbing formula varying from II—2½III—2III1⁺—2IV2½—1⁺V to I0⁺—1⁻III0⁺—1⁺III0⁺—1½IV1⁻—0⁺V; (5) dorsum varying from dark brown with light gray marks to cream with brown marks; (6) venter varying from light gray to dark brown with lighter dots and/or dark brown blotches; (7) cream suborbital mark present, clear labial stripe absent; (8) flanks cream with darker reticulations anteriorly and dark marks; (9) dermal roofing bones of the skull weakly exostosed; (10) in life, bones green; (11) in life, iris bronze with irregular reticulations; (12) paired vocal sacs small, located laterally, behind jaw articulation, (13) in life, juveniles with bronze iris, without pale elbows, knees, and heels; (14) larvae unknown.

Osteocephalus cannatellai is most similar to *O. buckleyi* and *O. vilmae* sp. n. The three species differ from other *Osteocephalus* by the combination of a bronze iris with irregular black reticulations (in life), areolate skin on the flanks, prominent tubercles in the tarsus and absence of a row of conspicuous tubercles in the lower jaw. *Osteocephalus cannatellai* differs from *O. buckleyi* in having: (1) scattered and weakly keratinized dorsal tubercles (more abundant and keratinized in *O. buckleyi*), (2) smaller tympanum (1/5 of head length in *O. cannatellai* vs. 1/4 in *O. buckleyi*; Fig. 5), (3) larger size (*O. cannatellai* mean male SVL = 46.83, SD = 4.31, *n* = 33; *O. buckleyi* mean male SVL = 41.12, SD = 2.45, *n* = 24; differences are significant: *t* = 5.82, *P* < 0.001; Fig. 5), (4) darker venter (cream with brown speckling in most *O. buckleyi*; Figs 4 and 9.), (5) more extensive areolate area on flanks (from axillary region to groin in *O. cannatellai*, restricted to anterior one third of flank in *O. buckleyi*), (6) contrasting coloration between flanks and venter (change in coloration is gradual in *O. buckleyi*), and (7) advertisement call (Fig. 11). Our phylogenetic analyses show that *O. cannatellai* and *O. buckleyi* are not sister species (Fig. 1).

Osteocephalus cannatellai differs from *O. vilmae* in having a narrower head (relative to SVL, mean male HW/SVL = 0.323, SD = 0.034, *n* = 33; *O. vilmae* mean male HW/SVL = 0.355, SD = 0.012, *n* = 5; differences are significant: *t* = 2.06, *P* = 0.046) and a smaller tympanum (relative to SVL, mean male TD/SVL = 0.069, SD = 0.007, *n* = 33; *O. vilmae* mean male TD/SVL = 0.087, SD = 0.006, *n* = 5; differences are significant: *t* = 5.17, *P* < 0.001). According to the phylogeny, *O. cannatellai* and *O. vilmae* are not sister species (Fig. 1). *Osteocephalus cannatellai* differs from *O. cabrerai* in (1) lacking prominent tubercles on the lower jaw, (2) having smooth to tuberculate outer edge of Finger IV (outer edge with fringe in *O. cabrerai*), and (3) having less webbing in the hands (in *O. cannatellai* webbing reaches two thirds of the distance between the ultimate and penultimate tubercle of Finger IV, in *O. cabrerai* it reaches the proximal border of the ultimate tubercle; Fig. 12). *Osteocephalus cannatellai* differs from other species of *Osteocephalus* (except *O. buckleyi*, *O. cabrerai*, and *O. vilmae*) in having a combination of prominent tubercles in the tarsus and areolate skin in the flanks. A bronze iris with black reticulations further distinguishes *O. cannatellai* from *O. deridens*, *O. oophagus*, *O. planiceps*, and *O. taurinus* which have black straight lines radiating from the pupil; iris coloration also differs in *O. carri*, *O. festae*, *O. heyeri*, *O. subtilis*, and *O. verruciger* which have predominantly dark irises (Jungfer 2010; Jungfer

and Lehr 2001; Lynch 2002). *Osteocephalus cannatellai* is larger than *O. exophthalmus* (maximum male SVL in *O. cannatellai* 57.21, $n = 33$; in *O. exophthalmus* 32.7 mm, $n = 3$; Smith and Noonan 2001) and *O. fuscifacies* (maximum SVL 44.17, $n = 21$). Skin texture in the flanks distinguishes *O. cannatellai* (areolate) from *O. mutabor* (smooth). *Osteocephalus inframaculatus* differs from *O. cannatellai* in coloration of the ventral surfaces of hindlimbs (bold brown blotches in *O. inframaculatus* are absent in *O. cannatellai*; Jungfer 2010).

Description of holotype. Adult male, 52.85 mm SVL, head length 18.61, head width 18.53, eye diameter 5.08, tympanum diameter 3.31, femur length 25.84, tibia length 30.05, foot length 22.73. Head narrower than body, slightly longer than wide; snout truncate in lateral and dorsal views; distance from nostril to eye longer than diameter of eye; canthus rostralis distinct and rounded; loreal region concave; internarial area depressed; nostrils moderately protuberant, directed laterally; interorbital area flat, lateral margins of the frontoparietals inconspicuous through skin; eye large, strongly protuberant; tympanic membrane clearly evident, large, slightly wider than high, about two thirds of eye diameter, separated from eye by ca. 85% of its diameter; tympanic annulus distinct except dorsally where it is covered by supratympanic fold; posterior end of supratympanic fold reaches arm insertion. Arm slender, axillary membrane present, reaching one third of arm length; four small low tubercles present along ventrolateral edge of forearm; relative length of fingers I<II<IV<III; fingers bearing large, oval discs, that of third finger about three fourths of tympanum diameter; subarticular tubercles prominent, round to ovoid, single; supernumerary tubercles present; palmar tubercle small, elongated; prepollical tubercle large, flat, elliptical; prepollex enlarged; large dark keratinous nuptial excrescences covering inner surface of prepollex up to half the distance between subarticular tubercle and proximal border of disk of thumb; webbing formula of fingers I basal II¹/₃—2²/₃, III2½—2*IV. Medium sized to small tubercles on tibiotarsal articulation; scattered tubercles on tarsus, more abundant on outer edge; small tubercles scattered along ventrolateral edge of foot; toes bearing discs slightly wider than long, smaller than those of fingers; relative length of toes I<II<V<III<IV; outer metatarsal tubercle ill defined, small, round; inner metatarsal tubercle large, ovoid; subarticular tubercles single, round, protuberant; supernumerary tubercles restricted to the soles; webbing formula of toes I1—2II1—2*III1+—2*IV2—1V. Skin on dorsum, head, and dorsal surfaces of limbs smooth, with scattered tubercles; skin on flanks areolate; skin on venter coarsely granular; skin on ventral surfaces of head and thighs granular, those of shanks smooth. Cloacal opening directed posteriorly at upper level of thighs; short simple cloacal sheath covering cloacal opening; round tubercles below vent; two conspicuous white tubercles ventrolateral to vent. Tongue cordiform, widely attached to floor of mouth; dentigerous processes of the vomer angular, adjacent medially, posteromedial to choanae, bearing 12 and 9 (left/right) vomerine teeth; choanae trapezoidal, oblique; vocal sac barely distinct above the arm and below the ear.

Color of holotype in preservative. Dorsum brown with light gray to cream peripheral marks; dark brown, ill defined, transversal bar between orbits (Fig. 8); cream middorsal line from tip of snout to end of sacrum; dorsal surfaces of forearms brown with light



Figure 8. Adult *Osteocephalus cannatellai* showing variation in dorsal coloration of preserved specimens. Left to right, upper row (dark morphs): QCAZ 49439, 31051 (females), 40258, 49022, 45271 (males); lower row (light morphs): QCAZ 37175, 48744, 48797, 39633, 46472 (males). Ecuador, Provincia Morona Santiago, Napo, Orellana, Pastaza and Zamora Chinchipe. All specimens are shown at the same scale.



Figure 9. Adult *Osteocephalus cannatellai* showing variation in ventral coloration of preserved specimens. Specimen identity and arrangement is the same as in Figure 8. All specimens are shown at the same scale.

gray and dark gray marks, dorsal surfaces of thighs light gray with dark gray transversal bands, dorsal surfaces of shanks and feet brown with dark gray marks. Venter brown with light cream yellowish spots, more abundant on posterior half of the body (Fig. 9); ventral surfaces of hindlimbs and forelimbs brown with dark brown marks and conspicuous white tubercles on forearms; outer half of ventral surfaces of forearms dark brown; sides of head brown with oblique white bar from posteroventral border of orbit to border of jaw, below tympanum (Fig. 10); vertical dark brown bar below eye, anterior to white bar; area behind white bar and eye dark brown except for brown

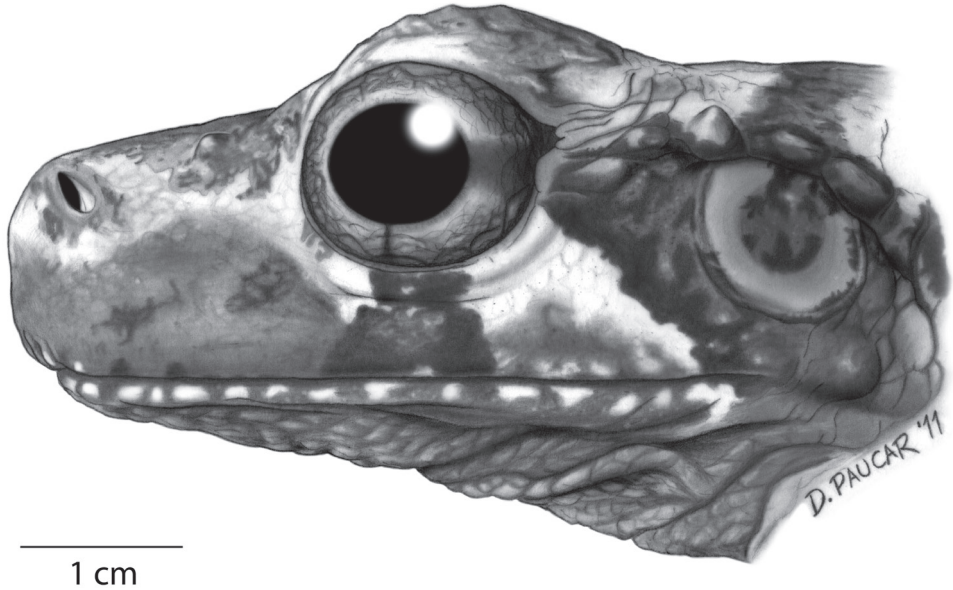


Figure 10. Lateral view of the head of the holotype of *Osteocephalus cannatellai* (QCAZ 49572).

periphery of tympanum; iris light gray with black reticulations; flanks light gray anteriorly, cream posteriorly, areolate region with gray reticulation.

Color of holotype in life. Based on digital photographs. Dorsum brown with green peripheral marks; dark brown, ill defined, transversal bar between orbits (Fig. 7E); dorsal surfaces of forearms brown with green and dark brown marks, dorsal surfaces of thighs dark green with dark brown transversal bands, dorsal surfaces of shanks and feet brown with dark brown marks. Sides of head brown with oblique lime bar from posteroventral border of orbit to border of jaw, below tympanum; vertical dark brown bar below eye, anterior to lime bar; area posterior to lime bar and eye dark brown except for brown periphery of tympanum; flanks light green, areolate region with dark reticulation.

Etymology. The specific name *cannatellai* is a noun in the genitive case and is a patronym for David C. Cannatella, who with his research has enriched the understanding of the evolution of Neotropical amphibians. He has also contributed to amphibian studies in Ecuador by providing funding and training to local scientists.

Variation. Variation in dorsal and ventral coloration of preserved specimens is shown in Figures 8 and 9. Dorsal background coloration varies from cream to light gray or brown; irregular dark brown or dark gray marks are always present (Fig. 8). Some specimens have a cream middorsal line from the tip of the snout to the mid sacrum (QCAZ 49570) or the vent (QCAZ 39633). In females, the dorsum always lacks tubercles while in males it varies between lacking tubercles (QCAZ 32508) and having scant and ill-defined non-keratinized tubercles (e.g., QCAZ 48814 and 49569). The prominence of the tubercles seems to decrease in preserved specimens: when collected, QCAZ 48744 had large conspicuous dorsal tubercles (Fig. 7), in preservative tubercles are barely noticeable.

Table 3. Descriptive statistics for morphometric measurements of species of the *Osteocephalus buckleyi* complex. Mean \pm SD is given with range below. Bold figures are averages for individuals of all populations. Abbreviations are: SVL = snout-vent length; FOOT = foot length; HL = head length; HW = head width; ED = eye diameter; TD = tympanum diameter; TL = tibia length; FL = femur length. All measurements are in mm.

	SVL	FOOT	HL	HW	ED	TD	TL	FL
<i>O. cabrerai</i> Males (n = 7)	42.54 \pm 2.51 (39.66–45.72)	17.46 \pm 0.92 (16.15–18.57)	15.33 \pm 0.73 (14.33–16.29)	14.86 \pm 0.73 (14.11–15.66)	4.11 \pm 0.38 (3.54–4.56)	3.4 \pm 0.34 (3–3.9)	23.62 \pm 1.04 (22.37–25.14)	21.93 \pm 1.11 (20.09–22.9)
<i>O. cannatellai</i> Males (n = 33)	46.84 \pm 4.31 (38.46–57.21)	19.68 \pm 2.05 (15.96–24.30)	16.27 \pm 1.48 (13.86–19.10)	15.12 \pm 1.94 (11.39–19.80)	5.14 \pm 1.65 (4.24–6.40)	3.22 \pm 0.48 (2.16–4.21)	25.83 \pm 2.47 (20.68–31.45)	23.40 \pm 2.52 (18.87–29.0)
Females (n = 3)	66.55 \pm 5.44 (62.64–72.77)	28.31 \pm 2.69 (26.12–31.32)	21.68 \pm 1.25 (20.76–23.11)	18.36 \pm 1.59 (17.3–20.2)	5.86 \pm 0.43 (5.42–6.28)	3.85 \pm 0.16 (3.7–4.02)	37.15 \pm 3.25 (34.17–40.62)	34.64 \pm 2.19 (32.89–37.11)
Bobonaza Males (n = 2)	44.79 \pm 2.72 (42.86–46.72)	18.55 \pm 0.80 (17.98–19.12)	15.34 \pm 1.39 (14.36–16.33)	12.85 \pm 0.45 (12.53–13.17)	4.94 \pm 0.12 (4.85–5.03)	2.91 \pm 0.18 (2.78–3.04)	4.82 \pm 1.64 (23.66–25.98)	21.34 \pm 0.69 (20.85–21.83)
Pomona Males (n = 3)	49.65 \pm 5.54 (43.67–54.61)	21.06 \pm 2.69 (18.5–23.88)	17.66 \pm 1.72 (15.27–18.31)	14.29 \pm 1.41 (12.66–15.23)	5.02 \pm 0.68 (4.44–5.78)	3.21 \pm 0.36 (2.83–3.56)	26.08 \pm 2.98 (23.52–29.36)	24.21 \pm 2.86 (21.52–27.22)
Yawi Males (n = 5)	41.86 \pm 2.91 (38.46–45.46)	17.11 \pm 0.78 (15.96–18.1)	14.65 \pm 0.95 (13.86–16.24)	12.53 \pm 0.98 (11.39–13.67)	4.61 \pm 0.42 (4.24–5.34)	2.92 \pm 0.47 (2.16–3.48)	22.41 \pm 1.21 (20.68–23.77)	20.22 \pm 1.05 (18.87–21.69)
Female (n = 1)	64.25	27.5	20.76	17.58	5.42	3.7	36.66	32.89
Zanjarajuno Males (n = 2)	50.07 \pm 0.96 (49.39–50.75)	21.46 \pm 1.34 (20.51–22.41)	17.73 \pm 0.07 (17.68–17.79)	14.15 \pm 0.16 (14.03–14.27)	5.07 \pm 0.09 (5.01–5.14)	3.24 \pm 0.16 (3.13–3.36)	28.17 \pm 2.24 (26.59–29.76)	24.75 \pm 1.36 (23.79–25.75)
Female (n = 1)	72.77	31.32	23.11	20.2	6.28	4.02	40.62	37.11
<i>O. buckleyi</i> Males (n = 14)	41.34 \pm 2.41 (38.01–45.25)	16.42 \pm 1.07 (14.51–18.34)	14.46 \pm 0.74 (13.05–15.82)	12.49 \pm 1.26 (10.84–15.35)	4.26 \pm 0.30 (3.76–4.84)	3.51 \pm 0.19 (3.20–3.88)	22.05 \pm 1.21 (20.07–24.24)	20.14 \pm 1.20 (17.76–22.37)
Females (n = 2)	45.68 \pm 7.44 (40.42–50.95)	18.06 \pm 1.52 (16.99–19.14)	16.08 \pm 2 (14.67–17.5)	13.47 \pm 1.49 (12.42–14.53)	4.69 \pm 0.53 (4.32–5.07)	3.66 \pm 0.2 (3.52–3.81)	25.14 \pm 3.63 (22.57–27.71)	23.49 \pm 2.8 (21.51–25.47)
<i>O. germami</i> Males (n = 2)	41.26–41.45	17.97–18.17	12.79–12.99	14.23–14.82	4.51–5.23	3.79–3.99	23.10–23.50	22.30–22.70
Females (n = 2)	49.16–50.76	21.00–22.10	13.67–15.00	17.23–17.67	5.10–5.35	3.80–4.17	26.80–27.70	25.00–27.00
<i>O. vilmae</i> Males (n = 6)	50.74 \pm 3.17 (48.23–55.77)	21.06 \pm 1.16 (19.61–22.11)	16.78 \pm 1.32 (14.90–18.09)	18.03 \pm 1.13 (16.46–19.22)	6.092 \pm 0.62 (5.27–6.80)	4.43 \pm 0.29 (4.10–4.90)	27.90 \pm 0.64 (27.00–28.70)	25.93 \pm 1.50 (24.20–28.00)

Ventral surfaces of preserved specimens (Fig. 9) vary from light gray (QCAZ 40909) to brown (QCAZ 31031). In most specimens, there are dark brown or dark gray spots, more abundant posteriorly (e.g., QCAZ 49439); QCAZ 39633 has brown blotches on the chest and venter; QCAZ 48804 has similar marks that also reach the gular region. In two Peruvian specimens ventral surfaces are light gray with few brown spots posteriorly (CORBIDI 09553) or with light brown spots, slightly visible, on gular region and belly (MUSM 28050). The gular regions in some Peruvian specimens are brown (e.g., CORBIDI 09507, 10532). Ventrally, limbs vary from light gray or light brown to dark brown; in QCAZ 33256 and 39587 black dots are present on limbs; scant cream tubercles can be present in the external edge of the forearm (e.g., QCAZ 32512). The skin of the anterior and posterior surfaces of thighs and the concealed surfaces of shanks are pale in the Peruvian specimens. The vent region is light gray to dark brown with dark brown dots. Flanks are cream to light gray, areolate in the anterior two-thirds and smooth posteriorly. In specimens from Peru the flanks are completely areolate. The areolate portion has a dark brown reticulation.

Head shape is truncate in dorsal and lateral view (e.g., QCAZ 39579). Lateral head coloration varies between dark brown (QCAZ 49569) to cream (QCAZ 32506). There is a cream subocular mark. The tympanic annulus is concealed dorsally and has lighter color than the background. The distal subarticular tubercle on Finger IV is single (e.g., QCAZ 40909) or bifid (e.g., QCAZ 45272).

Morphometric data pertain to adults and are summarized in Table 3. In the examined series, the largest male has a SVL of 57.21 mm and the largest female 72.77 mm; mean male SVL = 46.84 mm ($n = 33$, $SD = 4.31$), mean female SVL = 66.55 mm ($n = 3$, $SD = 5.44$). Females are significantly larger than males ($t = 7.66$, $df = 33$, $P < 0.001$). A MANOVA on the residuals of the regressions between SVL and the other measured variables indicates lack of significant differences between sexes in size-free morphometry ($F = 0.239$, $df = 17$, $P = 0.060$).

Color in life. Based on digital photograph of adult male QCAZ 48744 (Fig. 7 C–D): dorsum green with irregular light and dark brown marks; canthal region green with cream subocular mark and olive green diffuse band along the posterior half of upper lip; tympanum light brown; flanks light green with dark brown reticulation anteriorly and irregular dark brown blotches posteriorly; dorsal surfaces of thighs, shanks and forelimbs green with transversal brown bands; venter brown with irregular dark brown and cream marks; iris bronze with diffuse brown mid-horizontal line and black reticulations.

Based on digital photograph of juvenile QCAZ 40859 (Fig. 7 F): dorsum green with dark brown marks; upper lip cream with transversal brown bars; flanks light green with brown marks; dorsal surfaces of arms, thighs and shanks green with brown transversal bars; external edge of tarsus with white tubercles; iris bronze with black reticulations and diffuse mid-horizontal dark band between the pupil and posterior border of iris.

In life the Peruvian specimens have extensive blue coloration in the groins, concealed surfaces of thighs and tibia, dorsal surfaces of tarsus, armpits and posterior surfaces of arms (e.g., CORBIDI 10534; Fig. 7 G–H). The iris is highly variable from

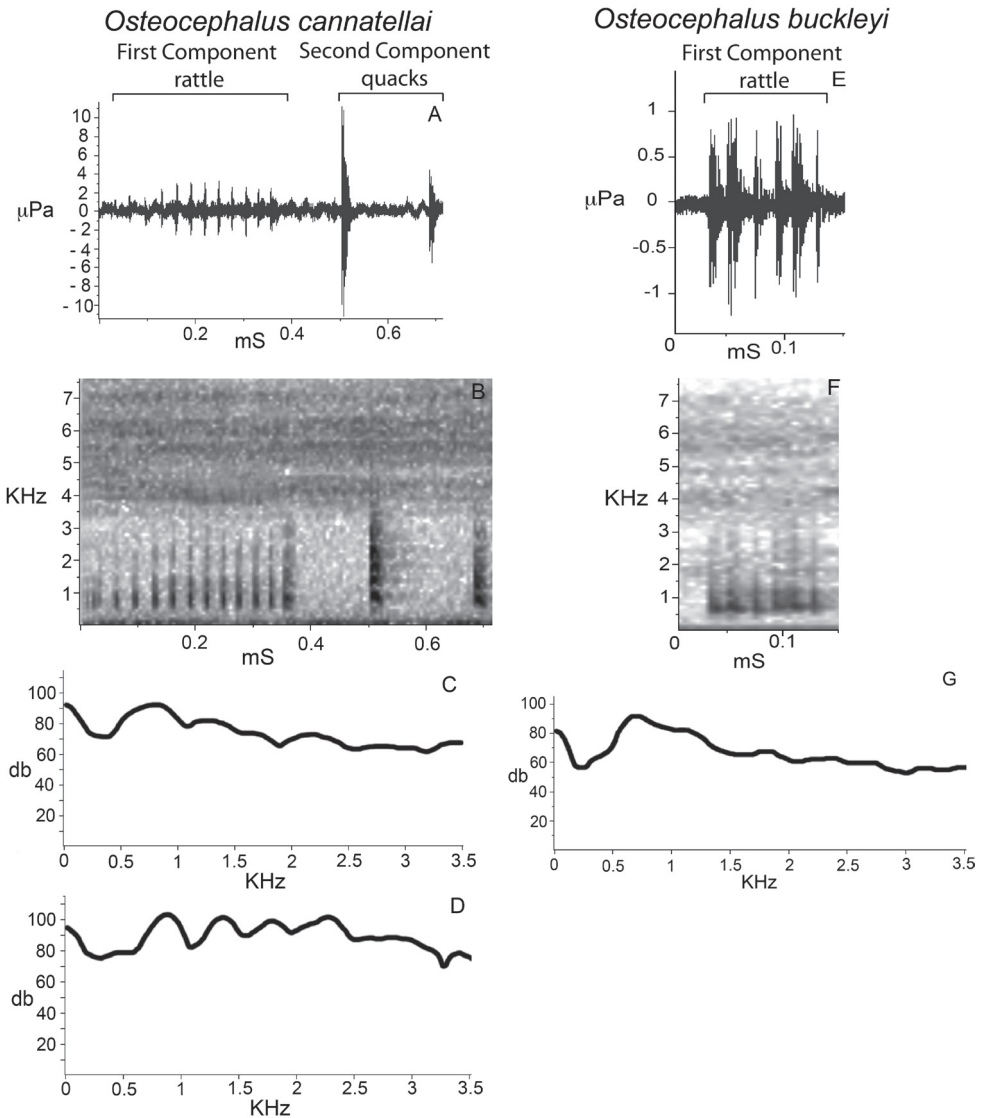


Figure 11. Advertisement calls of *Osteocephalus*. **A–D** *O. cannatellai* (QCAZ8322) from Río Piraña, Provincia Orellana, Ecuador; **E–G** *O. buckleyi*, from Jatun Sacha, Provincia Napo, Ecuador. **A** and **E** are oscillograms, **B** and **F** spectrograms, **C** and **G** power spectra of complete call, and **D** power spectra of quacks (second component).

light cream to brownish cream and dark brown (CORBIDI 09394); there are always black reticulations and a diffuse mid-horizontal dark band. Some individuals have a diffuse vertical dark band below the pupil.

Green coloration in life changes to cream in preserved specimens.

Call. Males call from vegetation next to rivers or streams. Acoustic parameters of the advertisement call of *O. cannatellai* are shown in Table 4. The call consists of two

Table 4. Descriptive statistics for call parameters of *Osteocephalus buckleyi* and *O. cannatellai* sp. n. Mean \pm SD is given with range below. The calls of both species have an obligatory first component consistent of a rattle-like note. *Osteocephalus cannatellai* has a facultative second component consistent of one to three quack notes. Sample sizes are number of males. Temporal characters are shown in seconds; spectral characters in Hertz.

	<i>O. cannatellai</i>			<i>O. buckleyi</i>
	Combined (n = 5)	Río Piraña (n = 1)	Río Pucayacu (n = 4)	Jatun Sacha (n = 2)
Duration of first component note	0.425 \pm 0.053 (0.356–0.489)	0.356	0.442 \pm 0.042 (0.389–0.489)	0.059 \pm 0.004 (0.056–0.063)
Call Rate	0.3066 \pm 0.113 (0.208–0.454)	0.454	0.269 \pm 0.090 (0.208–0.402)	1.524 \pm 0.151 (1.417–1.631)
First component interval	4.114 \pm 1.722 (2.142–6.004)	2.142	4.607 \pm 1.528 (2.568–6.004)	0.725 \pm 0.140 (0.625–0.824)
Dominant Frequency	1049.54 \pm 247.18 (771.6–1412.6)	771.616	1119.02 \pm 221.99 (765.68–1472.26)	745.66 \pm 0.87 (745.04–746.28)
Number of pulses	12.213 \pm 1.585 (9.8–14.2)	12	12.266 \pm 1.825 (9.8–14.2)	3.328 \pm 0.181 (3.2–3.457)
Pulse rate	28.932 \pm 4.095 (23.847–34.016)	33.661	27.749 \pm 3.610 (22.004–33.495)	55.833 \pm 1.565 (41.772–69.893)
Duration of second component	0.307 \pm 0.106 (0.216–0.488)	0.216	0.329 \pm 0.108 (0.25–0.488)	NA
Duration of second component note	0.032 \pm 0.004 (0.027–0.037)	0.027	0.033 \pm 0.004 (0.027–0.037)	NA
Number of second component notes	0.866 \pm 0.339 (0.445–1.287)	1	0.832 \pm 0.381 (0.225–1.439)	NA
Quack rate	0.140 \pm 0.026 (0.108–0.177)	0.108	0.148 \pm 0.022 (0.125–0.177)	NA

components. The first is obligatory and consists of one to five rattle-like notes. The second component is facultative and consists of one to three quacks. The first component is pulsed and lacks harmonic structure; the second component has visible harmonics and reaches higher amplitude than the first component (Fig. 11).

The advertisement calls of *O. cannatellai* differ markedly from those of *O. buckleyi*. Calls of *O. buckleyi* (Fig. 11) consist of a pulsed rattle-like note repeated at irregular intervals and without a second component. Those calls have a shorter duration, higher repetition rate, and fewer pulses than calls of *O. cannatellai*.

Distribution and ecology. *Osteocephalus cannatellai* has been recorded at twelve localities, all of them south of the Napo river, in the Ecuadorian and Peruvian Amazon basin (Provincias Morona Santiago, Napo, Orellana, Pastaza, Zamora-Chinchipec, and Datem del Marañón; Fig. 2). Localities with known elevation (El Edén, Huino, Yachana, Zanjarajuno, Río Maderoyacu, Hola Vida, Bobonaza, Nuevo Israel, Yawi, and Kampankis) have a range between 200 and 1290 m above sea level. Maximum airline distance between localities is 531 km. *Osteocephalus cannatellai* occurs sympatrically with *O. buckleyi* at Reserva Yachana and with *O. fuscifacies* and *O. mutabor* at Río Pucayacu, Nuevo Israel and Hola Vida.

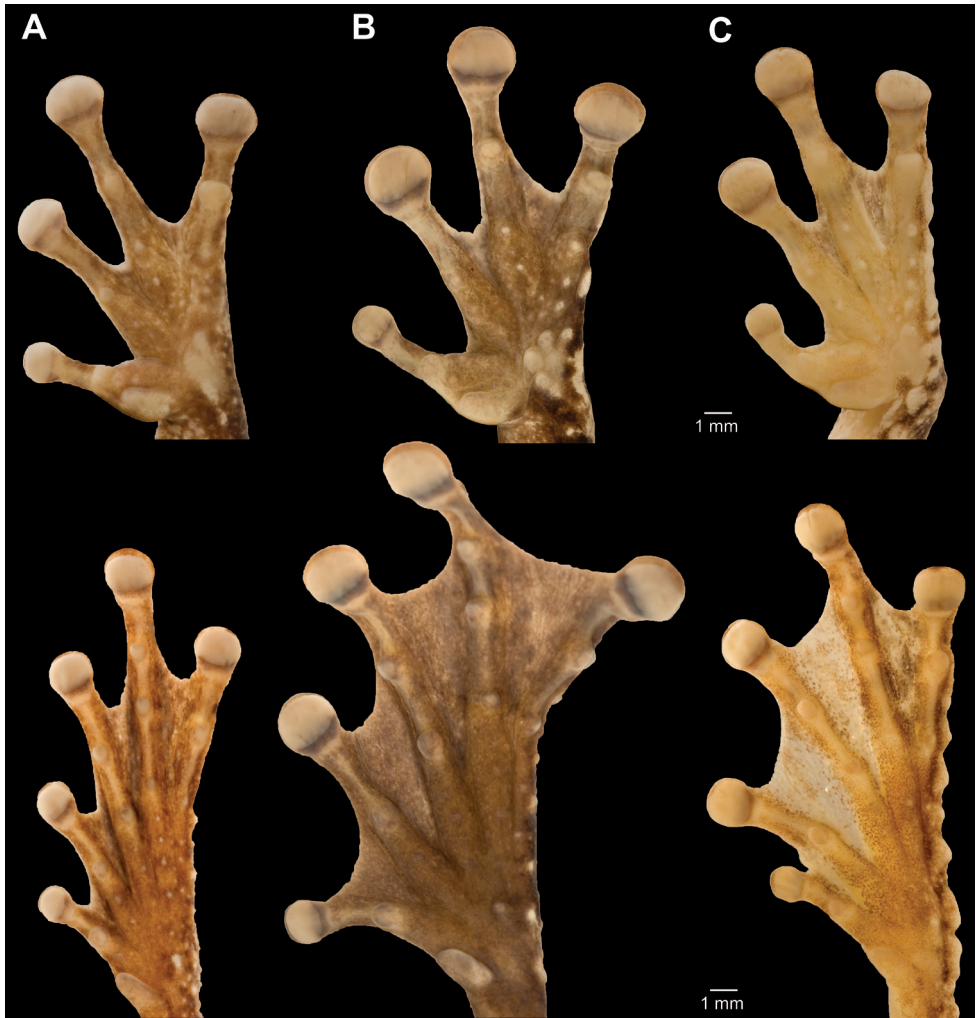


Figure 12. Ventral views of the left hand and foot of *Osteocephalus*. **A** *Osteocephalus buckleyi* (Tarangaro, Ecuador, SVL = 39.8 mm, QCAZ 39191) **B** *O. cannatellai* (Zanjarajuno, Ecuador, SVL = 45.32 mm, QCAZ 45907) and **C** *O. cabrenai* (Cuyabeno, Ecuador, SVL = 41.62 mm, EPN-H 7204). Hand and foot are shown at the same scale.

Most specimens were collected at Río Pucayacu, a river surrounded by a mixture of primary and secondary forest. Frogs were found next to the river, perching over broad leaves or on tree branches 50 to 230 cm above the ground. At the collection site, the river has an average width of approximately 10 m, fast running water, and a rocky bottom. Males were calling next to the river between June 26 and July 3 2010. Several adults and a juvenile were found on a small stream, tributary of Río Rivadeneira, surrounded by secondary forest, near Río Pucayacu, in March 2008.

Vegetation types (according to the classification of Sierra et al. 1999) are: (1) Amazonian Mountain Range Evergreen Foothill Forest, characterized by a mixture of



Figure 13. Lateral view of the head of the holotypes of *Osteocephalus germani* (above CORBIDI 05462) and *O. vilmae* (below CORBIDI 04773).

Amazonian and Andean vegetation with a canopy of 30 m (Río Pucayacu, Bobonaza, and Yawi), (2) Amazonian Lowland Evergreen Forests, characterized by high plant alpha-diversity and a canopy of 30 m with emergent trees that reach 40 m (Huino, Río Maderoyacu, Reserva Yachana), and (3) Amazonian Lower Montane Evergreen Forest, with an elevational range of 1300 to 2000 m above sea level, its canopy can reach 25 to 30 m (Nuevo Israel; Sierra et al. 1999, Cerón et al. 1999).

Specimens from Peru were collected in Cordillera de Kampankis within an elevational range of 300 to 365 m above sea level in tall, closed-canopy forest on low hills with well-drained soils at the base of the mountains. The soils have variable proportions of silt, clay and sand, but there are some small patches of sandy soil and limestone outcrops. The forest canopy is about 30 m tall, with emergent trees reaching 45 m. All individuals were collected in riparian vegetation of low-velocity and low-volume streams with rounded slate rocks lining the stream bed. Some individual were found on leaf of dense populations of rheophytic plants or shrubby *Pitcairnia aphelandriflora* (Bromeliaceae). Other individuals were found on branches of bushes between 50 and 200 cm above the ground. Other arboreal frogs at the site were *O. mutabor*, *Hypsiboas cinerascens*, and *Gastrotheca longipes*.

***Osteocephalus germani* sp. n.**

urn:lsid:zoobank.org:act:556B14DE-AA7D-4112-9C1B-D2814A7D6351

http://species-id.net/wiki/Osteocephalus_germani

Holotype. (Fig. 13, 14) CORBIDI 05462, adult male from Peru, Región Cusco, Provincia La Convención, near Pongo de Mainique in the vicinity of Santuario Natural Megantoni (12.2581°S, 72.8425°W), 670 m above sea level, collected by G. Chavez on 23 April 2010.

Paratotypes. (Fig. 15 A, C) CORBIDI 06633, adult female, and CORBIDI 06660, adult male, collected with the holotype; CORBIDI 05505, adult female, collected by G. Chavez on 8 November 2009.

Paratypes. (Fig. 15 B, D) Peru: Provincia La Convención, Comunidad Nativa Poyentimari (12.18853°S, 73.00092°W), 725 m above sea level, CORBIDI 08267, 08284, adult females, collected by G. Chavez and D. Vasquez on 28 November 2010; Comunidad Nativa Chokoriari (11.9569°S, 72.9410°W), 434 m above sea level, CORBIDI 08059, adult female, collected by D. Vasquez on 8 December 2010.

Diagnosis. Throughout this section, coloration refers to preserved specimens unless otherwise noted. *Osteocephalus germani* is a medium-sized species of *Osteocephalus* having the following combination of characters: (1) size sexually dimorphic; maximum SVL in males 41.45 mm ($n = 2$), in females 50.76 ($n = 2$); (2) skin on dorsum bearing tubercles in males, smooth in females; (3) skin on flanks areolate; (4) hand webbing formula varying from I basal II2⁻—3—III2½—2IV to I basal II2—3III3⁻—3—IV; foot webbing formula varying from I1—1½II1⁻—2III1—2IV1½—1—V to I1⁺—2II1⁺—2III1⁺—2—IV2—1V; (5) dorsum varying from brown with dark brown marks to light



Figure 14. Adult *Osteocephalus germani* showing variation in dorsal and ventral coloration of preserved specimens. Left to right, upper row: CORBIDI 08267 (female), 05505 (female), 05462 (male, holotype), 06660 (male), CORBIDI 06663 (female), 08284 (female), 08059 (female); third and fourth rows show ventral views of the same specimens, in the same order as in the first two rows. Peru, Region Cusco.

gray with dark brown marks; (6) venter light cream with or without dark brown flecks; (7) cream suborbital mark present, clear labial stripe absent; (8) flanks cream to brownish cream with dark brown blotches and flecks; (9) dermal roofing bones of the skull weakly exostosed; (10) bones green in life; (11) in life, iris golden to reddish golden

with fine dark reticulation; (12) paired vocal sacs, located laterally, behind jaw articulation, (13) juvenile coloration unknown; (14) larvae unknown.

Osteocephalus germani is most similar to *O. buckleyi*, *O. cabrerai*, *O. cannatellai* sp. n., and *O. vilmae* sp. n. It differs from all of them in lacking prominent tarsal tubercles (tubercles are indistinct in *O. germani*). It further differs from *O. buckleyi*, *O. cannatellai*, and *O. vilmae* in having a white to light cream venter with or without dark brown flecks (cream with brown speckling in most *O. buckleyi* and *O. vilmae*, light gray to dark brown in *O. cannatellai*). *Osteocephalus germani* also differs from *O. cannatellai* and *O. vilmae* in having more abundant and keratinized dorsal tubercles (dorsal tubercles are scattered and weakly keratinized in *O. cannatellai* and *O. vilmae*) and smaller size (*O. germani* male SVL range = 41.26–41.45, $n = 2$; *O. cannatellai* male SVL range = 38.46–57.21, $n = 33$; *O. vilmae* male SVL range = 48.23–55.77, $n = 5$). Mitochondrial DNA sequences show that *O. germani* is the sister species of *O. cabrerai* (Fig. 1). *Osteocephalus germani* can be easily distinguished from *O. cabrerai* by (*O. cabrerai* in parenthesis): (1) absence of prominent tubercles on the lower jaw (present), (2) smooth outer edge of Finger IV (outer edge with fringe), (3) row of inconspicuous tubercles in the outer edge of tarsus (conspicuous), and (4) less webbing in the hands (in *O. germani* web reaches the antepenultimate tubercle of Finger IV, in *O. cabrerai* it reaches the proximal border of the ultimate tubercle; Figs 12 and 16). *Osteocephalus germani* differs from other species of *Osteocephalus* in having a combination of a dark golden to tan golden iris, a row of indistinct tubercles in the tarsus, and areolate skin in the flanks. A golden iris with black reticulations further distinguishes *O. germani* from *O. deridens*, *O. oophagus*, *O. planiceps*, and *O. taurinus* which have bronze to golden irises with black lines radiating from the pupil; iris coloration also differs in *O. carri*, *O. festae*, *O. heyeri*, *O. subtilis*, and *O. verruciger* which have predominantly dark irises, and in *O. leoniae* which have a bicolor iris (Jungfer 2010; Jungfer and Lehr 2001; Lynch 2002). *Osteocephalus germani* differs from *O. exophthalmus*, *O. fuscifacies* and *O. leoniae* in having abundant keratinized dorsal tubercles in males (tubercles are absent in the three last species). Skin texture in the flanks distinguishes *O. germani* (areolate) from *O. mutabor* (smooth). *Osteocephalus inframaculatus* differs from *O. germani* in coloration of the ventral surfaces of hindlimbs (bold brown blotches in *O. inframaculatus* are absent in *O. germani*; Jungfer 2010).

Description of holotype. Adult male, 41.26 mm SVL, head length 12.79, head width 14.23, eye diameter 5.23, tympanum diameter 3.79, femur length 22.3, tibia length 23.1, foot length 17.97. Head narrower than body, slightly wider than long; snout rounded in dorsal view and truncate in lateral view; distance from nostril to eye longer than diameter of eye; canthus rostralis distinct and straight; loreal region concave; internarial area depressed; nostrils moderately protuberant, directed laterally; interorbital area with tiny keratinized conical tubercles, lateral margins of frontoparietals inconspicuous through skin; eye large, strongly protuberant; tympanic membrane clearly evident, large, slightly wider than high, about two thirds of eye diameter, separated from eye by ca. 85% of its diameter; tympanic annulus distinct except dorsally where it is covered by supratympanic fold; posterior end of supratympanic fold reaches

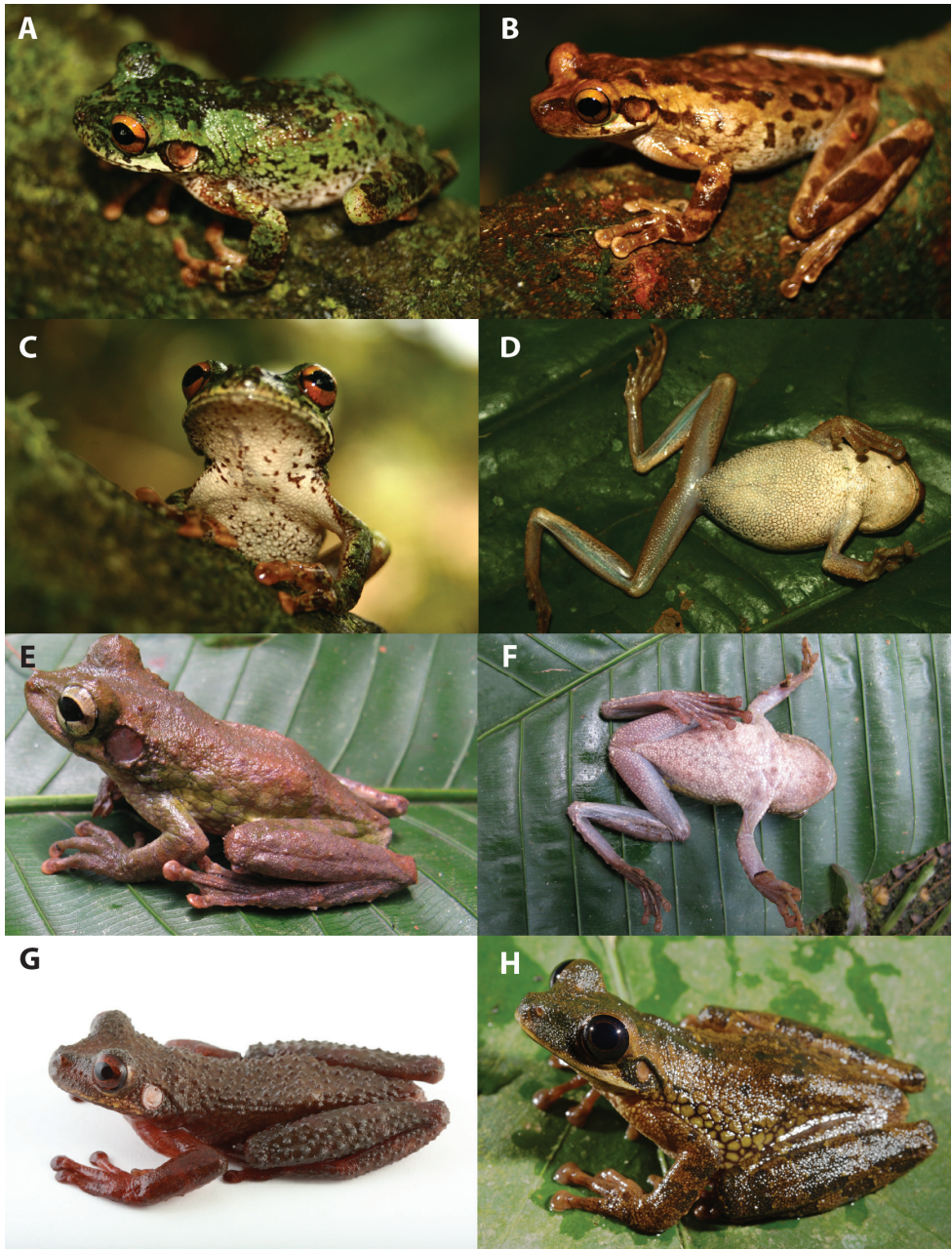


Figure 15. Dorsolateral, frontal, and ventral views of *Osteocephalus*. **A, C** *Osteocephalus germani*, CORBIDI 05505, adult female, SVL = 49.16 mm, Pongo de Mainique, Peru **B, D** *O. germani*, CORBIDI 08284, adult female, SVL = 49.00 mm, Comunidad Nativa Poyentimari, Peru **E–F** *O. vilmae* CORBIDI 04773 (holotype), adult male, SVL = 51.85 mm, Pampa Hermosa, Peru **G** *Osteocephalus verruciger*, QCAZ 41115, adult male, 52.37 mm, Pacto Sumaco, Ecuador **H** *Osteocephalus festae*, QCAZ 39801, adult female, SVL = 51.54 mm, Río Napinaza, Ecuador. Photographs **A–D** by G. Chavez, and **E–F** by V. Durán.

arm insertion. Arm slender, axillary membrane present, reaching less than one third of arm length; four small low tubercles present along ventrolateral edge of forearm; relative length of fingers I<II<IV<III; fingers bearing large, oval discs, that of third finger about three fourths of tympanum diameter; subarticular tubercles prominent, round to ovoid except for bifid distal subarticular tubercle of Finger IV; supernumerary tubercles present; palmar tubercle small, elongated; prepollical tubercle large, flat, elliptical; prepollex enlarged; large dark keratinous nuptial excrescences covering inner surface of prepollex up to two thirds the distance between subarticular tubercle and proximal border of disk of thumb; webbing absent between fingers I and II; webbing formula of fingers II²—3III²¹/₂ —3—IV. Small tubercles on tibiotarsal articulation; dorsal surface of tarsus covered by tiny keratinized conical tubercles, more abundant on outer edge; minute tubercles scattered along ventrolateral edge of foot; toes bearing discs slightly wider than long, smaller than those of fingers; relative length of toes I<II<V<III<IV; outer metatarsal tubercle ill defined, small, round; inner metatarsal tubercle low, ovoid; subarticular tubercles single, round, protuberant; supernumerary tubercles restricted to the soles; webbing formula of toes II—2III—2III¹+—2IV²—1V. Skin on dorsum, head, and dorsal surfaces of limbs shagreen covered by conical tubercles with keratinized tips, tiny on head and limbs; skin on flanks areolate; skin on venter coarsely granular; skin on ventral surfaces of head and thighs granular, those of shanks smooth. Cloacal opening directed posteriorly at upper level of thighs; short simple cloacal sheath covering cloacal opening; round tubercles below vent; two conspicuous white tubercles ventrolateral to vent at lower level of thighs. Tongue cordiform, widely attached to floor of mouth; dentigerous processes of the vomers angular, adjacent medially, posteromedial to choanae, bearing 5 and 6 (left/right) vomerine teeth; choanae trapezoidal, oblique; vocal slits moderately long, extending diagonally from lateral end of tongue toward to the angle of snout; vocal sac indistinct above the arm and below the ear.

Color of holotype in preservative. Dorsum light brown with dark brown peripheral marks; dark brown transversal bar between orbits with fine pale borders; dorsal surfaces of forearms grayish brown with dark brown marks, dorsal surfaces of thighs, shanks, and feet grayish brown with diffuse brown transversal bars. Venter light cream with dark brown flecks on the throat and thoracic region and absent on posterior half of the body; ventral surfaces of hindlimbs and forelimbs dirty cream with dark brown flecks on the lateral borders of shanks; outer half of ventral surfaces of forearms dirty cream; sides of head brown with white subocular band extending, below tympanum, two little brown blotches below the eye; tympanic membrane dark brown and area in the periphery of tympanum light brown dorsally and grayish brown behind the tympanum; flanks grayish white, areolate region with dark brown reticulation and flecks. Iris silver with dark brown mid-horizontal line and thin black reticulations.

Color in life. Dorsum brown with irregular dark brown marks; flanks brownish cream with dark brown spots and flecks; dorsal surfaces of thighs, shanks, and forelimbs brown with transversal dark brown bands. Venter whitish cream with brown flecks in throat; ventral surfaces of thighs tan. Iris bronze with thin black reticulations (G. Chávez field notes April 2010).

Etymology. The new species is dedicated to our colleague German Chávez (CORBIDI), one of the best friends of PJV, for his contributions to Peruvian herpetology and collecting the type series and tissues of this new species.

Variation. Variation in dorsal and ventral coloration of preserved specimens is shown in Figure 14. Dorsal background coloration varies from light brown to light gray; irregular dark brown marks are always present. In females, the dorsum lacks tubercles while in males tubercles are present. The single male paratype (CORBIDI 06660) differs from the holotype in having non-keratinized tubercles.

Ventral surfaces of preserved specimens (Fig. 14) are whitish cream. All the specimens have scattered dark brown flecks on the anterior half of the venter. Ventrally, limbs vary from whitish cream to tan; scant white tubercles can be present in the external edge of the forearm of males (e.g., CORBIDI 06660). The vent region is light brown or dark. Flanks are whitish cream to light gray, areolate in the anterior half and nearly smooth posteriorly. The areolate portion is completely covered by dark brown reticulation and flecks.

Snout is truncate in lateral view except for a female with rounded snout (CORBIDI 06633). Lateral head coloration varies from dull brown (CORBIDI 06633) to cream with dark brown blotches (CORBIDI 05505). The tympanic annulus is concealed dorsally and has lighter color than the background. The distal subarticular tubercle on Finger IV is bifid in all the specimens.

Adult morphometric data are summarized in Table 3. In the examined series, the largest male has a SVL of 41.45 mm and the largest female 50.76 mm; mean male SVL = 41.35 mm ($n = 2$, $SD = 0.13$), mean female SVL = 49.96 mm ($n = 2$, $SD = 1.13$).

Color in life. Based on digital photograph of adult male CORBIDI 06660: dorsum brown with irregular dark brown marks and some scattered light green blotches; canthal region greenish brown with greenish cream subocular mark and dark labial bars; tympanum light brown; flanks light green with dark brown reticulation and dark brown blotches posteriorly; dorsal surfaces of thighs, shanks, and forelimbs brown with transversal dark brown bands and scattered light green blotches. Iris bronze with brown horizontal midline and thin black reticulations.

Based on digital photograph of adult female CORBIDI 06633: dorsum brown with few scattered irregular dark brown marks; canthal region dark brown with greenish cream subocular mark speckled by three small dark brown blotches; tympanum light brown; flanks light brown with dark brown blotches; ventrolateral region cream with fine dark reticulation; dorsal surfaces of thighs, shanks, and forelimbs brown with transversal dark brown bands. Anterior half of venter whitish cream with fine brown reticulation in throat and chest; posterior half of venter and ventral surfaces of thighs tan; iris bronze with diffuse brown mid-horizontal line and thin black reticulations.

Based on digital photograph of adult female CORBIDI 05505 (Fig. 15): dorsum green with irregular dark brown marks; canthal region green with brown mottling and white subocular mark extending to the lips as a white labial stripe along posterior half of the jaw; tympanum light brown; flanks white with dark brown reticulation and small dark brown blotches posteriorly; dorsal surfaces of thighs, shanks, and forelimbs green with transversal dark brown bands and flecks. Venter white with scattered brown

flecks on throat and chest. Iris reddish gold with diffuse brown mid-horizontal line and thin black reticulations. Based on digital photograph of adult female CORBIDI 08284 (Fig. 15): dorsum light brown with irregular dark brown marks; canthal region brown and greenish white subocular mark; tympanum light brown; flanks light brown with small dark brown blotches; dorsal surfaces of thighs, shanks, and forelimbs light brown with transversal dark brown bands. Venter dull cream. Iris bronze with diffuse brown mid-horizontal line and thin black reticulations.

Distribution and ecology. *Osteocephalus germani* is known from three localities in southern Peru (Fig. 6). Pongo de Manique and Comunidad Nativa de Poyentimari are in premontane forest on the Upper Urubamba River basin (vegetation types according to ONERN 1976) in the Amazonian foothills of the southern Peruvian Andes, at elevations of 670–725 m; Comunidad Nativa de Chokoriari is *Terra Firme* Amazonian lowland forests on the lower Urubamba River basin in the southern Peruvian Amazon lowlands, at elevation of 434 m. In Pongo de Mainique the new species was found close to rocky streams in low-hill primary forest with arboreal ferns and abundant epiphytes. At this locality, *O. germani* was sympatric with *O. castaneicola* and *O. mimeticus*. In Comunidad Nativa de Poyentimari, *O. germani* was found close to rocky streams in a step area of very wet high-hill primary forest with abundant ferns (including arboreal), epiphytes, lichens and mosses. At this locality the new species was sympatric with *O. mimeticus*. In Comunidad Nativa de Chokoriari, *O. germani* was found close to a black-water slow-running creek in a patch of secondary forest, surrounded by pastures for cattle and plantations. The forest was dominated by bamboo and *Cecropia* spp. and the creek had sandy soils covered by leaf litter. No other species of *Osteocephalus* were found in this locality.

All specimens were collected next to temporary pools, perching over broad leaves or on tree branches 100 to 200 cm above the ground. Many streams surround the collection sites.

Remarks. In the phylogeny (Fig. 1), two specimens from gen bank (EF376030 from French Guiana and AY843705 from Río Jurua, Brazil) are grouped with *O. germani* in a strongly supported clade (PP = 0.96) and are likely conspecific or represent one or two closely related species. The specimen from French Guiana was reported as “*O. oophagus*” by Salducci et al. (2002, 2005); the specimen from Brazil was reported as “*O. cabrerai*” by Faivovich et al. (2005). Both individuals appear to be misidentified.

***Osteocephalus vilmae* sp. n.**

urn:lsid:zoobank.org:act:681AAC6A-8710-4276-AA79-BD1F5C58C1DC
http://species-id.net/wiki/Osteocephalus_vilmae

Holotype. (Figs 13 and 15) CORBIDI 04773, adult male from Peru, Region Loreto, Provincia Datem del Marañón, Pampa Hermosa (3.0650°S, 75.8264°W), 200 m above sea level, collected by V. Duran on 28 March 2008.

Paratypes. Five adult males: Ecuador: Provincia de Orellana: Pompeya-Iro road, km 80, Río Beye, QCAZ 51205, collected by E. Toral, I. G. Tapia, T. Camacho, and S.



Figure 16. Ventral views of left hand and foot of *Osteocephalus vilmae* and *O. germani*. **A** *O. vilmae* (Jibarito, Peru, SVL = 48.31 mm, CORBIDI 06469), and **B** *O. germani* (Comunidad Nativa Poyentimari, Peru, SVL = 49.00 mm, COBIDI 08284).

R. Ron on 31 May 2011; Provincia Pastaza: Nuevo Corrientes, 250 m above sea level, QCAZ 14947, collected by F. Villamarín on August 2000. Peru: Provincia Datem del Marañón: Andoas (2.6516°S, 76.5137°W), 151 m above sea level, CORBIDI 01086,

collected by A. Delgado on September 2008; Jibarito (2.7356°S, 76.0318°W), 197 m above sea level, CORBIDI 06469, collected by A. Delgado on 14 July; Capihuari Norte (2.6642°S, 76.5012°W), 270 m above sea level, CORBIDI 05031, collected by J. C. Chaparro on March 2008.

Diagnosis. Throughout this section, coloration refers to preserved specimens unless otherwise noted. *Osteocephalus vilmae* is a medium-sized species of *Osteocephalus* having the following combination of characters in males (females are unknown): (1) maximum SVL in males 55.77 mm ($n = 6$); (2) skin on dorsum bearing few scattered to abundant tubercles; (3) skin on flanks areolate with big flattened warts; (4) hand webbing formula varying from I basal II basal III2⁻—2IV to I basal II1^{2/3}—2^{2/3}III2^{2/3}—2^{1/2}IV; foot webbing formula varying from I1—1^{1/2}II1—2—III1⁻—2IV2⁻—1⁻V to I1⁺—2 II1—2III1⁺—2⁺IV2—1⁺V (Fig. 16); (5) dorsum varying from light brown with dark brown marks to light gray with dark brown marks; (6) venter varying from light gray to tan with lighter dots and/or dark brown blotches; (7) cream suborbital mark present, clear labial stripe absent; (8) flanks cream with darker reticulations and dark marks; (9) dermal roofing bones of the skull weakly exostosed; (10) in life, bones green; (11) in life, iris light cream to dirty cream with irregular reticulations; (12) paired vocal sacs small, located laterally, behind jaw articulation, (13) juveniles unknown; (14) larvae unknown.

Osteocephalus vilmae is most similar to *O. buckleyi* and *O. cannatellai*. It differs from *O. buckleyi* in having (1) scattered and weakly keratinized dorsal tubercles (abundant and keratinized in *O. buckleyi*), (2) larger size (*O. vilmae* mean male SVL = 55.77, SD = 3.17, $n = 5$; *O. buckleyi* mean male SVL = 41.12, SD = 2.49, $n = 24$; differences are significant: $t = 6.50$, $P < 0.001$; Fig. 5), and (3) more extensive and conspicuous areolate area on flanks (from axillary region to groin, with big flattened warts, in *O. vilmae*; restricted to anterior one half of flank in *O. buckleyi*). The range of genetic distances (uncorrected p for gen 12S) between *O. vilmae* and *O. buckleyi* is 0.9 to 1.6%. Both species are sympatric at km 80 Pompeya-Iro road indicating the existence of reproductive barriers between them.

Osteocephalus vilmae differs from *O. cannatellai* in having a larger tympanum ($\sim 1/4$ of head length in *O. vilmae* vs. $\sim 1/5$ in *O. cannatellai*), and areolate flanks with big flattened warts (areolate with small flattened warts in *O. cannatellai*). Mitochondrial DNA sequences show that *O. vilmae* and *O. cannatellai* are not sister species (Fig. 1). *Osteocephalus vilmae* differs from *O. cabrerai* in (1) lacking prominent tubercles on the lower jaw, (2) having smooth outer edge of Finger IV (outer edge with fringe in *O. cabrerai*), (3) having less webbing in the hands (in *O. vilmae* webbing reaches two thirds of the distance between the ultimate and penultimate tubercle of Finger IV, in *O. cabrerai* it reaches the proximal border of the ultimate tubercle; Figs 12 and 16), and (4) low to indistinct tubercles in the tarsus (prominent in *O. cabrerai*).

A cream to bronze iris with black reticulations distinguishes *O. vilmae* from *O. deridens*, *O. oophagus*, *O. planiceps*, and *O. taurinus* which have bronze to golden irises with black lines radiating from the pupil; iris coloration also differs from *O. carri*, *O. festae*, *O. heyeri*, *O. subtilis*, and *O. verruciger* which have predominantly dark irises, and from *O. leoniae* which have a bicolor iris (Jungfer 2010; Jungfer and Lehr 2001; Lynch 2002).

Osteocephalus vilmae is larger than *O. exophthalmus* (maximum male SVL in *O. vilmae* 55.77 mm, $n = 5$; in *O. exophthalmus* 32.7 mm, $n = 3$; Smith and Noonan 2001) and *O. fuscifacies* (maximum SVL = 44.17, $n = 21$). Skin texture in the flanks distinguishes *O. vilmae* (coarsely areolate) from *O. mutabor* and *O. yasuni* (smooth). *Osteocephalus inframaculatus* differs from *O. vilmae* in coloration of the ventral surfaces of hindlimbs (bold brown blotches in *O. inframaculatus* are absent in *O. vilmae*; Jungfer 2010).

Description of holotype. Adult male, 51.85 mm SVL, head length 18.9, head width 19.0, eye diameter 6.8, tympanum diameter 4.9, femur length 28.0, tibia length 28.7, foot length 22.1. Head narrower than body, nearly as wide as long; snout truncate in lateral and dorsal views; distance from nostril to eye longer than diameter of eye; canthus rostralis distinct and straight; loreal region concave; internarial area depressed; nostrils moderately protuberant, directed laterally; interorbital area flat, lateral margins of frontoparietals distinct through skin; eye large, strongly protuberant; tympanic membrane clearly evident, slightly wider than high, about two thirds of eye length, separated from eye by ca. 85% of its diameter; tympanic annulus distinct except dorsally where it is covered by supratympanic fold; posterior end of supratympanic fold reaches mid arm insertion. Arm slender, axillary membrane present, reaching one third of arm length; three small low tubercles present along ventrolateral edge of forearm; relative length of fingers $I < II < IV < III$; fingers bearing large, oval discs, that of third finger about three fourths of tympanum diameter; subarticular tubercles prominent, round to ovoid, bifid



Figure 17. Adult male *Osteocephalus vilmae* showing variation in dorsal and ventral coloration of preserved specimens. Upper row, from left to right: CORBIDI 5031, CORBIDI 6469, CORBIDI 1086, CORBIDI 4773 (holotype), Peru, Región Loreto, Provincia Datem del Marañón, Jibarito, Capihuari Norte, Andoas, Pampa Hermosa.

in distal subarticular tubercle of Finger IV; supernumerary tubercles present; palmar tubercle small, elongated; prepollical tubercle large, flat, elliptical; prepollex enlarged; large dark keratinous nuptial excrescences covering inner surface of prepollex almost reaching the proximal border of disk of thumb; webbing basal between fingers I and II; webbing formula of fingers I basal II1½—2½III2+—2IV. Medium sized to small tubercles on tibiotarsal articulation; scattered low tubercles on tarsus, more abundant on outer edge; small tubercles scattered along ventrolateral edge of foot; toes bearing discs slightly wider than long, smaller than those of fingers; relative length of toes I<II<V<III<IV; outer metatarsal tubercle ill defined, small, round; inner metatarsal tubercle large, ovoid; sub-articular tubercles single, round, protuberant; supernumerary tubercles restricted to the soles; webbing formula of toes I1—2-II1—2III1—2IV2—1-V. Skin on dorsum, head, and dorsal surfaces of limbs shagreen, with scattered tubercles; minute keratinized conical tubercles present on the eyelids and dorsal surface of head; skin on flanks areolate with big flattened warts; skin on venter coarsely granular; skin on ventral surfaces of head and thighs granular, that on shanks smooth. Cloacal opening directed posteriorly at upper level of thighs; short simple cloacal sheath covering cloacal opening; round tubercles below vent; two distinct white tubercles ventrolateral to vent. Tongue cordiform, widely attached to floor of mouth; dentigerous processes of the vomers angular, adjacent medially, posteromedial to choanae, bearing 9 and 6 (left/right) vomerine teeth; choanae trapezoidal, oblique; vocal slits short and curved posteroventral to the angle of snout at the base of tongue; vocal sac barely distinct above the arm and below the ear.

Color of holotype in preservative. Dorsum brown with a single diffuse interorbital mark; dorsal surfaces of forearms brown with diffuse brown bands; dorsal surfaces of hindlimbs brown with diffuse dark brown marks on shanks and feet. Venter dirty cream with light brown spots, more abundant on posterior half of the body; ventral surfaces of hindlimbs and forelimbs dirty cream without marks but with distinct white tubercles on forearms; outer half of ventral surfaces of forearms dark brown; sides of head light brown with oblique white bar from posteroventral border of orbit to border of jaw, below tympanum; vertical diffuse brown bar below eye, anterior to white bar; area behind white bar and eye dark brown including periphery of tympanum; flanks dirty cream, areolate region with brown reticulation. Iris silver with a brown mid-horizontal line and thin black reticulations.

Color of holotype in life. Based on digital photograph (Fig. 15). Dorsum pale brown without marks; canthal region pale brown with diffuse pale green subocular mark and dark stripe along the posterior half of upper lip; tympanum pink; flanks light green without marks; dorsal surfaces of thighs and tarsus pale brown with greenish brown transversal bands, forearms greenish brown; tibia pale brown without marks; anterior and posterior surfaces of thighs, concealed surfaces of tibia, and metatarsus pale blue. Venter dirty cream with light brown spots, more abundant on posterior half of the body; ventral surfaces of hindlimbs and forelimbs dirty cream. Iris dirty cream with brown transversal midline and black reticulations.

Etymology. The specific name is a patronym for Vilma Duran, in recognition of her continued work and efforts toward the improvement of the herpetological collection of CORBIDI and also for collecting the holotype and tissue of this new species.

Variation. Dorsal and ventral coloration of preserved specimens is shown in Figure 17. Dorsal background coloration varies from light brown to brown; irregular dark brown or dark gray marks are always present (Fig. 17). Flanks are always cream to grayish cream. Two specimens have a cream middorsal line from the tip of the snout to the vent (CORBIDI 06469, QCAZ 51205). The prominence of the tubercles can decrease in preserved specimens: when collected, CORBIDI 01086 had large conspicuous dorsal tubercle, in preservative tubercles are barely noticeable.

Ventral surfaces of preserved specimens (Fig. 17) vary from cream to vanilla. In most specimens, there are dark brown spots, more distinct posteriorly or in the throat (e.g., CORBIDI 06469); ventrally, limbs vary from dirty cream to light brown; all specimens have small white tubercles in the external edge of the forearm. The vent region is gray to brown with dark brown flecks or dots. Flanks are cream to gray, areolate, with dark brown reticulations, dots, and blotches along the entire flank or restricted to the posterior half (e.g. CORBIDI 05031).

Head shape is truncate in dorsal view and truncate in lateral view. Lateral head coloration varies from light brown with dark mottling (CORBIDI 01086) to grayish white with dark brown canthus rostralis and preocular stripes (CORBIDI 05031). All specimens have a white to cream subocular mark. The tympanic annulus is concealed dorsally and has lighter color than the background. The distal subarticular tubercle on Finger IV is bifid in all specimens.

Adult morphometric data are summarized in Table 3. In the examined series, the largest male has a SVL of 55.77 mm; mean male SVL = 50.74 mm ($n = 6$, $SD = 3.17$).

Color in life. Based on a digital photograph of adult male CORBIDI 01086: dorsum light brown with irregular dark brown and light green marks; canthal region greenish brown with white subocular mark and dark brown band along posterior half of upper lip; tympanum pink contrasting with dark brown tympanic annulus; flanks light green with dark brown reticulation anteriorly and few irregular dark brown blotches posteriorly; dorsal surfaces of thighs, shanks and forelimbs brown with dark brown transversal bands; posterior surfaces of thighs light green; venter white speckled with light brown blotches; iris light cream with brown mid-horizontal line and fine black reticulations.

Distribution and ecology. *Osteocephalus vilmae* is known from seven localities in the Peruvian and Ecuadorian Amazon basin (northern Loreto region), four at Río Corrientes (Jibarito, Nuevo Corrientes, Pampa Hermosa, and Shiviayacu), two near Río Pastaza in the border Ecuador-Peru (Andoas and Capahuari Norte) and one at Provincia de Orellana, Pompeya-Iro road (Fig. 2). The elevations of these localities are between 150 to 270 m above sea level. Maximum airline distance between localities is 158 km. The Peruvian localities are dominated by *Terra Firme* forest. Specimens collected in Capahuari Norte were found in a stream surrounded by a mixture of primary and secondary forest. In Jibarito, Pampa Hermosa, and Shiviayacu the frogs were found in primary forest in a swamp close to a stream. All specimens were next to the streams, perching on tree branches 100 to 200 cm above the ground. *Osteocephalus vilmae* occurs sympatrically with *O. buckleyi* at km 80 Pompeya-Iro road. At the Peruvian localities it co-occurs with *O. mutabor* and *O. planiceps*.

Table 5. Character loadings and eigenvalues for Principal Components (PC) I–III. The analysis was based on seven morphometric variables of adult *Osteocephalus buckleyi*, *O. cabrerai*, *O. cannatellai* sp. n., *O. festae*, *O. germani* sp. n., *O. verruciger* and *O. vilmae* sp. n. Bold figures indicate highest loadings.

Variable	PCA Males			PCA Females		
	PC I	PC II	PC III	PC I	PC II	PC III
Femur length	0.557	0.126	0.052	0.553	0.030	0.193
Foot length	0.425	−0.400	0.046	0.451	0.374	−0.106
Head length	0.106	0.459	0.715	−0.004	−0.326	0.649
Head width	0.433	−0.053	−0.480	0.161	0.652	−0.083
Eye diameter	0.173	0.554	−0.332	−0.018	0.349	0.690
Tympanum diameter	0.066	0.540	−0.233	−0.376	0.421	0.201
Tibia length	0.525	−0.108	0.298	0.568	−0.164	0.080
Eigenvalue	2.451	1.432	1.083	2.311	1.768	1.222

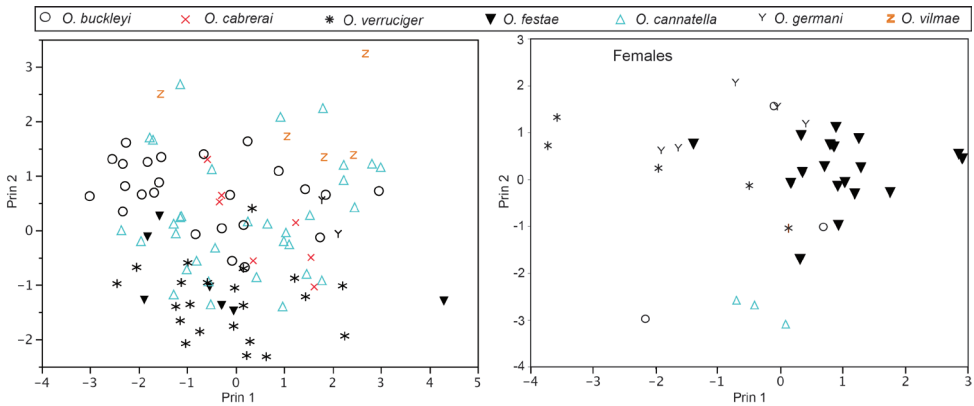


Figure 18. Principal components from analysis of seven size-corrected morphological variables. See Table 5 for character loadings on each component.

Morphometric comparisons among species

Three components with eigenvalues > 1.0, accounting for 70.9% of the total variation, were extracted from the PCA for males (Table 5). The highest loadings were femur length and tibia length for PC I, eye diameter and tympanum diameter for PC II, and head length for PC III (Table 5). Some species pairs have at least partly segregating morphometric spaces: *O. festae*-*O. buckleyi*, *O. festae*-*O. cabrerai*, *O. vilmae*-*O. buckleyi*, and *O. vilmae*-*O. cabrerai* (Fig. 18). *Osteocephalus germani* does not overlap with *O. vilmae*, *O. festae* and *O. cabrerai* but this differentiation requires to be verified with larger sample sizes for *O. germani* (currently *n* = 2). Principal Component I mainly describes hindlimb length (Table 5). There is low interspecies differentiation along PC I. Species with low scores on PC II are *O. festae* and *O. verruciger*; *O. vilmae* has high scores. Pairwise comparisons between *O. festae* and all other species (except *O.*

verruciger) are significant (all P values for t tests < 0.04); *O. verruciger* also shows significant differences with all the remaining species (all P values < 0.004).

Three components with eigenvalues > 1.0 were extracted from the PCA for females (Table 5). The three components accounted for 75.7% of the total variation. The highest loadings for the PCA for females were tibia length and femur length for PC I, head width for PC II, and eye diameter and head length for PC III (Table 5). As in the PCA for males, there is wide overlap in morphometric space among species (Fig. 18). The only exception is *O. cannatellai*, which segregates from the other species along PC II. However, larger sample sizes are required to confirm this differentiation.

In the DFA classification on males, all *O. cabrerai*, *O. festae*, *O. germani*, *O. verruciger*, and *O. vilmae* were correctly classified ($n = 7, 7, 2, 22,$ and 5 respectively). In *O. buckleyi*, 17 out of 24 specimens were correctly classified (4 were misclassified as *O. cabrerai*, 2 as *O. germani*, and 1 as *O. vilmae*); in *O. cannatellai*, only 4 out of 33 specimens were incorrectly classified, 2 as *O. buckleyi* and 2 as *O. vilmae*. Overall, the DFA show morphometric differentiation among the analyzed species. The DFA on females shows even better discrimination because all individuals were correctly assigned to their own species.

Discussion

Similarly to previous studies on Amazonian amphibians (e.g., Elmer et al. 2007; Fouquet et al. 2007; Funk et al. 2011) our results document a large proportion (300% increase) of hidden diversity within a set of populations that were previously treated as a single widely distributed species. Moreover, because most of our sampling was restricted to Ecuador and Peru, it is likely that there are even more species than found in our study. These results highlight the need to carry out large-scale genetic surveys of Amazonian amphibians to achieve a more realistic understanding of their diversity and evolution.

Genetic evidence is a valuable taxonomic tool but, in most cases, is insufficient to define species boundaries without reference to other sets of characters like advertisement calls or external morphology. Taxonomic reviews of Amazonian amphibians suggest that morphological characters are too conservative to define species boundaries because closely related species share similar morphology (e.g., Elmer et al. 2007; Fouquet et al. 2012; Funk et al. 2011; Lougheed et al. 2006; Padial et al. 2009). Our results, however, indicate that in some groups, like the *O. buckleyi* species complex, this is not necessarily the case. The three new species described here are diagnosable with morphological evidence alone and are distinctive from the other species of the complex. Morphological differences are also evident between *O. buckleyi*, *O. cabrerai*, *O. carri*, *O. festae*, and *O. mutabor*. Thus, none of the species of the complex are strictly cryptic (i.e., all of them can be identified using morphological characters) although their diagnosis based on morphology is challenging. Other groups of Amazonian amphibians on which phylogenetic analyses of DNA have led to the discovery of species that turned out to be morphologically distinct are the *Hypsiboas fasciatus-calcaratus* complex (Funk et al. 2011) and the *Pristimantis "ockendeni"* complex (Elmer and Cannatella 2008).

We suspect that the difficulty in defining species boundaries based on morphology arises from the high intraspecific polymorphism in coloration characteristic of most groups of dull-colored Amazonian amphibians like *Osteocephalus* and *Pristimantis* (see for example Fig. 2 in Elmer and Cannatella 2008 and Figs 3, 8, 14, 17 herein). If this is the case, understanding the evolutionary processes that generate and maintain polymorphism in coloration could help to predict which Amazonian taxa are more likely to contain “cryptic” diversity. One plausible process is frequency dependent predation which, occurs when the probability of predation is inversely correlated to the frequency of a given prey type in the population (for a review see Punzalan et al. 2005). Under this scenario, predators use search images to find preys and are better at detecting previously seen prey types because they have learned to find them. Although other processes could also explain polymorphisms (e.g., deferential selection associated with spatial variation in backgrounds), the available evidence suggests that some form of frequency dependent selection is the most likely explanation for color polymorphism in anurans (Milstead et al. 1974; Wells 2007, pp. 715).

Most *Osteocephalus* have a predominantly and highly polymorphic brown coloration and are cryptic against the background where they are found by day (Deichmann 2008; Deichmann and Williamson 2007; SRR pers. obs.) If polymorphisms are an adaptation to avoid falling into search categories of visually oriented predators, the difficulties of species delimitation based on morphological characters could be a byproduct of this selective pressure. This hypothesis needs to be tested empirically because if verified it could help to understand why several groups of Neotropical amphibians contain a large proportion of cryptic species.

Biogeography and speciation

Examination of the geographic ranges of sister species can provide insights into modes of speciation. Our phylogeny of the *O. buckleyi* species complex recovered four sister species pairs of which one is sympatric (*O. buckleyi*-*O. vilmae*) and three are allopatric. Among the allopatric pairs, two involve a lowland species sister to a highland species. *Osteocephalus mutabor* occurs at lower altitudes (range 230–1240 m) than its sister species, *O. festae* (860–2383 m). Similarly, *O. cannatellai* has a lower distribution (200–1290 m) than its sister species, *O. verruciger* (950–2120 m). Because most species of *Osteocephalus* are restricted to elevations below 1000 m, the distributions of *O. festae* and *O. verruciger* probably represent parallel and recent colonization events from the lowlands. This geographic pattern suggests that speciation has been a result of ecological mediated selection along an altitudinal gradient. Interestingly, both highland species resemble each other closely in external morphology (Figs 15 and 18) suggesting convergence as a byproduct of adaptation to similar environments. Speciation associated with ecological divergence along altitudinal gradients was also reported by Graham et al. (2004) in dendrobatid frogs and more recently by Salerno et al. (2012) between *Tepuihyla* and its sister lowland species, “*Osteocephalus*” *exophthalmus*.

At the intraspecific level, we found low genetic divergence with the only exception of *Osteocephalus festae* (up to 2.8% of uncorrected *p* distance in gene 12S). We also

found a concordant geographic pattern of divergence in *O. buckleyi* and *O. mutabor* because in both the most divergent population was the most northern of them, in the Cuyabeno region. High divergence of samples from Cuyabeno relative to others to the south was also reported for *Pristimantis kichwarum* (Elmer and Cannatella 2008). Samples of *O. mutabor*, *O. buckleyi* (*sensu stricto*) and *O. cannatellai* show genetic structure generally congruent with geography (i.e., geographically close localities tend to be genetically similar). Overall, our intraspecific sampling reveals low levels of genetic differentiation and genetic variation geographically structured.

Acknowledgments

This study was supported by grants from the Secretaría Nacional de Educación Superior, Ciencia, Tecnología e Innovación de Ecuador SENESCYT (PI-C08-0000470) and Dirección General Académica of Pontificia Universidad Católica del Ecuador. For the loan of specimens and access to collections we are indebted to A. Almendáriz and Barry Clarke. Santiago Castroviejo y J. M. Padial provided tissues of Colombian *O. cabrerai*. William E. Duellman shared information on type material. Ministerio de Ambiente of Ecuador and the Dirección General Forestal y Fauna Silvestre (DGFFS) of Peru issued collection permits. PJVs fieldwork in northern Loreto was part of the Rapid Biological Inventories led by the Field Museum, Chicago. PJV is grateful to Programa de Monitoreo Biológico COGA, Transportadora de Gas del Peru (TGP), and Knight Piesold Consultores S.A. for support of the fieldwork where *Osteocephalus germani* were collected. We are indebted to A. Catenazzi, A. Delgado, C. Landauro, G. Chavez, J. C. Chaparro, M. Cuyos, V. Duran, J. Delia, D. Acosta-López, S. Aldás-Alarcón, A. Almendáriz, L. Bustamante, L. A. Coloma, P. Peña-Loyola, N. Peñafiel, D. Almeida-Reinoso, J. Brito-Molina, K. Elmer, S. North, D. Salarzar, I. G. Tapia, and R. Tarvin for providing specimens and photos. Centro Científico Zanjarauno and Estación Científica Yasuní of Universidad Católica del Ecuador provided accommodation during fieldwork. Daniel Moen kindly gave advice on laboratory protocols. Rebecca Tarvin and P. Peña-Loyola provided audio recordings of *O. cannatellai*. Diego Paucar made a drawing of the holotype and P. Santiana helped to prepare illustrations. Open access to this paper was supported by the Encyclopedia of Life (EOL) Open Access Support Project (EOASP).

References

- Bass MS, Finer M, Jenkins CN, Kreft H, Cisneros-Heredia DF, McCracken SF, Pitman NC, English PH, Swing K, Villa G, Di Fiore A, Voigt CC, Kunz TH (2010) Global conservation significance of Ecuador's Yasuni National Park. *Plos One* 5: e8767. doi: 10.1371/journal.pone.0008767
- Boulenger GA (1882) Catalogue of the Batrachia Salientia. Ecaudata in the Collection of the British Museum. British Museum, London.

- Brandley MC, Schmitz A, Reeder TW (2005) Partitioned Bayesian analyses, partition choice, and the phylogenetic relationships of scincid lizards. *Systematic Biology* 54: 373–390. doi: 10.1080/10635150590946808
- Cerón C, Palacios W, Valencia R, Sierra R (1999) Las formaciones naturales de la Costa del Ecuador. In: Sierra R (Ed) Propuesta preliminar de un sistema de clasificación de vegetación para el Ecuador continental. Proyecto INEFAN/GERF-BIRF y Ecociencia, Quito.
- Charif RA, Clark CW, Frstrup KM (2004) Raven 1.2 User's Manual. Cornell Laboratory of Ornithology, Ithaca, NY, USA.
- Cochran DM, Goin CJ (1970) Frogs of Colombia. United States National Museum Bulletin 288: 1–655. doi: 10.5479/si.03629236.288.1
- Crump ML (1974) Reproductive strategies in a Tropical Anuran Community. Miscellaneous Publications Museum of Natural History University of Kansas 61: 1–68.
- Darst CR, Cannatella DC (2004) Novel relationships among hyloid frogs inferred from 12S and 16S mitochondrial DNA sequences. *Molecular Phylogenetics and Evolution* 31: 462–475. doi: 10.1016/j.ympev.2003.09.003
- Deichmann JL (2008) *Osteocephalus oophagus* (NCN). Terrestrial behavior. *Herpetological Review* 39: 338–339.
- Deichmann JL, Williamson GB (2007) *Osteocephalus yasuni* (NCN) and *Osteocephalus planiceps* (NCN). Terrestrial behavior. *Herpetological Review* 38: 189.
- Duellman WE (1970) Hylid frogs of Middle America. Monograph of the Museum of Natural History University of Kansas 1: 1–753. doi: 10.5962/bhl.title.2835
- Duellman WE, Mendelson JR (1995) Amphibians and reptiles from northern Departamento Loreto, Peru: taxonomy and biogeography. *University of Kansas Science Bulletin* 55: 329–376.
- Edwards SV, Liu L, Pearl DK (2007) High-resolution species trees without concatenation. *Proceedings of the National Academy of Sciences of the United States of America* 104: 5936–4941. doi: 10.1073/pnas.0607004104
- Elmer KR, Cannatella DC (2008) Three new species of leaf litter frogs from the upper Amazon forests: cryptic diversity within *Pristimantis "ockendeni"* (Anura: Strabomantidae) in Ecuador. *Zootaxa* 1784: 11–38.
- Elmer KR, Davila JA, Lougheed SC (2007) Cryptic diversity and deep divergence in an upper Amazonian leaf litter frog, *Eleutherodactylus ockendeni*. *BMC Evolutionary Biology* 7: 247. doi: 10.1186/1471-2148-7-247
- Faivovich J, Haddad CFB, Garcia PCA, Frost DR, Campbell JA, Wheeler WC (2005) Systematic review of the frog family Hylidae, with special reference to Hylinae: phylogenetic analysis and taxonomic revision. *Bulletin of the American Museum of Natural History* 294: 6–228. doi: 10.1206/0003-0090(2005)294[0001:SROTFF]2.0.CO;2
- Fouquet A, Gilles A, Vences M, Marty C, Blanc M, Gemmell NJ (2007) Underestimation of species richness in neotropical frogs revealed by mtDNA analyses. *Plos Biology* 2: e1109. doi: 10.1371/journal.pone.0001109
- Fouquet A, Recoder R, Teixeira M, Cassimiro J, Amaro RC, Camacho A, Damasceno R, Carnaval AC, Moritz C, Rodriguez MT (2012) Molecular phylogeny and morphometric analyses reveal deep divergence between Amazonia and Atlantic forest species of *Dendrobrynisus*. *Molecular Phylogenetics and Evolution* 62: 826–838. doi: 10.1016/j.ympev.2011.11.023

- Frost DR (2010) Amphibian Species of the World: an Online Reference v. 5.4. <http://research.amnh.org/vz/herpetology/amphibia/> [accessed 8-04-2010]
- Funk WC, Caminer M, Ron SR (2011) High levels of cryptic species diversity uncovered in Amazonian frogs. *Proceedings of the Royal Society B-Biological Sciences* 279: 1806–1814 doi: 10.1098/rspb.2011.1653
- Gaige HT (1929) Three new tree-frogs from Panama and Bolivia. *Occasional Papers of the Museum of Zoology, University of Michigan* 207: 1–6.
- Goebel AM, Donnelly MA, Atz M (1999) PCR primers and amplification methods for 12S ribosomal DNA, the control region, cytochrome oxidase I, and cytochrome b in bufonids and other frogs, and an overview of PCR primers which have amplified DNA in amphibians successfully. *Molecular Phylogenetics and Evolution* 11: 163–199. doi: 10.1006/mpev.1998.0538
- Graham CH, Ron SR, Santos JC, Schneider CJ, Moritz C (2004) Integrating phylogenetics and environmental niche models to explore speciation mechanisms in dendrobatid frogs. *Evolution* 58: 1781–1793. doi: 10.1554/03-274
- Jungfer KH (2010) The taxonomic status of some spiny-backed treefrogs, genus *Osteocephalus* (Amphibia: Anura: Hylidae). *Zootaxa* 2407: 28–50.
- Jungfer KH (2011) A new tree frog of the genus *Osteocephalus* from high altitudes in the Cordillera del Cóndor, Ecuador (Amphibia: Anura: Hylidae). *Herpetological Journal* 21: 247–253.
- Jungfer KH, Hödl W (2002) A new species of *Osteocephalus* from Ecuador and a redescription of *O. lepreurii* (Duméril & Bibron, 1841) (Anura: Hylidae). *Amphibia-Reptilia* 23: 21–46. doi: 10.1163/156853802320877609
- Jungfer KH, Lehr E (2001) A new species of *Osteocephalus* with bicoloured iris from Pozuzo (Peru: Departamento de Pasco) (Amphibia: Anura: Hylidae). *Zoologische Abhandlungen Staatliches Museum für Tierkunde Dresden* 19: 321–329.
- Jungfer KH, Weygoldt P (1999) Biparental care in the tadpole-feeding Amazonian treefrog *Osteocephalus oophagus*. *Amphibia-Reptilia* 20: 235–249. doi: 10.1163/156853899507040
- Katoh K, Misawa K, Kuma K, Miyata T (2002) MAFFT: a novel method for rapid multiple sequence alignment based on fast Fourier transform. *Nucleic Acids Research* 30: 3059–3066. doi: 10.1093/nar/gkf436
- Lougheed SC, Austin JD, Bogart JP, Boag PT, Chek AA (2006) Multi-character perspectives on the evolution of intraspecific differentiation in a neotropical hylid frog. *BMC Evolutionary Biology* 6: 23. doi: 10.1186/1471-2148-6-23
- Lynch JD (2002) A new species of the genus *Osteocephalus* (Hylidae: Anura) from the Western Amazon. *Revista de la Academia Colombiana de Ciencias Exactas, Físicas, y Naturales* 26: 289–292.
- Lynch JD (2006) The amphibian fauna in the Villavicencio region of eastern Colombia. *Caldasia* 28: 135–155.
- Lynch JD, Duellman WE (1997) Frogs of the genus *Eleutherodactylus* in Western Ecuador. *Special Publication The University of Kansas Natural History Museum* 23: 1–236. doi: 10.5962/bhl.title.7951

- Maddison WP, Maddison DR (2009) Mesquite: a modular system for evolutionary analysis. Version 2.72. <http://mesquiteproject.org>
- Milstead WW, Rand AS, Stewart MM (1974) Polymorphism in cricket frogs: an hypothesis. *Evolution* 28: 489–491. doi: 10.2307/2407175
- Moen DS, Wiens JJ (2009) Phylogenetic evidence for competitively driven divergence: body-size evolution in Caribbean treefrogs (Hylidae: *Osteopilus*). *Evolution* 63: 195–214. doi: 10.1111/j.1558-5646.2008.00538.x
- Moravec J, Aparicio J, Guerrero-Reinhard M, Calderón G, Jungfer KH, Gvozdík V (2009) A new species of *Osteocephalus* (Anura: Hylidae) from Amazonian Bolivia: first evidence of tree frog breeding in fruit capsules of the Brazil nut tree. *Zootaxa* 2215: 37–54.
- Myers CW, Duellman WE (1982) A new species of *Hyla* from Cerro Colorado, and other tree frog records and geographical notes from Western Panama. *American Museum Novitates* 2752: 1–32.
- ONERN (1976) Mapa Ecológico del Perú. Guía Explicativa. Oficina Nacional de Evaluación de Recursos Naturales (ONERN), Lima.
- Padial JM, Castroviejo-Fisher S, Köhler J, Vilá C, Chaparro JC, De la Riva I (2009) Deciphering the products of evolution at the species level: the need for an integrative taxonomy. *Zoologica Scripta* 38: 431–447. doi: 10.1111/j.1463-6409.2008.00381.x
- Padial JM, De la Riva I (2009) Integrative taxonomy reveals cryptic Amazonian species of *Pristimantis* (Anura: Strabomantidae). *Zoological Journal of the Linnean Society* 155: 97–122. doi: 10.1111/j.1096-3642.2008.00424.x
- Peracca MG (1904) Viaggio del Dr. Enrico Festa nell'Ecuador e regioni vicine. *Bollettino dei Musei di Zoologia ed Anatomia comparata, Università di Torino* 465: 1–41.
- Posada D (2008) Phylogenetic model averaging. *Molecular Biology and Evolution* 25: 1253–1256. doi: 10.1093/molbev/msn083
- Punzalan D, Rodd FH, Hughes KA (2005) Perceptual processes and the maintenance of polymorphism through frequency-dependent predation. *Evolutionary Ecology* 19: 303–320. doi: 10.1007/s10682-005-2777-z
- Rambaut A, Drummond AJ (2007) Tracer v1.4. University of Edinburgh. Available from <http://beast.bio.ed.ac.uk/Tracer>
- Ron SR, Santos JC, Cannatella DC (2006) Phylogeny of the túngara frog genus *Engystomops* (= *Physalaemus pustulosus* species group; Anura; Leptodactylidae). *Molecular Phylogenetics and Evolution* 39: 392–403. doi: 10.1016/j.ympev.2005.11.022
- Ron SR, Toral E, Venegas PJ, Barnes CW (2010) Taxonomic revision and phylogenetic position of *Osteocephalus festae* (Anura: Hylidae) with description of its larva. *ZooKeys* 70: 67–92. doi: 10.3897/zookeys.70.765
- Ronquist F, Teslenko M, van der Mark P, Ayres DL, Darling A, Höhna S, Larget B, Liu L, Suchard MA, Huelsenbeck JP (2012) MrBayes 3.2: efficient bayesian phylogenetic inference and model choice across a large model space. *Systematic Biology* 61(3): 539–542. doi: 10.1093/sysbio/sys1029
- Salducci MD, Marty C, Chappaz R, Gilles A (2002) Molecular phylogeny of French Guiana Hylinae: implications for the systematic and biodiversity of the Neotropical frogs. *Comptes Rendus Biologies* 325: 141–153. doi: 10.1016/S1631-0691(02)01423-3

- Salducci MD, Marty C, Fouquet A, Gilles A (2005) Phylogenetic relationships and biodiversity in Hylids (Anura: Hylidae) from French Guiana. *Comptes Rendus Biologies* 328: 1009–1024. doi: 10.1016/j.crv.2005.07.005
- Salerno PE, Ron SR, Señaris JC, Rojas-Runjaic FJM, Noonan BP, Cannatella DC (2012) Ancient Tepui summits harbor young rather than old lineages of endemic frogs. *Evolution* 66: 3000–3013. doi: 10.1111/j.1558-5646.2012.01666.x
- Sambrook J, Fritsch EF, Maniatis T (1989) *Molecular Cloning: a Laboratory Manual*. Cold Spring Harbor Laboratory Press, New York, USA.
- SAS Institute (2008) *User guide. Version 8.01*. SAS Institute, Cary.
- Sierra R, Cerón C, Palacios W, Valencia R (1999) Mapa de vegetación del Ecuador Continental 1:1'000.000. Proyecto INEFAN/GEF-BIRF, Wildlife Conservation Society y Ecociencia, Quito.
- Simmons JE (2002) Herpetological collecting and collection management. *Herpetological Circular* 31: 1–153.
- Smith EN, Noonan BP (2001) A new species of *Osteocephalus* (Anura: Hylidae) from Guyana. *Revista de Biología Tropical* 49: 347–357.
- Trueb L, Duellman WE (1971) A synopsis of Neotropical hylid frogs, genus *Osteocephalus*. *Occasional Papers of the Museum of Natural History University of Kansas* 1: 1–47.
- Wells KD (2007) *The Ecology and Behavior of Amphibians*. The University of Chicago Press, London.
- Werner F (1901) Über Reptilien und Batrachier aus Ecuador und Neu-Ginea. *Verhandlungen des Zoologisch-Botanischen Vereins in Wien* 50: 593–614.
- Wiens JJ, Morrill MC (2011) Missing data in phylogenetic analysis: reconciling results from simulations and empirical data. *Systematic Biology* 60(5): 719–731. doi: 10.1093/sysbio/syr025
- Wiens JJ, Fetzner JW, Parkinson CL, Reeder TW (2005) Hylid frog phylogeny and sampling strategies for speciose clades. *Systematic Biology* 54: 778–807. doi: 10.1080/10635150500234625
- Wiens JJ, Graham CH, Moen DS, Smith SA, Reeder TW (2006) Evolutionary and ecological causes of the latitudinal diversity gradient in hylid frogs: treefrog trees unearth the roots of high tropical diversity. *American Naturalist* 168: 579–596. doi: 10.1086/507882
- Wiens JJ, Kuczynski CA, Hua X, Moen DS (2010) An expanded phylogeny of treefrogs (Hylidae) based on nuclear and mitochondrial sequence data. *Molecular Phylogenetics and Evolution* 55: 871–882. doi: 10.1016/j.ympev.2010.03.013

Appendix I

Osteocephalus alboguttatus. ECUADOR: PROVINCIA PASTAZA: Canelos (QCAZ 15981).

Osteocephalus buckleyi. ECUADOR: PROVINCIA NAPO: Cando, 700 m (QCAZ 24446–48); Cabañas Pimpilalo, 600 m (QCAZ 23043); Ahuano, 410 m (QCAZ 36703); Jatun Sacha, 420 m (QCAZ 2876, 48093, 48827); Serena, Río Jatun-yacu, 520 m (QCAZ 25321); Tena, 550 m (QCAZ 8809–10); Juan Pablo II, Río Punino, 360 m (EPN-H 5476); Santa Rosa de Arapino, 570 m (EPN-H 6209); Nuevo Rocafuerte, Bloque 3, Pozo PCSA 1, 210 m (EPN-H 6516); PROVINCIA ORELLANA: El Edén, 235 m (QCAZ 33148); Río Yasuní (QCAZ 7360); Puente del Río Beque, 228 m (QCAZ 43071); Río Rumiyacu, Parque Nacional Yasuní, 250 m (QCAZ 16007); Taracoa, 251 m (QCAZ 34963); Aguarico, Parque Nacional Yasuní, Pozo Ewa, 320 m (EPN-H 2785–87); Pozo Sunka, 279 m (EPN-H 2757–58); Dayuano, Cotapino, 500 m (EPN-H 7471); Guiyero, 248 m (EPN-H 10909); Comuna Huatarco, Pozo Chonta, 300 m (EPN-H 11710, 11717–18); PROVINCIA PASTAZA: Canelos, 650 m, (BMNH 1947.2.13.44; lectotype); Tarangaro, 338 m (QCAZ 39073–74, 39081–82, 39146, 39172, 39191); Villano, 380 m (QCAZ 38503, 38704–05, 38713, 39285); Kurintza, 380 m (QCAZ 39033); PROVINCIA SUCUMBÍOS: Tarapoa (QCAZ 14948); Puerto Bolívar, 240 m (QCAZ 28231); Playas de Cuyabeno, 230 m (QCAZ 28277, 28280, 28395); Tarapoa-Puerto Carmen road, bridge over Río Cuyabeno, 290 m (QCAZ 28427); Comuna Shuar Chari, 280 m (EPN-H 4875); Cascales, Pozo Diamante, 410 m (EPN-H 5418, 5475); La Barquilla (EPN-H 7524–26); PERU: REGION LORETO: PROVINCIA DE REQUENA: Sierra del Divisor, 500 m (CORBIDI 03747); PROVINCIA DATEM DEL MARAÑÓN: Singasapa, 186 m (CORBIDI 06522); Sargento Puño, 206 m (CORBIDI 07458–59, 07462, 07473, 07516, 07558, 07560, 08675, 08714); PROVINCIA DE MAYNAS: Río Momon-San Luis de Vista Alegre (Puchana), 108 m (CORBIDI 2980–81).

Osteocephalus cabrerai. ECUADOR: PROVINCIA SUCUMBÍOS: Cuyabeno, Campamento Concienti, 260 m (EPN-H 7201–5); Puerto Bolívar, 240 m (QCAZ 27923, 28231); Campamento Guepicillo, 220 m (CORBIDI 00119–22, 00200); PERU: REGION LORETO: PROVINCIA DE REQUENA: Sierra del Divisor, 500 m (CORBIDI 02452, 02632, 05064); PROVINCIA DE MAYNAS: Gueppi, 220 m (CORBIDI 00199); Río Yanayacu, Campamento Curupa, 125 m (CORBIDI 05819–21, 05831).

Osteocephalus deridens. ECUADOR: PROVINCIA ORELLANA: Estación Científica Yasuní, Universidad Católica del Ecuador, Parque Nacional Yasuní (QCAZ 12556).

Osteocephalus festae. ECUADOR: PROVINCIA LOJA: San Francisco, Arco Iris Reserve, Parque Nacional Podocarpus (3.9884°S, 79.0930°W), 2200 m (QCAZ 39364); PROVINCIA MORONA SANTIAGO: Río Napinaza, 6.6 km N from General Leonidas Plaza (Limón) in the road to Mendez (2.9266°S, 78.4070°W), 1010 m (QCAZ 26283, 26304, 26488, 26552, 26561, 32835, 38081, 38420,

39799, 39804–6, 39798–803, 39808–12); San Carlos, San Miguel and Río Oro, 600–1200 m (QCAZ 11624–26); PROVINCIA ZAMORA CHINCHIPE: Miasí Alto (4.2502°S, 78.6174°W), 1250–1300 m (QCAZ 41039); Reserva Tapichalaca (4.5500°S, 79.1291°W), 1637 m (QCAZ 45674); PERU: REGIÓN DE AMAZONAS: PROVINCIA DE BAGUA: Cataratas de Paraiso-Chonza Alta (5.6026°S, 78.398°W), 1342 m (CORBIDI 760–64, 758–59); Camñopite (5.6147°S, 78.3319°W), 1650 m (CORBIDI 1962–65, 2992); PROVINCIA DE BONGARA: Quebrada Goca (on Yambrasbamba road) (5.7641°S, 77.9129°W), 1711 m (CORBIDI 10461); PROVINCIA DE YAMBRASBAMBA: Quebrada Goca (on Yambrasbamba road) (5.7641°S, 77.9129°W), 1711 m (CORBIDI 10461); REGIÓN DE SAN MARTÍN: PROVINCIA MARISCAL CACERES: Río Lejía (6.8365°S, 77.4860°W), 1500 m (CORBIDI 623, 624); PROVINCIA RIOJA: Bajo Naranjillo (5.8157°S, 77.3367°W), 844 m (CORBIDI 3386); PROVINCIA LAMAS: Cataratas de Ahuashiyacu (6.4174°S, 76.2893°W), 600 m (CORBIDI 09585, 09587).

Osteocephalus fuscifacies. ECUADOR: PROVINCIA NAPO: El Tena-Talag Road, 15 km from Tena, 550 m (QCAZ 8806); PROVINCIA ORELLANA: Pompeya-Iro Road, 38 km SE from Pompeya (QCAZ 8137); Estación Científica Yasuní, Universidad Católica del Ecuador, 240 m (QCAZ 20785).

Osteocephalus leoniae. —PERU: REGIÓN CUSCO: Provincia La Convención: Tangoshiari, 1135 m (CORBIDI 00306); REGIÓN SAN MARTIN: Provincia de Rioja: El Dorado, 844 m (CORBIDI 01415).

Osteocephalus mutabor. ECUADOR: PROVINCIA MORONA SANTIAGO: Cantón Morona, Nuevo Israel, 1290 m (QCAZ 46470–71); PROVINCIA NAPO: Chontapuntas, Comunidad Sumak Sacha-Pozo Yuralpa Centro 1 (QCAZ 28646–48); Huino, around the waterfall (QCAZ 30916–17, 30919–20, 30922–23, 30925–26); PROVINCIA ORELLANA: km 22 Pompeya-Iro Road, 287 m (QCAZ 42999); PROVINCIA PASTAZA: Pomona, Fundación Hola Vida, 846 m (QCAZ 25603, 25684); Cantón Santa Clara, Río Pucayacu, Colonia Mariscal Sucre (QCAZ 29430, 36935, 36946, 40253); Canelos (QCAZ 41030); PROVINCIA SUCUMBIOS: Puerto Bolívar, 240 m (QCAZ 28223). PERU: REGION LORETO, Provincia Loreto: Andoas, 187 m, (CORBIDI 04645); REGION AMAZONAS: Cordillera de Kampankis (CORBIDI 09369).

Osteocephalus planiceps. ECUADOR: PROVINCIA DE NAPO: Chontapuntas, Comunidad Sumak Sacha-Pozo Yuralpa Centro 1 (QCAZ 28648); PROVINCIA ORELLANA: Parque Nacional Yasuní, km 38 Pompeya-Iro Road, 280 m (QCAZ 5134, 14842); Estación Científica Yasuní, Universidad Católica del Ecuador, 240 m (QCAZ 14844, 20797–800); PROVINCIA SUCUMBIOS: La Selva lodge, 250 m (QCAZ 7408, 12093–95).

Osteocephalus taurinus. ECUADOR: PROVINCIA ORELLANA: Parque Nacional Yasuní, km 97 Pompeya-Iro road, 450 m (QCAZ 5301); Estación Científica Yasuní, Universidad Católica del Ecuador, 220 m (QCAZ 9007, 10604, 14804, 14954, 24449–50); PROVINCIA SUCUMBIOS: Reserva de Producción Faunís-

tica Cuyabeno, 220 m (QCAZ 5871–77); Puerto Bolívar, 240 m (QCAZ 27916, 27920); Zábalo, 220 m (QCAZ 27982, 28015); Chiritza-Puerto El Carmen road, bridge over Río Aguas Negras, 270 m (QCAZ 28485); Tarapoa-Puerto El Carmen road, bridge over Río Cuyabeno, 290 m (QCAZ 28435–36); PROVINCIA ZAMORA CHINCHIPE: Shaime, Nangaritza, 980 m (QCAZ 18230).

Osteocephalus verruciger. ECUADOR: PROVINCIA MORONA SANTIAGO: Nueve de Octubre (QCAZ 32266); Bosque Protector Abanico, Morona, 1647 m (EPN-H 11444); Morona, 1530 m (EPN-H 11445); Río Sardinayacu, Palora, Parque Nacional Sangay, 1600 m (EPN-H 5940–42, 5947); PROVINCIA NAPO: near Santa Rosa de Quijos, 1661 m (QCAZ 45344); E of Volcán Sumaco, 1570 m (QCAZ 1560, 1562); Nueva Loja road between Cascabel 1 and 2, 1600 m (QCAZ 7783–84); Río Salado (QCAZ 17285); Sumaco, 1800–2100 m (QCAZ 8964); Pacto Sumaco (QCAZ 10907); km 13 Loreto-Coca road, 1324 m (QCAZ 22201); Río Hollín (QCAZ 1681, 2405); Cordillera de los Guacamayos, Cosanga-Archidona road, 1600 m (QCAZ 12206, 41108); El Reventador (QCAZ 29208); Cascada San Rafael, 1553 m (QCAZ 363, 13225, 13247, 16954, 32032–36); Cosanga, 339 m (QCAZ 15942); PROVINCIA SUCUMBIOS: Quito-Lago Agrio road, Río Azuela, 1680 m (QCAZ 15149, 15991–97, 16220, 16953, 22497, EPN-H 6341, 11987, 12105–07, 12112, 12143); La Bonita (QCAZ 3175); Rosa Florida, 1185 m (QCAZ 20544); trail to Volcán Reventador, Gonzalo Pizarro, 1800 m (EPN-H 7052–53, 7059–60); PERU: REGIÓN DE AMAZONAS: Provincia Condorcanqui: Cabecera de la Quebrada Katerpiza, 1100 m (CORBIDI 09477); REGIÓN DE LORETO: Provincia Datem del Marañón: Cabecera de la Quebrada Wee, 1000 m (CORBIDI 09525).

Osteocephalus yasuni. ECUADOR: PROVINCIA SUCUMBIOS: Zábalo, 220 m (QCAZ 27998); Playas de Cuyabeno, 230 m (QCAZ 27816).

Trachycephalus jordani. ECUADOR: PROVINCIA EL ORO: Bosque Protector Puyango (QCAZ 35405).

Trachycephalus typhonius. ECUADOR: PROVINCIA PASTAZA: km 6 San Ramón-El Triunfo road, Colonia Mariscal Sucre, trail to Río Pucayaku (QCAZ 38075).

Revision of the freshwater genus *Atyaephyra* (Crustacea, Decapoda, Atyidae) based on morphological and molecular data

Magdalini Christodoulou^{1†}, Aglaia Antoniou^{2‡},
Antonios Magoulas^{2§}, Athanasios Koukouras^{1|}

1 Department of Zoology, School of Biology, Aristotle University of Thessaloniki, 54124 Thessaloniki, Macedonia, Greece **2** Institute of Marine Biology and Genetics, Hellenic Centre for Marine Research, Gournes Pediados, 71003, Heraklion, Crete, Greece

† [urn:lsid:zoobank.org:author:9C51EB19-3625-4BD3-9049-33B709EDEFEF](https://zoobank.org/urn:lsid:zoobank.org:author:9C51EB19-3625-4BD3-9049-33B709EDEFEF)

‡ [urn:lsid:zoobank.org:author:A9891030-7E7F-41EF-8970-BA949B002BA7](https://zoobank.org/urn:lsid:zoobank.org:author:A9891030-7E7F-41EF-8970-BA949B002BA7)

§ [urn:lsid:zoobank.org:author:17EED3B5-B7F5-4665-B97E-A0C729258224](https://zoobank.org/urn:lsid:zoobank.org:author:17EED3B5-B7F5-4665-B97E-A0C729258224)

| [urn:lsid:zoobank.org:author:BEF5A889-9F46-4212-92CC-52FFBA25E250](https://zoobank.org/urn:lsid:zoobank.org:author:BEF5A889-9F46-4212-92CC-52FFBA25E250)

Corresponding author: Magdalini Christodoulou (magchris@bio.auth.gr)

Academic editor: Niel Bruce | Received 30 August 2012 | Accepted 12 October 2012 | Published 19 October 2012

[urn:lsid:zoobank.org:pub:5F529BC5-C0D6-4F36-B9C7-D19BC139BEA4](https://zoobank.org/urn:lsid:zoobank.org:pub:5F529BC5-C0D6-4F36-B9C7-D19BC139BEA4)

Citation: Christodoulou M, Antoniou A, Magoulas A, Koukouras A (2012) Revision of the freshwater genus *Atyaephyra* (Crustacea, Decapoda, Atyidae) based on morphological and molecular data. ZooKeys 229: 53–110. doi: 10.3897/zookeys.229.3919

Abstract

Atyaephyra de Brito Capello, 1867 was described from the Mediterranean region almost 200 years ago. Since then, the genus has been recorded from various freshwater habitats in Europe, North Africa and the Middle East. Despite its long history, the taxonomic status of *Atyaephyra* species remains confusing and uncertain. Consequently numerous specimens from the known range of *Atyaephyra* were analysed using morphological characters and mitochondrial COI sequences in an attempt to clarify the taxonomy of this genus. The present study recognises seven *Atyaephyra* species, more than twice as many as previously recorded (three), four of which are considered as new. The new species are described, additional information to the original descriptions are provided for the remaining three taxa, while neotypes of *A. desmarestii* Millet, 1831 and *A. stankoi* Karaman, 1972 are designated to stabilize their taxonomy. Non-overlapping distinguishing morphological characters are used to discriminate the examined material into five species, e.g., *A. desmarestii*, *A. stankoi*, *A. orientalis* Bouvier, 1913, *A. thymensis* **sp. n.**, *A. strymonensis* **sp. n.** In

addition, the genetic analysis supports the existence of multiple phylogenetic clades in the broader Mediterranean area and distinguishes two new cryptic species, namely *A. tuerkayi* sp. n. and *A. acheronensis* sp. n. The geographic distribution of these species is confirmed and their phylogenetic relationships are described.

Keywords

Atyidae, *Atyaephyra*, new species, cryptic species, COI, freshwater shrimp, molecular data, morphology, taxonomy

Introduction

Atyidae is one of the most diverse shrimp families comprising at least 469 valid species (De Grave and Fransen 2011) being found in freshwater habitats world-wide with the exception of Antarctica. However, this high number of species is probably an underestimate of the family's species richness. The latter becomes evident given the current indication of numerous, yet undescribed species, many of which being characterized as cryptic (Cook et al. 2006, Page and Hughes 2007, Page et al. 2008, Cook et al. 2008) and pending further research to be confirmed or not as such. Currently, 43 atyid genera (De Grave and Fransen 2011, Richard et al. 2012) have been established, five of which (*Atyaephyra* de Brito Capello, 1867, *Dugastella* Bouvier, 1912, *Gallocaris* Sket and Zakšek, 2009, *Typhlatya* Creaser, 1936, *Troglocaris* Dormitzer, 1853) are found in the broader Mediterranean region.

Atyaephyra is the most widespread atyid taxon in the Mediterranean region with its native range spanning from the Middle East to North Africa, a large part of Southern Europe and to some Mediterranean islands (Corsica, Sardinia, Sicily) (d' Udekem d' Acoz 1999). Furthermore, it has been introduced into North and Central Europe through river canals opened in France (e.g. Dhur and Massard 1995, Moog et al. 1999, Grabowski et al. 2005, Straka and Špaček 2009).

Atyaephyra was first reported in the Mediterranean region almost 200 years ago (Rafinesque 1814) and like most of old taxa has a very confused taxonomic history. The oldest species of *Atyaephyra* (*A. desmarestii*) and only one until recently, was first described by Rafinesque (1814) as *Symethus fluviatilis*, based on material most likely collected from Simeto River in Sicily (Holthuis 1993). In 1831, Millet after studying material from the rivers of the Maine and Loire area (France) thought he found a different species which he described and named *Hippolyte desmarestii*. Joly (1843) stated that Millet erroneously placed the new species in the genus *Hippolyte* Leach, 1814 and transferred it to the genus *Caridina* H. Milne Edwards, 1837. A few years later, de Brito Capello (1867) described a new genus and a species named *Atyaephyra rosiana* from material collected from the surroundings of Coimbra (Portugal) most probably from the River Mondego that crosses the city or from one of its tributaries. Ortman (1890) assigned the species *Caridina desmarestii* to a new genus named *Hemicaridina*. However some years later, he realized that the species *Atyaephyra rosiana* and *Hemicaridina desmarestii* were actually the same and thus proposed a new name combination of this species and established *Atyaephyra desmarestii*.

In the beginning of the 20th century, Bouvier (1913) described two varieties of *A. desmarestii*: (a) a western variety named *A. desmarestii* var. *occidentalis* Bouvier, 1913, distributed in North Africa up to Tunisia, and the entire area of Southern Europe, up to and including Macedonia; (b) an eastern one, *A. desmarestii* var. *orientalis* Bouvier, 1913, found in Syria. Fifty years later, these two forms were elevated to subspecies level by Holthuis (1961) and since *A. d.* var. *occidentalis* contained the name-bearing type of the species it was re-named to *A. d. desmarestii*. A third subspecies, *A. d. stankoi*, was described by Karaman (1972) from Doirani Lake which is situated at the borders between Greece and Former Yugoslav Republic of Macedonia (F.Y.R.O.M.). Finally, Al-Adhub (1987) described *A. d. mesopotamica* from Shatt Al-Arab River and Hammar Lake (Iraq) thus increasing the number of subspecies to four.

Subsequent studies (Gorgin 1996, Anastasiadou et al. 2004) questioned the validity of these four subspecies based on the observed overlapping in the key characters used to separate them. However, Anastasiadou et al. (2004) stated that given the wide distribution of this species and the degree of isolation of its populations it is likely that a detailed examination of other morphological features could reveal real differences among the various populations of this species.

Recently, Anastasiadou et al. (2006) re-described *A. desmarestii* Millet, 1831 after studying specimens from Garrone River (France) and 2 years later they (Anastasiadou et al. 2008) re-validated and re-described *A. rosiana* de Brito Cappelo, 1867 based on specimens from São Barnabé River (Odelouca River, Algarve, Portugal).

After examining two mitochondrial genes (COI, 16S) from specimens collected mainly from the western Mediterranean area, Garcia Muñoz et al. (2009) proposed the existence of two species: *A. desmarestii*, distributed in West Europe and North Africa and *A. stankoi* Karaman, 1972 distributed in Greek freshwaters which was elevated from the subspecies to the species level. Furthermore, the authors argued about the existence of a third genetically distinguished group, *A. mesopotamica* Al-Adhub, 1987 (or *A. orientalis* Bouvier, 1913), without confirming its status as a distinct species. In addition, they synonymised *A. rosiana*, as described by Anastasiadou et al. (2008), with *A. desmarestii*. The species *A. stankoi* was characterized as cryptic since previous studies failed to detect any distinguishing morphological characters (Anastasiadou et al. 2004) that would enable its discrimination from the *A. desmarestii* complex (Garcia Muñoz et al. 2009).

A comprehensive revision of synonyms of the *Atyaephyra*, at species level, has been provided by De Grave and Fransen (2011) while a list of synonyms at genus level is given by Holthuis (1993).

This eventful taxonomic history, and the high intra- and inter-specific morphological variability observed among the *Atyaephyra* taxa make the recognition of discrete species intricate. Also, the wide distribution of the genus and the apparent isolation between populations may support the existence of new non-described species. Therefore the lack of any study including material covering all the known distribution of the genus provoked the present current multidisciplinary study.

In an attempt to recognize and delimit species within *Atyaephyra*, samples covering the known distribution of the genus were analysed, using morphological and

molecular methods to evaluate the consensus of groupings as inferred by both datasets. In the last decade molecular data have been widely used in conjunction with decapod morphology, and have been instrumental in discriminating cryptic or sibling species (e.g. Macpherson and Machordom 2005, Jesse et al. 2010, 2011).

This study specifically aims to: (a) test the status of the species already recognized based on morphological and molecular data; (b) describe new species based on morphological and molecular data; (c) provide knowledge on the current geographic distribution of the *Atyaephyra* species; (d) describe the phylogenetic relationships of new and previously described species based on COI gene.

Material and methods

Abbreviations used

MMNH: Macedonian Museum of Natural History, Skopje, F.Y.R.O.M.; ZMAUTH: Zoological Museum of the Department of Biology, Aristotle University of Thessaloniki, Greece; MNHN: Muséum National d'Histoire Naturelle, Paris, France; NHM: Natural History Museum, London, England; NMW: Naturhistorisches Museum Wien, Austria; OUMNH: Oxford University Museum of Natural History, England; SMF: Senckenberg Research Institute and Natural History Museum, Frankfurt, Germany and NHMC: Natural History Museum of Crete, Greece; CL: carapace length (measured from the posterior margin of the orbit to the posterior margin of the carapace); stn: station; ovig: ovigerous.

Morphological analyses

Specimens were collected with a hand dredge over the period 2000–2012 from numerous river catchments in Greece, while additional material from the rest of the Mediterranean region was either offered or loaned by researchers and Museum collections. Samples were loaned or offered from the following museums: NHM, NMW, MNHN, MMNH, ZMAUTH, OUMNH and SMF. In total 1,082 adult individuals (*A. acheronensis* sp. n.: 4, *A. desmarestii*: 431, *A. thymisensis* sp. n.: 194, *A. orientalis*: 111, *A. stankoi*: 106, *A. strymonensis* sp. n.: 92, *A. tuerkayi* sp. n.: 2; furthermore 112 and 30 additional individuals were examined pending their assignment to *A. acheronensis* and *A. tuerkayi* respectively) were examined from 122 different stations (49 river basins, 20 countries) spanning throughout the known distribution of the genus *Atyaephyra* from Middle East to North Africa and Europe (Fig. 1). Part of this examined material has been included in the studies of Kinzelbach and Koster (1987) and Anastasiadou et al. (2004, 2006, 2008). A total of 135 morphological characters including 68 somatometric distances were analysed (see Appendix: Table 1). Morphometric measurements were taken using a Carl Zeiss standard trinocular microscope or an Olympus VM stereoscope both with

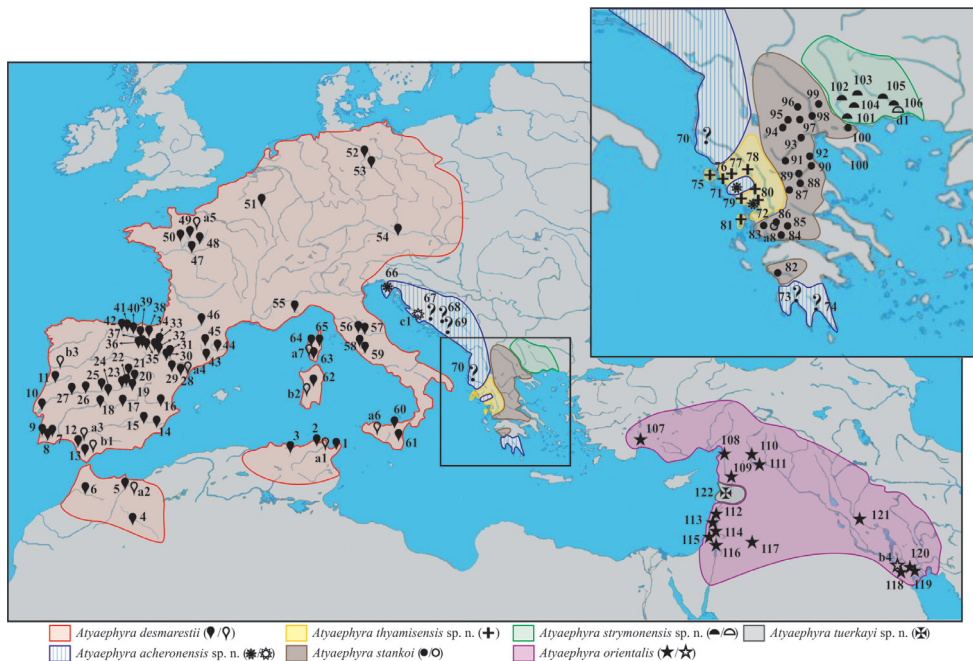


Figure 1. Map showing the sampling localities of *Atyaephyra* and the geographic distribution of the genus in Europe, Middle East and North Africa. Numbers 1–122, next to a solid symbol, indicate the different rivers, lakes or barrages from where samples were collected. Letters a–d, next to an open symbol, represent localities reported in the published sources of sequences. The symbols correspond to different *Atyaephyra* species. Question marks indicate station's unsure placement inside *A. acheronensis* (the clarification of their position will have to await the sequencing) while the general distribution of *A. acheronensis* shown is only speculation.

ocular micrometer. Only adult individuals were taken into account in order to exclude deviations in the features which appear in the juvenile individuals. A threshold of $CL \geq 5$ mm was set for all the specimens examined except for those belonging to *A. orientalis* for which the threshold was set to $CL \geq 3.8$ mm. The threshold corresponds to the smaller ovigerous individual found. *Atyaephyra orientalis* is of smaller size and thus the threshold must be lower than in the other species. Drawings were made based on photos taken which were subsequently digitized and processed with CoreDRAW® Graphics Suite X5.

Electronic publication

All data (e.g. taxon descriptions, figures, characters measured) underlying this publication can also be accessed on *Atyaephyra* Scratchpad (<http://atyaephyra.myspecies.info/>). Scratchpads (<http://scratchpads.eu>) is a Virtual Research Environment, that enable taxonomists to collaborate in the production of websites documenting the diversity of life (Blagoderov et al. 2010).

Molecular analyses

DNA extraction, amplification and sequencing

Genomic DNA was extracted exclusively from abdominal tissue using ammonium acetate protocol (provided by Poulakakis N, NHMC, University of Crete, Greece). Abdominal tissue was dissolved in 600µl extraction buffer (0.05M Tris-HCl pH 7.5, 1mM EDTA pH 8.0, 0.15M NaCl, 0.3% sodium dodecyl sulfate, and 0.6µg/µl proteinase K) and incubated in a shaking waterbath at 56°C overnight. Following the incubation, 340µl of 4M ammonium acetate were added to each sample and incubated at room temperature for 60 min. Samples were mixed several times during this period by inversion. The solution was centrifuged at 18,000g for 20 min and supernatant was transferred to 2.0ml centrifuge tubes and 1ml of absolute ethanol was added to each sample. The tubes were inverted several times and centrifuged at 18,000g for 30 min. Following the removal of ethanol samples were dried overnight. DNA pellet was diluted by adding 50µl ddH₂O and incubated at 4°C overnight. A fragment of the 5' region of mitochondrial (mtDNA) cytochrome c oxidase subunit I (COI) gene was amplified using the polymerase chain reaction (PCR). Two pairs of primers were used for each DNA extract, following the technique of nested PCR. Different combinations of primers were used as first pair: (a) LCO-1490 (5'-GGTCAACAAATCATAAAGATATTGG-3'; Folmer et al. 1994) and HCO-2198 (5'-TAAACTTCAGGGTGACCAAAAATCA-3'; Folmer et al. 1994); (b) LCO-1490 and C1-N-2191 (5'-CCCGGTTAAAAT-TAAAATATAAACTTC-3'; Simon et al. 1994); (c) Pals-COI-F1 (5'-GAGCTGAAC-TAGGTCAACC-3', designed on Palaemoninae sequences) and HCO-2198 specifying a ~700 bp to ~600 bp fragment of the COI gene. Thermocycling was performed with an initial denaturation step of two min at 94°C; followed by 35 cycles of one min at 94°C, one min at 42–52°C (depending on the primer pair used), and one min at 72°C, with a final extension of 72°C for 10 min. Then, the primary PCR product was directly used for another amplification reaction, without further purification, using two different combinations of primers as second pair: (a) the newly designed Pals-COI-F1 and Pals-COI-R1 (5'-AGTATAGTAATAGCTCCAGC-3', designed on Palaemoninae sequences) and (b) C1-J-1718, (5'-GGAGGATTTGGAAATTGATTAGTTCC-3'; Simon et al. 1994) and Pals-COI-R1 which amplified a ~450 bp and ~330 bp fragment respectively. The thermal profile for the secondary amplification reaction was the same as that of the primary amplification reaction. All amplification reactions were carried out in a final volume of 20µl. Each reaction contained 1.0µl template DNA, 0.15µM of each primer, 0.15mM dNTPs, 1.5mM or 3mM MgCl₂ (depending on the primer pair used), 1X PCR reaction buffer, and 0.5U Taq (Gennaxon).

In some cases after the nested PCR a re-amplification was made using a modified Band-stab PCR protocol (Bjourson and Cooper 1992). The re-amplification reaction was carried out in a final volume of 50µl containing: 0.1µM of each primer, 0.08mM dNTPs, 1mM MgCl₂, 1X PCR reaction buffer, and 1.25U Taq (Gennaxon). After an initial denaturation step of two min at 94°C, 25 cycles of one min at 94°C, one min at

45°C, and one min at 72°C were performed, followed by a final extension of five min at 72°C. The amplified fragments were then purified using ethanol and sodium acetate precipitation method and sequenced using Big Dye Terminator Cycle Sequencing 3.1 (Applied Biosystems) standard protocol on an ABI 3730 Genetic Analyzer (Applied Biosystems). All individuals were sequenced either with the forward or the reverse COI primer or with both (Pals-COI-F1, Pals-COI-R1).

Alignment and genetic divergence

Thirty-seven new COI sequences were generated (GenBank accession numbers JX289898–JX289919, JX289921–JX289933, JX289935–JX289936; Table 1). Our dataset was supplemented with eight COI sequences of *Atyaephyra* from the study of Garcia Muñoz et al. (2009), one from Franjević et al. (2010), one from Zakšek et al. (2007) and four from Page et al. (unpublished data). Furthermore, three COI sequences (Page et al. 2005a, Zakšek et al. 2007, Garcia Muñoz et al. 2009) from another two atyid genera, were included as outgroups (i.e. *Dugastella valentina* (Ferrer Galdiano, 1924) from Spain, *Dugastella marocana* Bouvier, 1912 from Morocco, and *Paratya curvirostris* (Heller, 1862) from New Zealand, accession numbers provided in Table 1). The choice of the taxa used as outgroup was based on their close relationship with the genus under study since they all belong to the same atyid group (*Paratya* group) (Von Rintelen et al. 2012).

COI sequences were aligned using FSA (Fast Statistical Alignment) (Bradley et al. 2009) and translated into amino acids prior to analysis, to ensure that no gaps or stop codons were present in the alignment. The number of distinct haplotypes was estimated with the software Arlequin version 3.5.1.3 (Excoffier and Lischer 2010). jModelTest (Posada 2008) was used to determine the model of DNA sequence evolution that best fit the data using AIC and BIC criteria. Sequence divergences were estimated with the software MEGA version 5.1 (Tamura et al. 2011).

Phylogenetic analyses

Phylogenetic inference analyses were conducted using Neighbor Joining (NJ), Maximum Likelihood (ML), and Bayesian Inference (BI) methods. The nucleotide substitution model selected by jModeltest [Tamura-Nei, 1993 (TrN) + gamma (G)] was applied to the data matrix in all analyses. A NJ tree was produced with the software MEGA where branch support was assessed with 1,000 bootstrap replicates. ML estimates were made using PhyML online web server (Guindon et al. 2010; <http://www.atgc-montpellier.fr/phyml/>). Nearest neighbor interchanges (NNIs) and subtree pruning and regrafting (SPR) topological moves were used to explore the space of tree topologies. Approximate likelihood-ratio test (aLRT) based on a non-parametric Shimodaira-Hasegawa-like (SH-like) procedure was employed to estimate branch support (Guindon et al.

Table 1. *Atyaephyra* specimens and COI sequences accession numbers listed by area and species. The sex and the CL are given for each specimen sequenced in parenthesis (first column). Museum accession numbers are given in parentheses (second column). GenBank accession numbers of published sequences, used in this study, are provided with their corresponding studies indicated by the letters a–e [a: Garcia Muñoz et al. 2009, b: Page et al. (unpub sequences), c: Franjević et al. 2010, d: Zakšek et al. 2007, e: Page et al. 2005a].

Specimen	Sampling site	Station number in Fig. 1	GenBank accession no. COI
<i>Atyaephyra desmarestii</i>			
Leb1 (♀, CL: 6.6 mm)	Tunisia, Lebna Barrage, 21.3.2010, coll. S. Dhaouadi-Hassen	1	JX289898
Met1 (♀, CL: 6.8 mm)	Tunisia, Ben Metir Barrage, 22.2.1974 (NHM 1515–1540.22.2.74)	2	JX289899
Moul1 (♀, CL: 6.1 mm)	Morocco, Moulouya River, 11.4.2011, coll. M. Melhaoui	5	JX289900
Krum2 (♀, CL: 6.9 mm)	Morocco, Krumane River, 22.7.1952, coll. J. Phillipson (NHM 1953.12.2.12–15)	6	JX289901
Bord2 (♀, CL: 5.7 mm)	Portugal, Bordeira River, 5.3.1985, coll. J. Paula (NHM 1986.261)	9	JX289902
Sint1 (♀, CL: 7.0 mm)	Portugal, Tagus Basin, Colares River, 1880 (NHM 1880.36)	10	JX289903
Mon1 (♀, CL: 7.2 mm)	Portugal, Mondego Basin, Ceira River, 24.5.2010, coll. V. Ferreira	11	JX289904
Mon2 (♀, CL: 6.8 mm)			JX289905
Vet1 (♀, CL: 8.0 mm)	Spain, Guadalquivir Basin, Guadiamar River, 8.5.2006, coll. C. Lejeusne	12	JX289906
Mu1 (♀, CL: 6.9 mm)	Spain, Segura Basin, Mundo River, 27.9.2001, coll. J.L. Moreno Alcaraz	15	JX289907
Vb1 (♀, CL: 6.1 mm)	Spain, Guadiana Basin, Vado Blanco River, 3.10.2001, coll. J.L. Moreno Alcaraz	17	JX289908
Ta1 (♀, CL: 7.8 mm)	Spain, Tagus Basin, Tajuna River, 7.8.2001, coll. J.L. Moreno Alcaraz	20	JX289909
Er1 (♀, CL: 8.2 mm)	Spain, Ebro Basin, Erro River, 25.5.2007, coll. J. Oscoz	38	JX289910
Fl1 (♂, CL: 5.3 mm)	Spain, Catalan Basin, Fluvia River, 4.2.2005, coll. M.L. Zettler	44	JX289911
Gar2 (♀, CL: 6.0 mm)	France, Garrone River, 25.8.2004, coll. R. Liasko and S. Combes	46	JX289912
Sart1 (♀, CL: 7.0 mm)	France, Loire Basin, Sarthe River, 20.9.2000, coll. P. Noël	48	JX289913
May2 (♀, CL: 5.6 mm)	France, Loire Basin, Mayenne River, 20.9.2000, coll. P. Noël	49	JX289914
Hav1 (♀, CL: 6.3 mm)	Germany, Elbe Basin, Havel River, 26.8.2005, coll. M.L. Zettler	53	JX289915
Dan1 (♀, CL: 7.4 mm)	Austria, Danube River, 8.10.1998, coll. Zipek and Melcher (NMW 18315)	54	JX289916
Sim3 (♀, CL: 6.5 mm)	Sicily, Simeto River, 1.9.1978, coll. C. Frogliola	61	JX289917
Riz1 (♂, CL: 5.8 mm)	Corsica, Rizzanese River, 13.8.2003, coll. M.L. Zettler	64	JX289918
Br1 (♀, CL: 7.9 mm)	Corsica, Bravone River, 16.8.2003, coll. M.L. Zettler	65	JX289919

Specimen	Sampling site	Station number in Fig. 1	GenBank accession no. COI
	Tunisia, Medjerda River	a1	FJ594343
	Morocco, Zegzel River	a2	FJ594340
	Spain, Guadalquivir River	a3	FJ594339
	Spain, Ebro River	a4	FJ594342
	France, Loire Basin, Mayenne River	a5	FJ594341
	Sicily, Frattina River	a6	FJ594344
	Corsica, Liamone River	a7	FJ594345
Guad1	Spain, Guadalhorce River, coll. C.N. Sánchez	b1	JX853921
Cog1	Sardinia, Coghinas River, coll. M. Jowers	b2	JX853920
Dour1	Portugal, Douro River, coll. M. Fidalgo	b3	JX289920
<i>Atyaephyra acheronensis</i> sp. n.			
Drag1 (♂, CL: 5.1 mm)	Slovenia, Dragonja River, Aug.1971	66	JX289921
Ach1 (♀ ovig., CL: 5.9 mm)	Greece, Acherontas River, 15.4.2012, coll. Ch. Anastasiadou (NHM 2012.1493)	71	JX289922
Lour1 (♀, CL: 7.6 mm)	Greece, Louros River, 15.4.2012, coll. Ch. Anastasiadou	72	JX289923 JX289924
Lour2 (♀ ovig., CL: 7.0 mm)			
	Croatia, Krka River	c1	DQ320047
<i>Atyaephyra thyamisensis</i> sp. n.			
Lour3 (♀, CL: 7.4 mm)	Greece, Louros River, 15.4.2012, coll. Ch. Anastasiadou	72	JX289925
Lef2 (♂, CL: 5.7 mm)	Greece, Lefkada Island, Vardas River, 2.10.1932, coll. Beier (NHMW 466)	81	JX289926
<i>Atyaephyra stankoi</i>			
Doir2 (♀, CL: 5.0 mm)	Greece–F.Y.R.O.M., Doirani Lake, 26.10.1994, coll. S. Jovanovich	99	JX289927
	Greece, Lisimakhia River	a8	FJ594346
<i>Atyaephyra strymonensis</i> sp. n.			
Myl1 (♀, CL: 5.2 mm)	Greece, Strymonas Basin, Mylopotamos Springs, 23.5.2011, coll. M. Christodoulou and M.S. Kitsos	102	JX289928 JX289929
Myl2 (♀, CL: 5.3 mm)			
	Greece, Nestos River	d1	DQ641570
<i>Atyaephyra orientalis</i>			
Kar2 (♀, CL: 4.5 mm)	Turkey, Orontes Basin, Karasu River, 22.9.1982, coll. R.K. Kinzelbach (SMF 12174)	108	JX289930
Or2 (♀, CL: 5.0 mm)	Syria, Orontes River, 30/31.3.1979, coll. R.K. Kinzelbach (SMF 12050)	109	JX289931
Euph2 (♀, CL: 4.7 mm)	Syria, Euphrates River, 17.8.1978, coll. R.K. Kinzelbach (SMF 12188)	110	JX289932
Shat2 (♀, CL: 5.3 mm)	Iraq, Euphrates–Tigris Basin, Shatt Al-Arab River, 2011, coll. M.D. Naser	120	JX289933
AlH1	Iraq, Euphrates–Tigris Basin, Al-Huaizah Marshes, coll. M.D. Naser	b4	JX289934
<i>Atyaephyra tuerkayi</i> sp. n.			
Nah1 (♀, CL: 6.2 mm)	Syria: Nahr Al-Kabir River, 5.3.1979, coll. R.K. Kinzelbach (SMF 43020-1)	122	JX289935 JX289936
Nah2 (♀, CL: 7.1 mm)			

Specimen	Sampling site	Station number in Fig. 1	GenBank accession no. COI
Outgroups			
<i>Dugastella valentina</i>	Spain	d2	DQ641569
<i>Dugastella marocana</i>	Morocco	a9	FJ594347
<i>Paratya curvirostris</i>	New Zealand (North Island), Marawara Stream	e1	AY661487

2010). BI analysis was performed in BEAST version 1.7.2. (Drummond et al. 2012) assuming an uncorrelated lognormal relaxed-clock model, setting the tree prior to Yule process, run for 100,000,000 generations (10% was discarded as burn-in period). Finally, TreeAnnotator was used to find the Maximum Clade Credibility tree. In order to show the geographic distribution of the distinct haplotypes, in all the analyses, not only the unique haplotypes were used, but all the sequences acquired.

Results

Phylogenetic analyses

Out of the 51 *Atyaephyra* COI sequences 35 distinct haplotypes were distinguished. Shared haplotypes were observed among individuals in close geographical proximity. Of the 600 nucleotide sites examined, 237 were variable of which 197 were parsimony informative (14% in the first, 2% in second, and 84% in third codon position). The nucleotide substitution model that best fits our data according to both AIC and BIC criteria is Tamura and Nei (1993) + gamma (G) based on which *Atyaephyra* sequence divergence ranged from 0% to 25.7%.

All employed methods yielded consistent tree topologies (Fig. 2). The monophyly of the genus is highly supported in all methodologies (BI posterior probability: 1.0, ML SH-like value: 96, NJ bootstrap value: 95).

In all phylogenetic analyses four main and well-supported phylogroups were identified, corresponding to different groups of species designated by morphology (presented in the next section) and/or well defined geographic regions throughout the Mediterranean region (Fig. 2). The first phylogroup comprises specimens from the Middle East which were classified to the nominal species, *A. orientalis* by morphology. Specimens from the topotypical populations of the subspecies *A. d. orientalis* (Orontes River, Syria) and *A. d. mesopotamica* (Shatt Al-Arab River, Iraq) were also included. However, present data do not allow for within clade fine scale resolution. The mean genetic distances between the Middle East phylogroup (*A. orientalis*) and the other groups/subgroups were very high ranging from 18.7% to 24.5% while the average intraspecific distance was 5.8% (Table 2).

The second phylogroup which is strongly supported by both BI and ML methodologies while in NJ yielded lower bootstrap values (BI posterior probability: 0.99, ML SH-like value: 94, NJ bootstrap value: 65) includes sequences exclusively from Greek

Table 2. Nucleotide mean distances (% Tamura-Nei 1993 + G model) of cytochrome c oxidase I (COI) within (first column) and among the *Atyaephyra* species. The range of pairwise distances is given in parenthesis.

	Within species	<i>A. desmarestii</i>	<i>A. acheronensis</i> sp. n.	<i>A. thyamensis</i> sp. n.	<i>A. stankoi</i>	<i>A. strymonensis</i> sp. n.	<i>A. orientalis</i>
<i>A. desmarestii</i>	0.016 (0.000–0.048)						
<i>A. acheronensis</i> sp. n.	0.001 (0.000–0.003)	0.083 (0.059–0.116)					
<i>A. thyamensis</i> sp. n.	0.000 (0.000)	0.239 (0.206–0.271)	0.238 (0.233–0.251)				
<i>A. stankoi</i>	0.024 (0.024)	0.236 (0.204–0.261)	0.232 (0.215–0.241)	0.167 (0.163–0.176)			
<i>A. strymonensis</i> sp. n.	0.003 (0.000–0.005)	0.233 (0.201–0.273)	0.219 (0.205–0.234)	0.182 (0.166–0.194)	0.119 (0.117–0.119)		
<i>A. orientalis</i>	0.058 (0.009–0.102)	0.222 (0.192–0.287)	0.238 (0.216–0.256)	0.187 (0.169–0.200)	0.226 (0.190–0.244)	0.245 (0.219–0.270)	
<i>A. tuerkayi</i> sp. n.	0.000 (0.000)	0.230 (0.208–0.260)	0.222 (0.215–0.232)	0.257 (0.237–0.278)	0.232 (0.215–0.242)	0.254 (0.243–0.267)	0.197 (0.172–0.221)

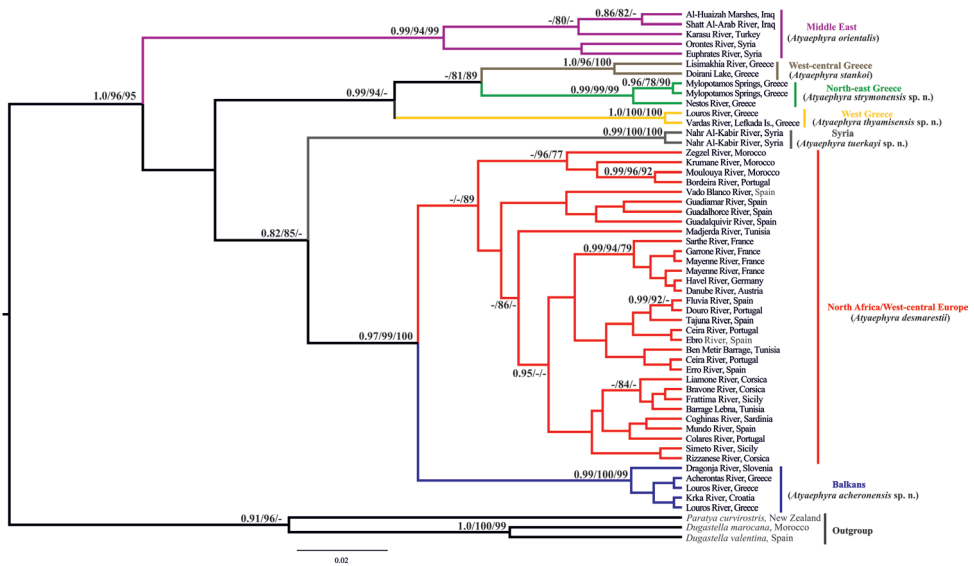


Figure 2. Bayesian inference phylogenetic tree of *Atyaephyra* based on COI dataset. Numbers on nodes indicate Bayesian Inference posterior probabilities, Maximum Likelihood SH-like branch support and Neighbor Joining bootstrap respectively. Only values above 0.75 and 75% are shown. Colours correspond to those used in Figure 1.

populations. The Greek phylogroup is further subdivided into three well supported groups. The first subgroup corresponds to the nominal species, *A. stankoi*, found in West-central Greece. It is worth noticing that specimens from the type locality (Doirani Lake) of *A. d. stankoi* are also included. The remaining Greek specimens are grouped in two well defined subgroups, one distributed in North-east Greece while the other is located in West Greece (Fig. 1). The mean genetic divergence among the three subgroups ranges from 11.9% to 18.2%, while the mean genetic distances within subgroups varied from 0% to 2.4% (Table 2).

The third phylogroup contains specimens from the Syrian River Nahr Al-Kabir and it is strongly supported in all methodologies (BI posterior probability: 0.99, ML SH-like value: 100, NJ bootstrap value: 100). The mean genetic distances between the Syrian subgroup and the other groups/subgroups were very high ranging from 19.7% to 25.7% (Table 2).

The fourth phylogroup which is well supported by BI, ML and NJ (BI posterior probability: 0.97, ML SH-like value: 99, NJ bootstrap value: 100) includes specimens originating from West-central Europe, North Africa and the Balkans. Within this phylogroup, specimens from Croatia, Slovenia and Greece form a distinct highly supported subgroup (BI posterior probability: 0.99, ML SH-like value: 100, NJ bootstrap value: 99). The remaining specimens within the phylogroup i.e. specimens from West-central Europe and North Africa, although classified as *A. desmarestii* (nominal species) by morphology (discussed in the next section) do not constitute a well supported subgroup

except in NJ analysis where it is relatively well supported (NJ bootstrap value: 89). Sequences from the topotypical populations of the *A. desmarestii* (Mayenne and Sarthe River), and *A. rosiana* described by de Brito Capello (Ceira River, tributary of Mondego River) were included in this subgroup as well as a sequence acquired from river Bordeira (Portugal) which is near to São Barnabé River from where *A. rosiana* was re-described by Anastasiadou et al. (2008). The genetic distances between these two subgroups are quite large, ranging from 5.9% to 11.6% (Table 2). The lowest values (5.9–6.8%) were observed between the specimens of the Balkan subgroup and those of South Iberian Peninsula and North Africa (Morocco), located in the distant end of *A. desmarestii* distribution. On the contrary higher values (7.5–10.2%) were observed between the nearest to the Balkan subgroup populations (e.g. Danube River) as well as between the topotypical populations of *A. desmarestii* (Mayenne and Sarthe River) and the Balkan populations. Furthermore, no haplotypes were shared between these two subgroupings.

Morphological analysis

Account of *Atyaephyra* species

The present study recognises five well defined by morphology species of *Atyaephyra*: *Atyaephyra desmarestii* (Millet, 1831), *A. stankoi* Karaman, 1972, *A. orientalis* Bouvier, 1913 and two new species, *A. thyamisensis* sp. n. and *A. strymonensis* sp. n. Neotypes are designated for *A. desmarestii* and *A. stankoi* in an attempt to stabilize their taxonomy. In addition, two cryptic species are defined by the molecular analysis. Descriptions are provided for all these species.

Taxonomy

Family Atyidae de Haan, 1849 (in de Haan, 1833–1850)

Genus *Atyaephyra* de Brito Capello, 1867

<http://species-id.net/wiki/Atyaephyra>

Type species: *Atyaephyra rosiana* de Brito Capello, 1867: 6–7, Pl. 1, Figs 1A–E [type locality: Coimbra, Portugal]; by monotypy.

Diagnosis. Carapace with supraorbital and antennal tooth. Rostrum long and armed up to the tip. Eyes well developed, pigmented. Exopods present only on the two first pairs of pereopods, carpus of first and second pair of pereopods with a distal excavation. Uropod diaeresis with a single spine (rarely two). Appendix masculina of male second pleopod long, sub-cylindrical and armed with numerous spiniform setae. Eggs small to medium, size 0.40–0.75 × 0.25–0.5 mm.

***Atyaephyra desmarestii* (Millet, 1831)**

http://species-id.net/wiki/Atyaephyra_desmarestii

Symethus fluviatilis Rafinesque, 1814: 23–24 [suppressed under the plenary powers for the purposes of the Principle of Priority but not for those of the Principle of Homonymy in Opinion 522 in 1958].

Acilius fluviatilis. – Rafinesque, 1815: 221.

Hippolyte Desmarestii Millet, 1831: 55–57, Pl. 1, Figs 1A–B [type locality: Mayenne River, Sarthe River, Loir River, Thouet River, Layon River (France)]. – H. Milne-Edwards 1837: 376; Taramelli 1864: 363–369.

Caridina Desmarestii. – Joly, 1843: 34–86, Figs 1–78; Heller 1863: 238, Pl. 8, Fig. 3; Pelseneer 1886: 211–216; Bolivar 1892: 131.

Atyaephyra Rosiana de Brito Capello, 1867: 6–7, Pl. 1, Figs 1A–E. [type locality: Coimbra, Portugal].

Hemicardina desmarestii. – Ortmann, 1890: 464–465.

Atyaephyra Desmaresti. – Ortmann 1895: 401; Bouvier 1925: 84–89, Figs 164–174, partim.

Atyaephyra Desmaresti var. *occidentalis* Bouvier, 1913: 65–74, Figs 2E–H, 2J–L, 3E–J, partim.

Atyaephyra desmarestii desmarestii. – Holthuis, 1961: 5–10, Figs 2A, 3A, partim.

Atyaephyra desmarestii. – Anastasiadou et al. 2004: 5–13, partim; Anastasiadou et al. 2006: 1195–1207, Figs 1–5; Garcia Muñoz et al. 2009: 32–42; Von Rintelen et al. 2012: 82–96, partim.

Atyaephyra rosiana. – Anastasiadou et al. 2008: 191–205, Figs 1–5.

Material examined. Type material. Neotype: 1 ovig. ♀ (CL 7.1 mm), MNHN-IU-2009-2270 (ex MNHN-Na480), Maine-et-Loire, France [here designated].

Non-type material. Tunisia: 8 ♀♀ (1 ovig.) (CL 5.4–7.4 mm), Barrage Lebna (Fig. 1, stn 1), 21.3.2010, coll. S. Dhaouadi-Hassen; 2 ♀♀ (CL 6.0–6.8 mm), NHM 1515–1540.22.2.74, Ain Draham, Barrage Ben Metir (Fig. 1, stn 2), 22.2.1974. **Algeria:** 1 ♂ (CL 5.1 mm), NHM 1955.5.3.15–18, Algiers, Seybouse River (Fig. 1, stn 3), 3.5.1955; 11 ♀♀ (6 ovig.) (CL 5.0–8.0 mm) and 1 ♂ (CL 5.2 mm), NHM 1949.5.2.1–12, Beni Abbes, Saoura River (Fig. 1, stn 4), 2.5.1949, coll. H. Munro Fox. **Morocco:** 4 ♀♀ (1 ovig.) (CL 5.5–6.5 mm) and 1 ♂ (CL 5.0 mm), Moulouya River (Fig. 1, stn 5), 11.4.2011, coll. M. Melhaoui; 1 ♀ (CL 6.9 mm) and 4 ♂♂ (CL 5.2–5.6 mm), NHM 1953.12.2.12–15, Krumane River (Fig. 1, stn 6), 22.7.1952, coll. J. Phillipson. **Portugal:** 21 ♀♀ (12 ovig.) (CL 5.8–7.3 mm) and 11 ♂♂ (CL 5.0–5.7 mm), Algarve, São Barnabé River (Odelouca River) (Fig. 1, stn 7), 23.7.1988, coll. C. d' Udekem d' Acoz; 7 ♀♀ (6 ovig.) (CL 6.2–7.7 mm) and 5 ♂♂ (CL 5.0–5.2 mm), NHM 1971.105, Portimao, Odelouca River (Fig. 1, stn 8), 1970; 18 ♀♀ (4 ovig.) (CL 5.5–8.0 mm) and 3 ♂♂ (CL 5.0–5.1 mm), NHM 1986.261, Bordeira River (Fig. 1, stn 9), 5.3.1985, coll. J. Paula; 5 ♀♀ (4 ovig.) (CL 7.0–8.1 mm) NHM 1880.36, Sintra, Colares River (Fig. 1, stn 10), 1880; 15 ♀♀ (3 ovig.) (CL 5.8–7.9

mm) and 5 ♂♂ (CL 5.3–6.1 mm), Coimbra, Ceira River (Fig. 1, stn 11), 24.5.2010, coll. V. Ferreira. **Spain:** 2 ♀ (CL 6.5–8.0 mm), Veta la Arena, Guadiamar River (Fig. 1, stn 12), 8.5.2006, coll. C. Lejeusne; 5 ♀♀ (CL 6.1–6.7 mm) and 17 ♂♂ (CL 5.0–6.5 mm), Cadiz, Guadalete River (Fig. 1, stn 13), 2000, coll. A. Rodriguez; 3 ♀♀ (CL 5.1–6.3 mm), Segura River (Fig. 1, stn 14), 28.9.2001, coll. J.L. Moreno Alcaraz; 10 ♀♀ (1 ovig.) (CL 6.1–7.5 mm) and 1 ♂ (CL 5.5 mm), Mundo River (Fig. 1, stn 15), 18/27.9.2001, coll. J.L. Moreno Alcaraz; 2 ♀♀ (CL 6.6–7.7 mm) and 1 ♂ (CL 5.5 mm), Villalva de la Sierra, Jucar River, 40°07.99'N, 02°08.38'W (Fig. 1, stn 16), 16.8.2001, coll. J.L. Moreno Alcaraz; 7 ♀♀ (CL 5.1–6.4 mm) and 1 ♂ (CL 5.3 mm), Ossa de Montiel, Vado Blanco River, 38°54.60'N, 02°48.03'W (Fig. 1, stn 17), 3.10.2001, coll. J.L. Moreno Alcaraz; 3 ♀♀ (CL 5.7–6.5 mm), El Torno, Bullaque River, 39°14.36'N, 04°15.57'W (Fig. 1, stn 18), 11.10.2001, coll. J.L. Moreno Alcaraz; 2 ♀♀ (CL 7.2–7.7 mm), Canavera, Guadiella River, 40°25.36'N, 02°28.95'W (Fig. 1, stn 19), 14.8.2001, coll. J.L. Moreno Alcaraz; 3 ♀♀ (CL 6.2–8.0 mm), Abanades, Tajuna River (Fig. 1, stn 20), 7.8.2001, coll. J.L. Moreno Alcaraz; 3 ♀♀ (1 ovig.) (CL 6.3–7.2 mm) and 6 ♂♂ (CL 5.5–6.5 mm), Henares River, (Fig. 1, stn 21), 1.8.2001, coll. J.L. Moreno Alcaraz; 1 ovig. ♀ (CL 7.4 mm), Naharros, Canamares River, 41°09.10'N, 02°55.14'W (Fig. 1, stn 22), 30.7.2001, coll. J.L. Moreno Alcaraz; 2 ovig. ♀♀ (CL 7.3–7.8 mm), Puebla de Valles, Jarama River (Fig. 1, stn 23), 31.7.2001, coll. J.L. Moreno Alcaraz; 1 ♀ (CL 5.9 mm) and 1 ♂ (CL 5.1 mm) La Guardia, Cedron River, 39°48.26'N, 03°20.33'W (Fig. 1, stn 24), 6.9.2001, coll. J.L. Moreno Alcaraz; 1 ♀ (CL 5.2 mm), Escalona, Alberche River, 40°09.45'N, 04°25.04'W (Fig. 1, stn 25), 27.8.2001, coll. J.L. Moreno Alcaraz; 1 ♀ (CL 5.1 mm) and 2 ♂♂ (CL 5.3–5.7 mm), Tietar River (Fig. 1, stn 26), 28.8.2001, coll. J.L. Moreno Alcaraz; 9 ♀♀ (1 ovig.) (CL 5.1 mm) and 1 ♂ (CL 5.0 mm), Tagus River (Fig. 1, stn 27), 14.8.2001 and 5.9.2001, coll. J.L. Moreno Alcaraz; 1 ♂ (CL 5.5 mm), Calanda, Guadalope River (Fig. 1, stn 28), 25.5.2004, coll. J. Oscoz; 1 ♀ (CL 7.2 mm) and 1 ♂ (CL 5.1 mm), Escatron, Martin River (Fig. 1, stn 29), 24.5.2001, coll. J. Oscoz; 1 ♀ (CL 5.6 mm) and 3 ♂♂ (CL 5.3–5.6 mm), Murillo de Gallego, Gallego River (Fig. 1, stn 30), 7.8.2007, coll. J. Oscoz; 1 ovig. ♀ (CL 6.5 mm), Gurrea de Gallego, Soton River (Fig. 1, stn 31), 14.6.2006, coll. J. Oscoz; 1 ♂ (CL 6.2 mm), Lumbier, Irati River (Fig. 1, stn 32), 8.7.2005, coll. J. Oscoz; 2 ovig. ♀♀ (CL 6.9–7.5 mm) and 4 ♂♂ (CL 5.2–5.8 mm), Aspurz, Salazar River (Fig. 1, stn 33), 3.7.2007, coll. J. Oscoz; 1 ovig. ♀ (CL 6.5 mm) and 1 ♂ (CL 5.2 mm), Ripodas, Areta River (Fig. 1, stn 34), 3.7.2007, coll. J. Oscoz; 5 ♀♀ (4 ovig.) (CL 5.0–7.5 mm) and 2 ♂♂ (CL 5.6 mm), Castejon, Alfaro, Tudela, Ebro River (Fig. 1, stn 35), 11/12.7.2007, coll. J. Oscoz; 6 ♀♀ (5 ovig.) (CL 7.0–8.6 mm), San Adrian, Ega River (Fig. 1, stn 36), 27.6.2007, coll. J. Oscoz; 1 ovig. ♀ (CL 7.3 mm) and 2 ♂♂ (CL 5.2–5.5 mm), Marcilla, Aragon River (Fig. 1, stn 37), 28.6.2007, coll. J. Oscoz; 2 (1 ovig.) ♀♀ (CL 8.2–8.5 mm) and 2 ♂♂ (CL 5.6–6.5 mm), Urroz, Erro River (Fig. 1, stn 38), 25.5.2007, coll. J. Oscoz; 1 ovig. ♀ (CL 7.5 mm) and 2 ♂♂ (CL 5.8–6.0 mm), Mendigorria, Salado River (Fig. 1, stn 39), 14.6.2007, coll. J. Oscoz; 1 ovig. ♀ (CL 7.6 mm), Puentealarreina, Arga River (Fig. 1, stn 40), 20.6.2007, coll. J. Oscoz; 1 ♀ (CL 7.2 mm), Iraneta, Arakil River

(Fig. 1, stn 41), 20.6.2007, coll. J. Oscoz; 1 ♀ (CL 7.4 mm), Palazuelos, Jerea River (Fig. 1, stn 42), 1.6.2004, coll. J. Oscoz; 3 ovig. ♀♀ (CL 7.3–8.0 mm) and 2 ♂♂ (CL 5.3–5.5 mm), NHM 1955.10.5.2–6 and NHM 1957.8.12.69–75, Barcelona, Llobregat River (Fig. 1, stn 43), 5.10.1955 and 12.8.1955; 8 ♂♂ (CL 5.2–6.1 mm), Bascara, Fluvia River (Fig. 1, stn 44), 4.2.2005, coll. M.L. Zettler; 3 ♀♀ (CL 5.6–6.6 mm), NHM 1955.10.5.8–10, Gerona, Lake of Banyoles (Fig. 1, stn 45), 5.10.1955. **France:** 30 ♀♀ (18 ovig.) (CL 5.0–7.0 mm) and 20 ♂♂ (CL 5.0–5.2 mm), Merville, Garrone River (Fig. 1, stn 46), 25.8.2004, coll. R. Liasko and S. Combes; 2 ♀♀ (CL 5.5–6.5 mm), NHM 1955.5.3.11–14, Maine et Loire, Loire River (Fig. 1, stn 47), 3.5.1955; 2 ♀♀ (CL 6.6–7.0 mm), Angers, Sarthe River (Fig. 1, stn 48), 20.9.2000, coll. P. Noël; 2 ♀♀ (CL 5.1–5.6 mm), Mayenne River (Fig. 1, stn 49), 20.9.2000, coll. P. Noël; 3 ♀♀ (CL 6.3–6.5 mm), NMW 467, Rennes, Vilaine River (Fig. 1, stn 50), coll. G. Laponge. **Belgium:** 31 ♀♀ (8 ovig.) (CL 5.2–8.3 mm) and 7 ♂♂ (CL 5.0–6.0 mm), Ombret, Meuse River, (Fig. 1, stn 51), 3.8.1979, coll. C. d' Udekem d' Acoz. **Germany:** 1 ♂ (CL 5.2 mm) Berlin, Tegel Lake, 52°34.98'N, 13°16.44'E (Fig. 1, stn 52), 13.9.1995, coll. K. Rudolph and M.L. Zettler; 4 ♀♀ (CL 5.7–7.0 mm) and 1 ♂ (CL 5.0 mm), Havel River (Fig. 1, stn 53), 52°23.82'N, 12°17.04'E, 26.8.2005 (Saxony–Anhalt) and 52°29.82'N, 12°24.30'E, 27.8.2005 (Brandenburg), coll. M.L. Zettler. **Austria:** 1 ♀ (CL 7.4 mm), NMW 18315, Danube River (Fig. 1, stn 54), 8.10.1998, coll. Zipel and Melcher. **Italy:** 2 ♂♂ (CL 5.0–5.7 mm), Centa River (Fig. 1, stn 55), 28.5.1989, coll. C. Frogliã; 4 ♀♀ (CL 5.3–5.8 mm) and 1 ♂ (CL 5.6 mm), Nestore River (Fig. 1, stn 56), 11.11.1974, coll. C. Frogliã; 2 ♂♂ (CL 5.2–5.6 mm), Ponte Nuovo, Chiascio River, (Fig. 1, stn 57), 9.9.1975, coll. Cianficoni; 2 ovig. ♀♀ (CL 7.0–7.5 mm) and 1 ♂ (CL 5.2 mm), Nera River (Fig. 1, stn 58), 5.6.1971, coll. Moretti; 5 ♀♀ (CL 6.2–6.8 mm) and 7 ♂♂ (CL 5.0–6.3 mm), Tiber River (Fig. 1, stn 59), 10.10.1975 (Nestore), 14.10.1975 (Orte), 13.11.1975 (Umbertide), coll. Cianficoni. **Sicily:** 1 ovig. ♀ (CL 7.5 mm) and 4 ♂♂ (CL 5.4–5.9 mm), San Bartolomeo, Rosmarino River (Fig. 1, stn 60), 13.5.1986, coll. C. Frogliã; 2 ♀♀ (CL 5.8–6.4 mm) and 1 ♂ (CL 5.5 mm), Simeto River (Fig. 1, stn 61), 1.9.1978, coll. C. Frogliã. **Sardinia:** 7 ♀♀ (4 ovig.) (CL 5.5–7.2 mm) and 2 ♂ (CL 5.0 mm), unknown locality (Fig. 1, stn 62), 13.9.1977, coll. Cav; 2 ♀ (CL 6.7–7.6 mm) and 1 ♂ (CL 5.6 mm), unknown locality, coll. R.B. Manning. **Corsica:** 3 ♀♀ (1 ovig.) (CL 6.3–6.9 mm) and 1 ♂♂ (CL 5.0 mm), Favello, Taravo River (Fig. 1, stn 63), 10.8.2003, coll. M.L. Zettler; 5 ♂♂ (CL 5.0–5.8 mm), Propriano, Rizzanese River (Fig. 1, stn 64), 13.8.2003, coll. M.L. Zettler; 2 ♀♀ (CL 7.2–7.9 mm) and 4 ♂♂ (CL 5.3–6.0 mm), Bravone, Bravone River, 42°12.36'N, 09°32.10'E (Fig. 1, stn 65), 16.8.2003, coll. M.L. Zettler.

Amendments to description. Rostrum long, dorsal margin straight or slightly curved in the middle and pointed upwards, 3.79–8.70, mostly (82% of the individuals examined) 4.64–6.50, × as long as high, shorter, equal to, or longer than scaphocerite. From 17 to 36 (21–28 in 86% of the individuals examined) pre orbital teeth on dorsal margin of rostrum arranged to tip. One to five, most frequently (90% of the individuals examined) 2–4, post orbital teeth and 1–13, most often (88% of the individuals examined) 4–9, teeth on ventral margin of rostrum. Carapace smooth with pterygos-

tomial angle not protruding, rounded (Anastasiadou et al. 2006; Fig. 1). Pleuron of fifth abdominal segment pointed with an acute posterior angle. Telson with 2–4, most frequently (95% of the individuals examined) 3–4, pairs of dorsal spines arranged in curved fashion. Distal border of telson with 7–15, mostly (89%) 9–13, spines (4–7 pairs) arranged in a fan-like way. Outermost pair of spines shortest, similar to dorsal spines, adjacent pair stronger, terminating before the inner, finely setulose pairs (Anastasiadou et al. 2006; Figs 2A–B). Antennulary stylocerite with its tip failing to reach, reaching or overreaching distal margin of basal peduncle segment. Anterolateral lobe of basal segment short, round or pointed. Distal segment of antennular peduncle with 0–2, predominantly (93%) 1–2, spines (Anastasiadou et al. 2006; Fig. 2D). Basal lower endite of maxilla densely covered with long simple setae arranged in 15–22, mostly (84%) 17–20, oblique parallel rows. Endite of maxilla 1.39–1.88, most often (90%) 1.49–1.71, \times as long as basal lower endite (Anastasiadou et al. 2006; Fig. 3C). Basal endite of first maxilliped reaching clearly beyond distal end of exopod (Anastasiadou et al. 2006; Fig. 3D). Distal one-third of terminal segment of third maxilliped bearing 0–8, (1–6 in 91% of the individuals examined), mesial spines and one subdistal lateral spine near the base of larger terminal spine, interpretable as dactylus (Anastasiadou et al. 2006; Fig. 3G). Armature along flexor margin of dactylus of third and fourth pereiopod consisting of 5–10 (6–8 in 95% of the individuals) and 5–10 (6–8 in 94% of the individuals) spines respectively. Merus of third and fourth pereiopod with 1–7 (3–5 in 95% of the individuals) and 2–6 (3–5 in 99% of the individuals) spines respectively (Anastasiadou et al. 2006; Figs 4C–D). Armature along flexor margin of dactylus of fifth pereiopod consisting of 18–43, mostly (87%) 25–35, spines (Anastasiadou et al. 2006; Figs 4E–F). Endopod of first male pleopod expanded proximally and with a distal portion elongated and tapering, often with a small protruding lobe in its outer subdistal part. Endopod with 14–30 (16–25 in 86% of the individuals examined), spines arranged on a slightly curved inner margin and 9–17 (10–15 in 92% of the individuals examined), setae arranged on outer margin (Anastasiadou et al. 2006; Fig. 5C, Anastasiadou et al. 2008; Fig. 5C). 133–848 eggs of 0.4–0.7 \times 0.25–0.4 mm size.

Size. *Atyaephyra desmarestii* is a large sized species with maximum carapace length to be 6.8 mm in ♂♂, 8.5 mm in ♀♀ and 8.6 mm in ovig. ♀♀.

Molecular characters. *Atyaephyra desmarestii* can be differentiated from all other species of *Atyaephyra* by molecular characters, as demonstrated by the phylogenetic analysis of mtDNA COI sequences. Furthermore, 22 haplotypes from 30 different localities found in *A. desmarestii* were not shared by any other species of the genus. Finally, it differs from all the other species in the following nucleotide positions in the COI gene of *A. desmarestii* specimen Dour1 (Genbank accession number JX289920), position 213: cytosine (C), position 234: cytosine (C) and position 444: adenine (A).

Distribution. *Atyaephyra desmarestii* is found in freshwater habitats of North Africa and West-central Europe (see material examined and Fig. 1).

Remarks. *A. desmarestii* has been exhaustively described and illustrated by Anastasiadou et al. (2006). Anastasiadou et al. (2008) also re-established and redescribed in detail *A. rosiana*, a species currently considered as a synonym of *A. desmarestii*. In

the present paper the same material used for the redescription of *A. desmarestii* and of *A. rosiana* (Anastasiadou et al. 2006, 2008) was examined. Although Anastasiadou et al. (2006) stated that the “holotype” of *A. desmarestii* could not be traced in French institutions, Bouvier (1913) clearly stated that he examined material from “*Maine-et-Loire* (*H. Milne Edwards, probablement des cotypes de Millet*)”. As Millet and H. Milne Edwards were contemporary, and it seemed possible that H. Edwards may have asked for some specimens from the MNHN, this material was recently looked for in the MNHN collection, where the material listed in Bouvier (1913) is indeed still present (registration number Na480). However, there appears to be a discrepancy (and thus possible clarification) on the actual specimen label to this information. The specimen label (see Appendix: Fig. 3) provides the following information: (1) “Maine et Loire”, (2) “*Caridina Desmarestii* Millet”, (3) “A. Milne Edwards det.”, (4) “E.L. Bouvier ver. 1899” and (5) “A. Milne Edwards, 1900”. It is difficult to definitively interpret the label information in view of what Bouvier (1913), a contemporary of A. Milne-Edwards, wrote, as he may have had access to direct, personal information. However, the sample is herein interpreted as having belonged to the A. Milne-Edwards collection, who died in 1900 (1835–1900) and was then accessioned in the museum collection (label item 5), with the material being examined and verified, i.e. “*ver.*” in 1899, by Bouvier (label item 4), but that the material originally was identified by A. Milne Edwards (label item 3), and that the material may not have been seen by H. Milne Edwards (although it may have passed from father to son without being recorded as such on the museum labels). It seems, therefore, impossible to certify that these are indeed syntypic specimens of *Hippolyte Desmarestii* Millet, 1831, as indicated by Bouvier (1913). However, in deference to Bouvier’s potential knowledge on the matter and in line with Recommendation 75A (ICZN, 1999), a neotype for *A. desmarestii* is herein selected from this lot, the largest ovigerous female. The designation of a neotype is deemed justified under Art. 75 (ICZN, 1999), as (1) the taxon is involved in a complex nomenclatorial problem which cannot be solved without fixing the identity of the oldest name; (2) the taxon is differentiated from the other taxa in this complex by having 0–8 mesial spines on terminal segment of third maxilliped, the basal endite of first maxilliped clearly reaching beyond distal end of exopod, having 1–5 post orbital rostral teeth, having a not protruding, rounded pterygostomial angle and by the slightly curved endopod of first male pleopod with its distal part elongated and tapering; (3) the selected specimen is the largest (of only two) ovigerous females in lot MNHN-Na480; (4) the reasons the name-bearing types are considered lost (or the contrary cannot be conclusively proven) are given above (see also Anastasiadou et al. 2006); (5) the neotype is from the general locality (Maine et Loire) of the type locality of *A. desmarestii* from which no other species is known and thus it corresponds morphologically and genetically with data presented herein and in Anastasiadou et al. (2006); (6) the neotype is selected from the “Maine et Loire” sample in Bouvier (1913), corresponding to the area mentioned in Millet (1831); and (7) the neotype has been selected from a sample already belonging to

MNHN (Na480). Therefore, all conditions of Art. 75 are considered to be met and the selection of neotype is justified.

In light of the current revision of the species complex across Europe, North Africa and the Middle East, a nomenclatorial problem exists with the nomen, *Atyaephyra desmarestii* var. *occidentalis* Bouvier (1913), for which Bouvier (1913) did not designate a holotype. As such, the syntypic material of this variety (considered to be equivalent to a subspecies under Art. 45.6.4) includes all the material listed by Bouvier (1913) to have originated from North Africa and southern Europe, up to Macedonia. As such, this includes material from the Vardar region as summarily listed in Bouvier (1913), the area from which subsequently *A. desmarestii stankoi* Karaman (1972) was described. As the name of Bouvier's variety would take precedence over *A. stankoi* as used in the present revision (a precedence which would cause considerable confusion), the herein selected neotype of *A. desmarestii* (see above) is simultaneously selected as the lectotype of *A. desmarestii* var. *occidentalis* Bouvier, 1913. This being fully justified by the inclusion of the "Maine et Loire" material in Bouvier (1913)'s type series. As a result of this action, the nomen *A. stankoi* Karaman, 1972 can be used for the Macedonian taxon (as used herein), whilst *A. desmarestii* var. *occidentalis* Bouvier, 1913 becomes a junior synonym of *A. desmarestii* (Millet, 1831).

Bouvier (1913) also mentions he examined material from Coimbra (Portugal), with those particular specimens sent by "Barboza" from the Museu Bocage under the name *Atyaephyra rosiana*. He further indicates that these almost surely are cotypes from Brito Capello ("presque sûrement des cotypes"). These specimens are still present in the collection of MNHN (registration number Na509), with the label information (see Appendix: Fig. 4) corroborating the statement in Bouvier (1913) and as such are herein interpreted as syntypes of *Atyaephyra rosiana* de Brito Capello, 1867. Under ICZN Art. 75.8, the neotype selected by Anastasiadou et al (2008) is thus set aside by the rediscovery of these syntypes. As the synonymy of *A. rosiana* with *A. desmarestii* seems certain at present, there appears currently no need to select a lectotype amongst the material. It should however be noted that the type locality of *A. rosiana* de Brito Capello, 1867 reverts back to Coimbra (Portugal) and is no longer São Barnabe River, Algarve, as listed in De Grave & Fransen (2011) (see also García Muñoz et al. 2009).

A. desmarestii can be distinguished among other characters from *A. stankoi*, *A. orientalis* and *A. thymisensis* sp. n. by the presence of 0–8 mesial spines (Anastasiadou et al. 2006; Fig. 3G) on the terminal segment of third maxilliped (vs. 10–38 in *A. orientalis*, *A. stankoi* and *A. thymisensis* sp. n.; Figs 4H, 6H, 8H respectively) and by the basal endite of first maxilliped reaching beyond distal end of exopod (Anastasiadou et al. 2006; Fig. 3D) (vs. basal endite fails to reach or reaches distal end of exopod in *A. orientalis*, *A. stankoi* and *A. thymisensis* sp. n.; Figs 4E, 6F, 8F respectively). *Atyaephyra desmarestii* is similar to *A. strymonensis* sp. n. in having 0–8 mesial spines on the terminal segment of third maxilliped (Fig. 10H) but it can be discriminated by the presence of 1–5 post orbital rostral teeth (Anastasiadou et al. 2006; Fig. 1) (vs. no post orbital teeth present leaving short unarmed proximal gap in *A. strymonensis* sp. n.; Fig. 9A).

***Atyaephyra orientalis* Bouvier, 1913**

http://species-id.net/wiki/Atyaephyra_orientalis

Figs 3–4

Hemicaridina Desmaresti. – Barrois 1893: 126–134: Figs 1–3.

Atyaephyra desmarestii var. *orientalis* Bouvier, 1913: 65–74, Figs 1, 3C [type locality: Syria].

Atyaephyra desmaresti. – Annandale and Kemp 1913: 241–244.

Atyaephyra Desmaresti. – Bouvier 1925: 84–89 Figs 159–162, partim.

Atyaephyra desmarestii orientalis. – Holthuis 1961: 5–10, Figs 2C–E, 3C–H; Kinzelbach and Koster 1985: 127–133, Fig. 1, partim.

Atyaephyra desmarestii mesopotamica Al-Adhub, 1987: 1–4, Fig. 1 [type locality: Shatt Al-Arab River and Hammar Lake, Iraq]. – Salman 1987: 27–42, Figs 1–8.

Atyaephyra desmarestii. – Gorgin 1996: 662–668, Figs 1–2; Anastasiadou et al. 2004: 5–13, partim; Von Rintelen et al. 2012: 82–96, partim.

Material examined. Turkey: 3 ♀♀ (CL 4.8–5.0 mm), Antalya, Kirkgoz Spring (Fig. 1, stn 107), 21.6.2006, coll. M. Özbek; 7 ♀♀ (CL 4.5–5.5 mm), SMF 12174, Akbez, Karasu River (Fig. 1, stn 108), 22.9.1982, coll. R.K. Kinzelbach. **Syria:** 10 ♀♀ (3 ovig.) (CL 5.0–6.0 mm) and 4 ♂♂ (CL 4.0–5.0 mm), SMF 12050, below the dam of Ascharna, Orontes River (Fig. 1, stn 109), 30/31.3.1979, coll. R.K. Kinzelbach; 34 ♀♀ (15 ovig.) (CL 4.1–4.8 mm), SMF 12188, north of M'adan, Euphrates River (Fig. 1, stn 110), 17.8.1978, coll. R.K. Kinzelbach; 3 ♀♀ (2 ovig.) (CL 4.5–5.6 mm), SMF SYR8, Euphrates River (Fig. 1, stn 111), 15/16.6.1998, coll. R. Beck. **Israel:** 3 ♀♀ (2 ovig.) (CL 4.7–5.3 mm) and 2 ♂♂ (CL 3.9–4.0 mm), SMF IES 1189, Te'o Spring (Fig. 1, stn 112), 16.2.1977; 9 ♀♀ (CL 4.3–6.0 mm) and 4 ♂♂ (CL 3.9–4.0 mm), Hula Lake (Fig. 1, stn 113), 29.1.1981, coll. D. Eurth; 2 ovig. ♀♀ (CL 3.8–3.9 mm), NHM 1913.7.24.3–12, Kinneret Lake (Fig. 1, stn 114), 24.7.1913; 1 ♀ (CL 3.9 mm), Samakh, Kinneret Lake, 6.5.1986, coll. R. Ortal; 1 ♀ (CL 4.4 mm), Zaki River (Fig. 1, stn 115), 6.5.1986, coll. R. Ortal; 1 ♀ (CL 4.0 mm), Jordan River (Fig. 1, stn 116), 6.5.1981, coll. R. Ortal; 1 ♀ (CL 4.2 mm) and 1 ♂ (CL 3.8 mm), NHM 1938.1.26.8.12, Jordan River, 26.1.1938. **Jordan:** 2 ♀♀ (1 ovig.) (CL 4.0–4.9 mm), SMF 12057, Al-Azraq Oasis (Fig. 1, stn 117), 24.3.1977, coll. H. Damian. **Iraq:** 12 ♀♀ (CL 5.6–6.8 mm) and 3 ♂♂ (CL 4.5–4.8 mm), Basrah, Garmat Ali marsh (Fig. 1, stn 118), 24.2.1987, coll. A.H.Y. Al-Adhub; 1 ♀ (CL 5.2 mm), NHM 1919.11.14.5–20, Basrah, Shatt Al-Arab River (Robat creek) (Fig. 1, stn 119), 14.11.1919, coll. Capt. Boulenger; 1 ♂ (CL 4.2 mm), NHM 1919.4.28.2–3, Basrah, Shatt Al-Arab River (Robat creek), 28.4.1919, coll. P.J. Barraud; 4 ♀♀ (1 ovig.) (CL 5.2–5.5 mm) and 1 ♂ (CL 4.8 mm), Basrah, Shatt Al-Arab River (Fig. 1, stn 120), 2011, coll. M.D. Naser; 1 ovig. ♀, NHM 1919.11.12.11, Amarah, Tigris River (Fig. 1, stn 121), 12.11.1919, coll. J.O. Cooper Esq.

Amendments to description. Rostrum long, slender, dorsal margin straight, slightly or strongly curved in the middle and pointed upwards or downwards, 6.0–10.0, most frequently (91% of the individuals examined) 6.5–9.25, × as long as high,

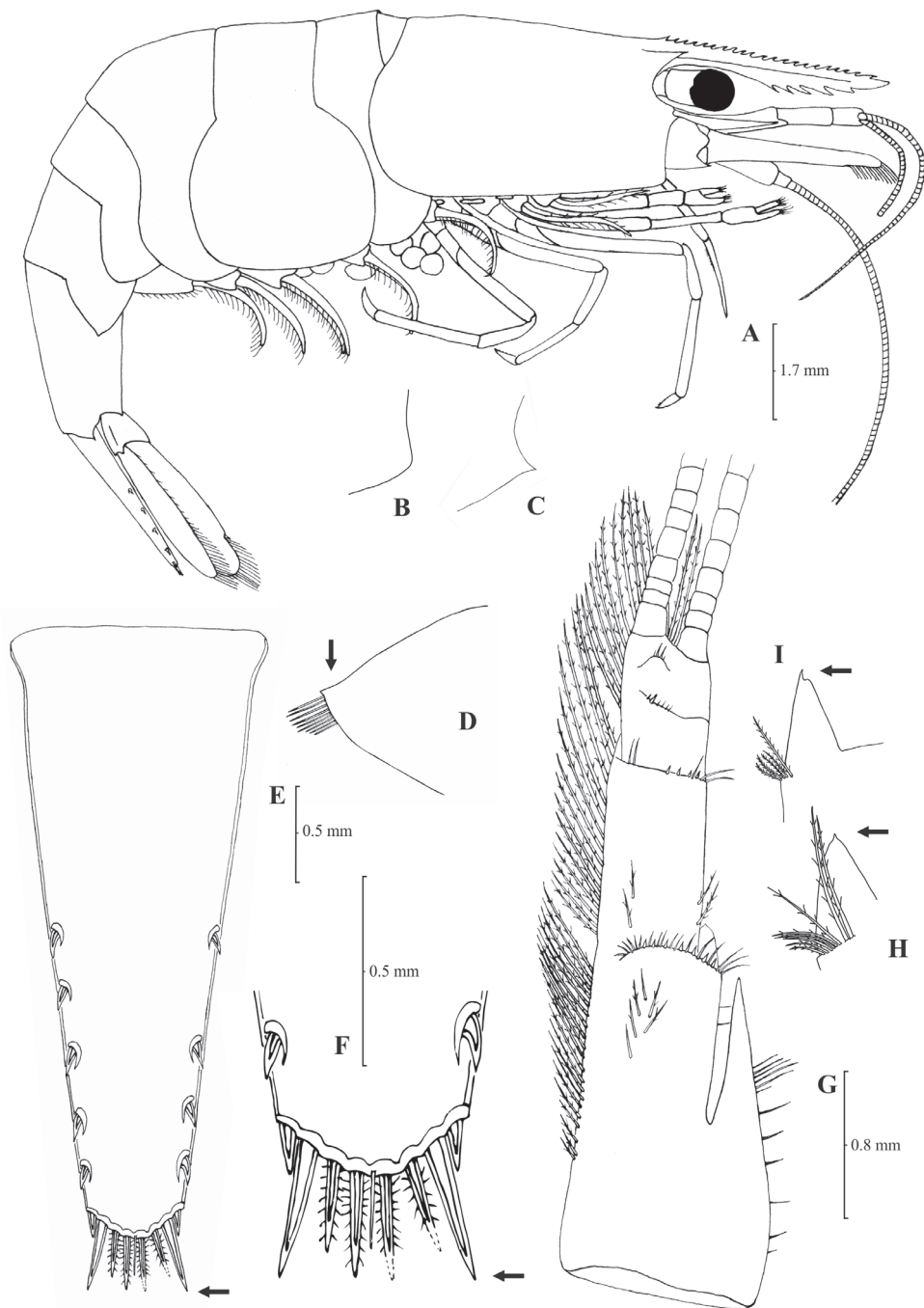


Figure 3. *Atyaephyra orientalis* Bouvier, 1913, adult ovig. ♀ (SMF 12050): **A** entire individual **B** detail of pterygostomial boarder **C** detail of pterygostomial boarder (adult ♀, SMF 12050) **D** right pleuron of fifth abdominal segment **E** telson **F** distal margin of telson **G** right antennular peduncle **H** right antennular lobe **I** right antennular lobe (adult ♀, SMF 12050).

shorter or equal to, or longer than scaphocerite (longer in 71% of the individuals examined). 14–29 (18–23 in 80% of the individuals) pre orbital teeth on dorsal margin of rostrum arranged to tip. 0–3, most often (85%) 1–3, post-orbital teeth. 3–13 teeth, mostly (96%) 4–10, arranged on ventral margin of rostrum (Fig. 3A). Carapace smooth with pterygostomial angle not protruding and rounded or bluntly produced (Figs 3B–C). Pleuron of fifth abdominal segment pointed ending in an acute or an obtuse posterior angle (Fig. 3D). Telson with 3–6, predominantly (93%) 4–5, pairs of dorsal spines arranged in curved fashion (Fig. 3E). Distal border of telson with 7–12, most often (91%) 8–10, spines (4–5 pairs) arranged in a fork-like or a fan-like way. Outermost pair of spines shortest, similar to dorsal spines, adjacent pair stronger terminating beyond, along with or before (beyond and along with in 64% of the individuals) the inner finely setulose pairs (Figs 3E–F). Basal segment of antennular peduncle with long stylocerite, with its tip failing to reach, reaching or overreaching the distal end of basal segment. Anterolateral lobe of basal segment short and pointed (Figs 3H–I). Distal segment of antennular peduncle with 0–3, most often (93%) 1–2, spines (Fig. 3G). Basal lower endite of maxilla densely covered with long simple setae arranged in 11–16 (12–15 in 93% of the individuals) oblique parallel rows. Endite of maxilla 1.75–2.20, mostly (93%) 1.81–2.07, \times as long as basal lower endite (Fig. 4G). Basal endite of first maxilliped failing or reaching to distal end of exopod distal margin (Fig. 4F). Distal one-third of terminal segment of third maxilliped bearing 10–36 (14–31 in 84% of the individuals), mesial spines and one subdistal lateral spine near the base of larger terminal spine (Fig. 4H). Armature along flexor margin of dactylus of third and fourth pereopod consisting of 6–11 (7–10 in 97% of the individuals) and 7–11 (8–10 in 89% of the individuals) spines (including terminal spine) respectively (Figs 4B, 4D). Merus of third and fourth pereopod with 6–10 (7–9 in 85% of the individuals) and 5–9 (6–7 in 83% of the individuals) spines respectively (Figs 4A, 4C). Dactylus of fifth pereopod with 33–55 (36–49 in 83% of the individuals) spines arranged in comb-like fashion on flexor margin (Fig. 4E). Endopod of first male pleopod expanded proximally with a distal portion stout and not tapering, often, with a, large protruding lobe in its outer subdistal part. Endopod with 13–38 spines arranged on a strongly curved inner margin and 5–8 setae arranged on outer margin (Fig. 4I, Bouvier et al. 1913: Fig. 1). 32–158 eggs of 0.5–0.75 \times 0.35–0.5 mm in size.

Size. *A. orientalis* is a small-medium sized species of *Atyaephyra*, with maximum carapace length to be 4.8 mm in ♂♂, 6.8 mm in ♀♀ and 5.5 mm in ovig. ♀♀.

Molecular characters. *A. orientalis* can be differentiated from all other species of *Atyaephyra* by molecular characters, as demonstrated by the phylogenetic analysis of mtDNA COI sequences. Additionally, 5 haplotypes, each from a different location, found in *A. orientalis* were not shared by any other species of the genus. It also differs from all the other species in the following nucleotide positions in the COI gene of *A. desmarestii* specimen Dour1, position 273: guanine (G), position 276: guanine (G) and position 369: cytosine (C).

Distribution. *Atyaephyra orientalis* is found in freshwater habitats of Middle East, from Turkey to Iraq (see material examined and Fig. 1).

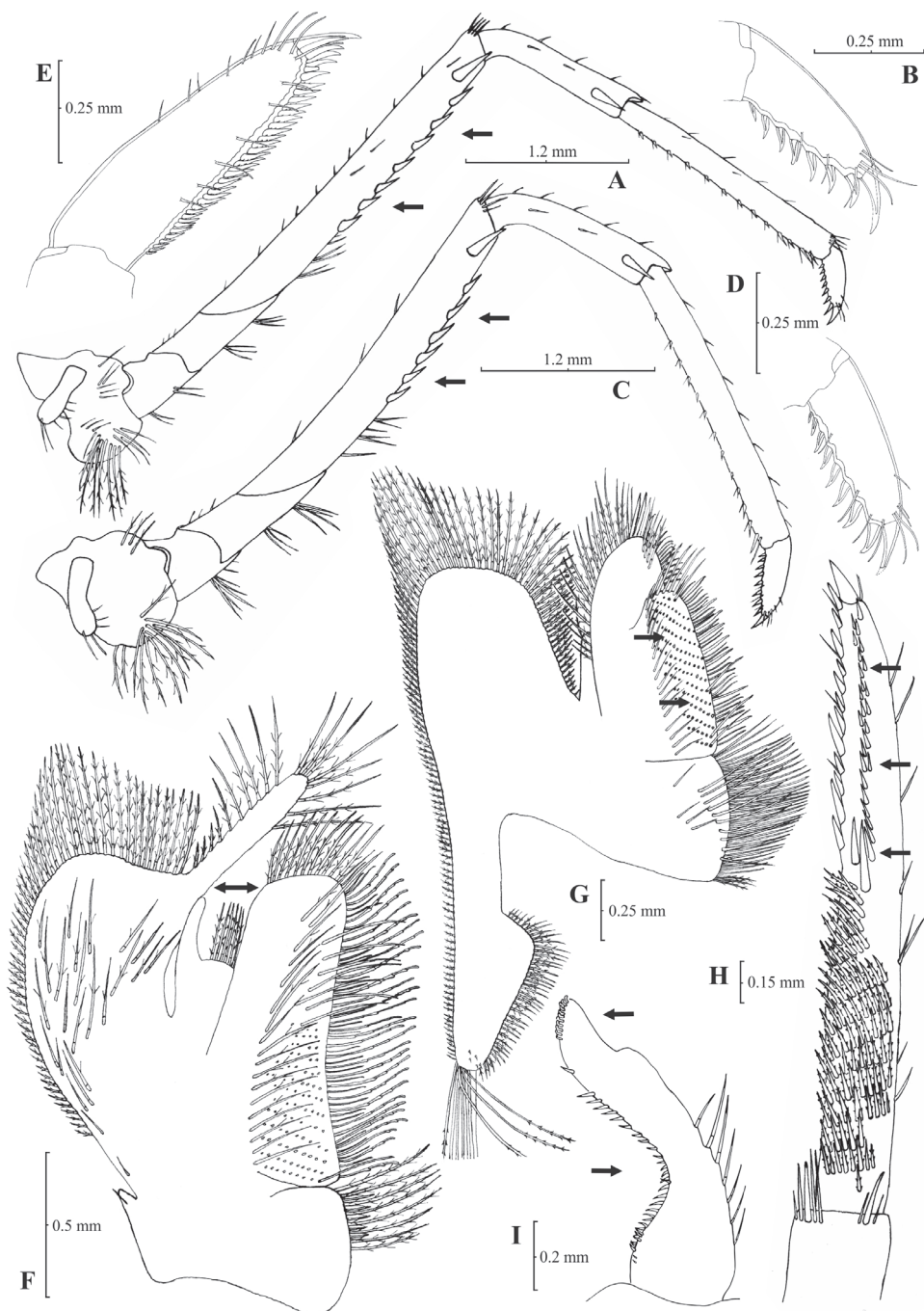


Figure 4. *Atyaephyra orientalis* Bouvier, 1913, adult ovig. ♀ (SMF 12050): **A** right third pereiopod **B** dactylus of third pereiopod **C** right fourth pereiopod **D** dactylus of fourth pereiopod **E** dactylus of right fifth pereiopod **F** right first maxilliped **G** right maxilla **H** right terminal segment of third maxilliped. Adult ♂ (SMF 12050): **I** right endopod of first male pleopod.

Remarks. Bouvier (1913) after examining the *Atyaephyra* material deposited in the MNHN collections he assigned it into two varieties (*A. d. var. orientalis* and *A. d. occidentalis*) based mainly on differences observed in the endopod of first male pleopod. *A. d. var. orientalis* was originally described from Syria (from Orontes River, near the Lake Qattinah (Lake Homs), from a stream in Kousseir (probably Qoussair) near Damascus and from Barada River, Ataibe, East of Damascus) and was elevated to subspecies level by Holthuis (1961). Apart from *A. d. orientalis*, a second subspecies, *A. d. mesopotamica*, was found to exist in the Middle East and was described by Al-Adhub (1987). Al-Adhub (1987) described the new subspecies based on the presence of a distinct subterminal process (vs. absent from *A. d. orientalis* and *A. d. desmarestii*) and the presence of 50 spines on dactylus of fifth pereopod (vs. 40 in *A. d. orientalis* and *A. d. desmarestii*). Furthermore he noticed that the rostrum of *A. d. mesopotamica* resembles that of *A. d. desmarestii* from Greece but differs in having the distal ventral part always devoid of teeth. Indeed the individuals from Shatt Al-Arab River had the highest number of spines on dactylus of fifth pereopod ranging from 41–55 but specimens from the River Orontes were also found with up to 47 spines (33–47). Additionally, male individuals having endopod with a distinct subterminal process were found again in River Orontes as well as in other Middle East Rivers. Gorgin (1996), after studying 150 males from two different localities in Iran found individuals with a distinct subterminal process and without inside the same population. Finally, specimens from Greece belonging to *A. stankoi* (as the sample of Holthuis to which Al-Adhub refers to) were found to be also devoid of teeth in the distal part of the rostrum. Even in the illustration included in Holthuis (1961) work, the Greek specimen is devoid of teeth in the distal part of the ventral margin. Although the genetic distances within the *A. orientalis* phylogroup were high (0.9%–10.2%) no firm conclusion could be drawn whether the hypothesis of multiple species is valid or not. Sequences from Orontes River (topotypical location of *A. d. orientalis*) and from Shatt Al-Arab River (topotypical location of *A. d. mesopotamica*) presented a noticeable mean genetic divergence (5.0%) but still not strong enough to support the hypothesis of different species. Detailed future studies on the morphological and genetic variability within the *Atyaephyra* distributed throughout the Middle East will help clarify the relationships between the populations in this region. However, only one species is currently considered to exist, *A. orientalis*. Therefore, *A. d. mesopotamica* is here proposed as a synonym.

Atyaephyra orientalis appears to be morphologically more similar to *A. stankoi* and *A. thyamisensis* sp. n. by sharing characters such as the presence of numerous mesial spines (10–38) on terminal segment of third maxilliped (Figs 4H, 6H, 8H). It also shares in common with the other two species the presence of fewer rows of setae (12–16) on basal lower endite of maxilla, the endite of maxilla being 1.75–2.24 × as long as basal lower endite (Figs 4G, 6G, 8G) and basal endite of first maxilliped failing or reaching to distal end of exopod distal margin (Figs 4F, 6F, 8F). *Atyaephyra orientalis* can be separated from *A. thyamisensis* sp. n. and *A. stankoi* by the presence of a pointed antennular lobe (Figs 3H–I) (vs. round in *A. stankoi* and *A. thyamisensis* sp. n. Figs 5H, 7H). Further, *A. orientalis* can be distinguished by the strongly curved and distally

stout and not tapering endopod of male first pleopod (Fig. 4I) (vs. slightly curved and distally more or less elongated but always tapering in *A. stankoi*, Fig. 6I; slightly or strongly curved but always its distal part is elongated and tapering (ribbon shaped) in *A. thyamisensis* sp. n., Fig. 8I). *Atyaephyra orientalis* differs from the other four species of *Atyaephyra* in having 10–36 spines on terminal segment of third maxilliped (Fig. 4H) (vs. 0–8 in *A. desmarestii*, *A. strymonensis* sp. n., *A. acheronensis* sp. n. and *A. tuerkayi* sp. n. Figs 10H, 12H, 14H).

***Atyaephyra stankoi* Karaman, 1972**

http://species-id.net/wiki/Atyaephyra_stankoi

Figs 5–6

Atyaephyra Desmaresti var. *occidentalis* Bouvier, 1913: 65–74, Figs 2I, 3I, partim.

Atyaephyra desmarestii desmarestii. – Holthuis 1961: 5–10, Figs 2B, 3B, partim.

Atyaephyra desmarestii stankoi Karaman, 1972: 81–84, Figs 3, 6, 9, 10 [type locality: Doirani Lake, Greece].

Atyaephyra desmarestii. – Anastasiadou et al. 2004: 5–13, partim

Atyaephyra stankoi. – Garcia Muñoz et al. 2009: 32–42, partim

Atyaephyra sp. n. 3. – Christodoulou et al. 2010: partim

Material examined. Type material. Neotype: NHM 2012.1475, adult ♀ (CL 6.0 mm), Greece–F.Y.R.O.M., Doirani Lake, (Fig. 1, stn 99), among aquatic plants, 9.11.1992, coll. S. Jovanovich and E. Stojkoska [here designated].

Non-type material. Greece: 4 ♀♀ (CL 5.4–5.9 mm), Peloponnesus, Alfeios River (Fig. 1, stn 82), 24.9.2001, coll. Ch. Anastasiadou; 4 ♀♀ (CL 5.4–5.7 mm), Aitoloacarnania, Ozeros Lake (Fig. 1, stn 83), 22.11.2001, coll. Ch. Anastasiadou; 2 ovig. ♀♀ (CL 5.5–7.0 mm), Aitoloakarnania, Aitoliko, Acheloos River (Fig. 1, stn 84), 4.4.2002, coll. Ch. Anastasiadou; 3 ♀♀ (CL 5.0–5.5 mm), Aitoloakarnania, Trichonida Lake (Fig. 1, stn 85), 22.10.2001, coll. Ch. Anastasiadou; 4 ♀♀ (CL 5.1–6.5 mm) Aitoloacarnania, Lysimachia Lake (Fig. 1, stn 86), 22.11.2001, coll. Ch. Anastasiadou; 1 ♀ (CL 6.9 mm) and 2 ♂♂ (CL 5.1–5.3 mm), Thessalia, Tavropou Lake (Fig. 1, stn 87), 14.11.2001, coll. Ch. Anastasiadou; 17 ♀♀ (CL 6.0–8.0) and 2 ♂♂ (CL 5.0 mm), Thessalia, Enipeas River (Fig. 1, stn 88), 14.10.2001, coll. Ch. Anastasiadou; 3 ♀♀ (CL 6.5–7.6 mm) and 1 ♂ (CL 5.5 mm), ZMAUTH G1-910, Thessalia, Mati Tyrnavou Lake (Fig. 1, stn 89), 15.11.1977, coll. A. Koukouras; 1 ♀ (CL 6.8 mm) and 1 ♂ (CL 5.2 mm) Thessalia, Pineios River (Fig. 1, stn 90), 15.11.2001, coll. Ch. Anastasiadou; 1 ♀ (CL 7.0 mm), Thessalia, Lithaios River (Fig. 1, stn 91), 14.11.2001, coll. Ch. Anastasiadou; 5 ♀♀ (CL 6.0–7.0 mm) and 1 ♂ (CL 5.0 mm), Thessalia, Gritsas River (Fig. 1, stn 92), 15.11.2001, coll. Ch. Anastasiadou; 3 ♀♀ (CL 6.0–6.7 mm), Macedonia, Aliakmonas River (Fig. 1, stn 93), 9.9.1974 and 26.11.1978; 4 ♀♀ (2 ovig.) (CL 5.7–6.8 mm), ZMAUTH G1-1005, Macedonia, Vegoritida Lake (Fig. 1, stn 94), 17.6.1968; 4 ♀♀ (1 ovig.) (CL 5.5–6.3 mm), ZMAU-

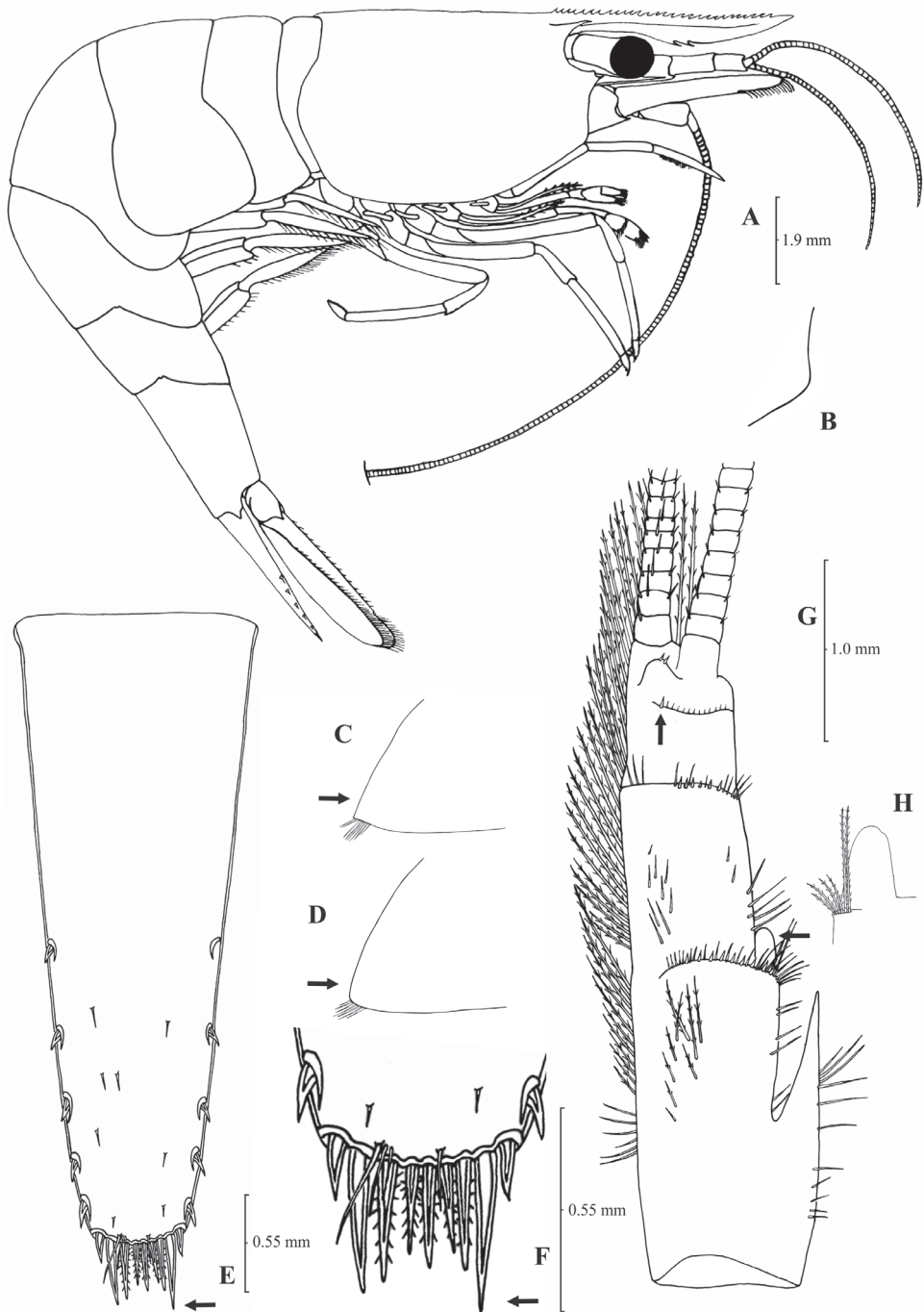


Figure 5. *Atyaephyra stankoi* Karaman, 1972. Neotype, adult ♀ (NHM 2012.1475): **A** entire individual **B** right detail of pterygostomial boarder **C** right pleuron of fifth abdominal segment **D** right pleuron of fifth abdominal segment (adult ♀) **E** telson **F** distal margin of telson **G** right antennular peduncle **H** right antennular lobe.

TH G1-1018, Thessalia, Agra Lake (Fig. 1, stn 95), 17.6.1968, coll. P. Economides; 12 ♀♀ (CL 5.5–7.0 mm) and 3 ♂♂ (CL 5.0–5.5 mm), Thessalia, Edessaïos River (Fig. 1, stn 96), 19.10.2001, coll. Ch. Anastasiadou; 5 ♀♀ (CL 5.0–5.5 mm) and 1 ♂ (CL 5.0 mm), Thessalia, Kariotissa, Moglenitsa River (Fig. 1, stn 97), 18.10.2001, coll. Ch. Anastasiadou; 4 ♀♀ (CL 6.0–7.0 mm) and 1 ♂ (CL 5.0 mm), ZMAUTH G1-988, Macedonia, Axios River (Fig. 1, stn 98), 16.7.1971, coll. P. Economides; 11 ♀♀ (CL 5.9–7.3 mm) and 1 ♂ (CL 5.1 mm), Macedonia, Richios River (Fig. 1, stn 100), 26.10.01, coll. Ch. Anastasiadou; **Greece–F.Y.R.O.M.:** 4 ♀♀ (CL 5.0–5.7 mm), Doirani Lake, (Fig. 1, stn 99), 9.11.1992, coll. S. Jovanovich and E. Stojkoska.

Description. Rostrum long, slender, dorsal margin straight or slightly curved in the middle and pointed upwards, 6.12–8.67, mostly (83% of the examined individuals) 6.25 to 7.54, × as long as high, shorter, equal to, or longer than scaphocerite (longer in 76% of the individuals examined). From 17 to 28 (19–27 in 91% of the individuals) pre orbital teeth on dorsal margin of rostrum arranged up to tip. 0–3, predominantly (96%) 1–3, post-orbital teeth. 2–8, most often (96%) 2–6, teeth arranged on ventral margin of rostrum (Fig. 5A). Carapace smooth with pterygostomial angle not protruding, rounded (Fig. 5B). Pleuron of fifth abdominal segment usually pointed ending in an obtuse (ending in an acute angle in 11% of the individuals) posterior angle (Figs 5C–D). Telson with 3–6, most often (93%) 5–6, pairs of dorsal spines arranged in curved fashion (Fig. 5E). Distal border of telson with 6–11, mostly (87%) 8–10, spines (3–6 pairs), arranged in a fork-like pattern. Outermost pair of spines shortest, similar to dorsal spines, adjacent pair stronger terminating beyond (or along with) the inner finely setulose pairs (Figs 5E–F). Basal segment of antennular peduncle with long stylocerite, with its tip failing to reach, reaching or overreaching the distal end of basal segment. Anterolateral lobe of basal segment short and rounded (Fig. 5H). Distal segment of antennular peduncle with 1–4, mostly (93%) 1–3, spines (Fig. 5G). Basal lower endite of maxilla densely covered with long simple setae arranged in 12–16, (13–15 in 89% of the individuals), oblique parallel rows. Endite of maxilla 1.78–2.08, mostly (89%) 1.84–1.99, × as long as basal lower endite (Fig. 6G). Basal endite of first maxilliped failing or reaching to distal end of exopod (Fig. 6F). Distal one-third of terminal segment of third maxilliped bearing 11–35, frequently (85%) 16–28, mesial spines and one subdistal lateral spine near the base of larger terminal spine (Fig. 6H). Armature along flexor margin of dactylus of third and fourth pereopod consisting of 7–11 (7–9 in 98% of the individuals) and 7–10 (7–9 in 98% of the individuals) spines (including terminal spine) respectively (Figs 6B, 6D). Merus of third and fourth pereopod with 3–8 (4–6 in 83% of the individuals examined) and 2–6 (3–5 in 88% of the individuals) spines respectively (Figs 6A, 6C). Dactylus of fifth pereopod with 26–47, most often (80%) 32–41, spines arranged in comb-like fashion on flexor margin (Fig. 6E). Endopod of first male pleopod expanded proximally and with a distal portion either elongated (ribbon shape) or more stout but always tapering. Endopod with 13–17 spines arranged on a slightly curved inner margin and 7–12 setae arranged on the outer margin (Fig. 6I). 96–195 eggs of 0.6–0.7 × 0.4 mm in size.

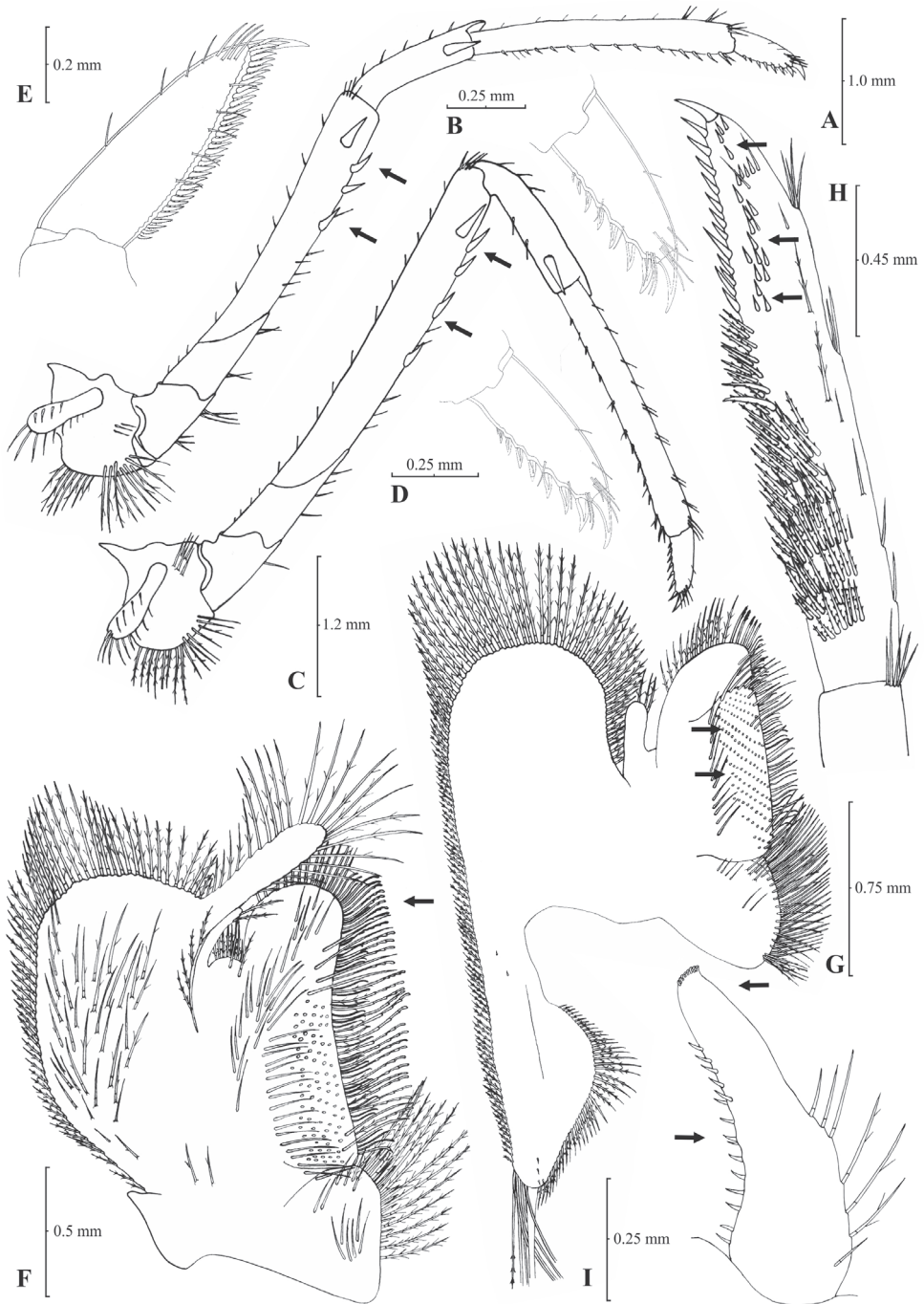


Figure 6. *Atyaephyra stankoi* Karaman, 1972. Neotype, adult ♀ (NHM 2012.1475): **A** right third pereiopod **B** dactylus of third pereiopod **C** right fourth pereiopod **D** dactylus of fourth pereiopod **E** dactylus of fifth pereiopod **F** right first maxilliped **G** right maxilla **H** right terminal segment of third maxilliped. Adult ♂ (ZMAUTH G1 988): **I** right endopod of first male pleopod.

Size. *Atyaephyra stankoi* is a large sized species with maximum carapace length of 5.50 mm in ♂♂, 7.60 mm in ♀♀ and 6.8 mm in ovig. ♀♀.

Molecular characters. *Atyaephyra stankoi* can be distinguished from all other species of *Atyaephyra* by molecular characters, as shown by the phylogenetic analysis of mtDNA COI sequences, such as the two unique *A. stankoi* haplotypes. Furthermore, it differs from all the other species in the following nucleotide positions in the COI gene of *A. desmarestii* specimen Dour1, position 192: cytosine (C), position 282: adenine (A), position 320: cytosine (C), position 342: cytosine (C) and position 423: cytosine (C).

Distribution. *Atyaephyra stankoi* is found in freshwater habitats in the mainland of West-central Greece and South F.Y.R.O.M. (see material examined and Fig. 1).

Remarks. Bouvier (1913) assigned the material of MNHN originating from Portugal, France, Corsica, Macedonia, Tunisia, Algeria and Morocco to var. *occidentalis* while the material from Syria he assigned to var. *orientalis*. The material from Macedonia was collected from the region of Vardar (Axios) north of Thessaloniki, from the Lake of Amatovo (drained in the early twentieth century) near Kirdzalar (today called Adendron). The two varieties described by Bouvier were elevated in subspecies level by Holthuis (1961) and the var *occidentalis* was re-named to *A. desmarestii desmarestii* since it contained the name-bearing type of the species. Few years later, Karaman (1972) described a new subspecies from Doirani Lake which is part of the Vardar (Axios) basin and named it *A. desmarestii stankoi* ignoring the available name of Bouvier's (*A. d. var. occidentalis*). However, after designating a neotype of *A. desmarestii* from Bouvier's material the nomen *A. d. var. occidentalis* becomes unavailable since it becomes a junior synonym of *A. desmarestii* (see *A. desmarestii* remarks) and thus the nomen *A. stankoi* can be used for the Macedonian taxon (as used herein).

Efforts made to trace Karaman's type material in the MMNH were unsuccessful. According to the director of the Museum, Dr Petkovski S. (pers. comm.), Karaman's material is considered lost after a fire that took place in the Museum.

A neotype for *A. stankoi* is proposed for reasons of taxonomic clarification and stability, as foreseen by Art. 75 (ICZN, 1999). The neotype will contribute to the stability of the taxonomic status of the species and avoid further confusion due to nomenclature (see also *A. desmarestii* remarks). Furthermore, it incorporates novel characteristics that distinguish it from the remaining *Atyaephyra* species such as: having 11–35 mesial spines on terminal segment of third maxilliped, basal endite of first maxilliped failing or reaching to distal end of exopod, distal boarder of telson with spines arranged in a fork-like pattern, a rounded antennular lobe, a pterygostomial angle not protruding, and a slightly curved and distally more or less elongated but always tapering endopod of male first pleopod. The name-bearing types are considered lost while the neotype has been collected from Doirani Lake, the same locality from where Karaman (1972) collected *A. d. stankoi* type material and it will replace the lost type material.

A. stankoi is similar to *A. thyamisensis* sp. n. in having: 11–38 mesial spines on terminal segment of third maxilliped (Figs 6H, 8H), 12–16 rows of setae on basal lower endite of maxilla (Figs 6G, 8G), 3–6 pairs (mostly 4–5) of spines on distal boarder of telson with the second pair to be the strongest and terminating beyond (or along with)

the other pairs arranged in a fork-like pattern (Figs 5E–F, 7E–F), a rounded antennular lobe (Figs 5H, 7H) and the basal endite of first maxilliped failing or reaching to distal end of exopod (Figs 6F, 8F). *Atyaephyra stankoi* differs from *A. thyamisensis* sp. n. in not having a sharply protruding pterygostomial angle (Figs 5B, 7B). *A. stankoi* can be distinguished from *A. orientalis* by the presence of a rounded antennular lobe (Fig 5H) (vs. pointed in *A. orientalis*; Figs 3H–I). Further, *A. stankoi* can be distinguished by the slightly curved and distally more or less elongated but always tapering endopod of male first pleopod (Fig. 6I) (vs. strongly curved and distally stout and not tapering in *A. orientalis*; Fig. 4I). *A. stankoi* can be separated from *A. desmarestii*, *A. strymonensis*, *A. acheronensis* and *A. tuerkayi* by the presence of numerous mesial spines (11–35) on terminal segment of third maxilliped (Fig 6H) (vs 0–8 mesial spines; Figs 10H, 12H, 14H).

***Atyaephyra thyamisensis* sp. n.**

urn:lsid:zoobank.org:act:E57CE407-D38C-4EF2-B4AC-C0B9BEE6EFB1

http://species-id.net/wiki/Atyaephyra_thyamisensis

Figs 7–8

Atyaephyra desmarestii. – Anastasiadou et al. 2004: 5–13, partim; Anastasiadou et al. 2011: 41–54, Figs 1–6.

Atyaephyra sp. n. 1. – Christodoulou et al. 2008: Fig. 4B.

Atyaephyra sp. n. 3. – Christodoulou et al. 2010: Fig. 2, partim.

Material examined. Type material. Holotype: NHM 2012.1476, adult ovig. ♀ (CL 7.1 mm), Greece, Epirus, Thyamis River, 39°32.26'N, 20°09.76'E (Fig. 1, stn 76), among aquatic plants, 19.3.2005, coll. Ch. Anastasiadou; Allotype: NHM 2012.1477, adult ♂ (CL 5.3 mm), same data collection as holotype; Paratypes: NHM 2012.1478–1483, 4 ♀♀ (3 ovig.) (CL 6.0–6.8 mm) and 2 ♂♂ (CL 5.0–5.3 mm) same data collection as holotype. NHM 2012.1484–1485, 2 ♀ (CL 6.5–7.4 mm), Greece, Epirus, Louros River, 39°03.14'N, 20°46.26'E (Fig. 1, stn 72), among aquatic plants, 25.3.2012, coll. Ch. Anastasiadou. OUMNH.ZC 2012-08-001, 4 ♀♀ (2 ovig.) (CL 6.0–7.8 mm) and 2 ♂ (CL 5.2 mm) same data collection as holotype. SMF 43022, 4 ♀♀ (2 ovig.) (CL 5.8–7.1 mm) and 2 ♂♂ (CL 5.0–5.2 mm) same data collection as holotype. NHMW 25453, 4 ♀♀ (2 ovig.) (CL 5.5–7.5 mm) and 1 ♂♂ (CL 5.0 mm) same data collection as holotype

Non-type material. Greece: 2 ♀♀ (CL 5.2–5.5 mm), NHMW 462, Corfu Island (Fig. 1, stn 75), 1.9.1937, coll. Stephanides; 13 ♀♀ (1 ovig.) (CL 5.3–8.1 mm) and 8 ♂♂ (CL 5.2–6.2 mm), Epirus, Thyamis River (Fig. 1, stn 77), 20.5.2000 and 26.10.01, coll. Ch. Anastasiadou; 20 ♀♀ (15 ovig.) (CL 6.5–7.5 mm) and 3 ♂♂ (CL 5.0–5.7 mm), Epirus, Pamvotida Lake (Fig. 1, stn 78), 24.3.2006, coll. Ch. Anastasiadou; 20 ♀♀ (CL 5.0–7.0) and 8 ♂♂ (CL 5.0–5.5), Epirus, Ziros Lake (Fig. 1, stn 79), 28.10.2001, coll. Ch. Anastasiadou; 20 ♀♀ (CL 5.8–8.5 mm) and 4 ♂♂ (CL 5.2–6.4

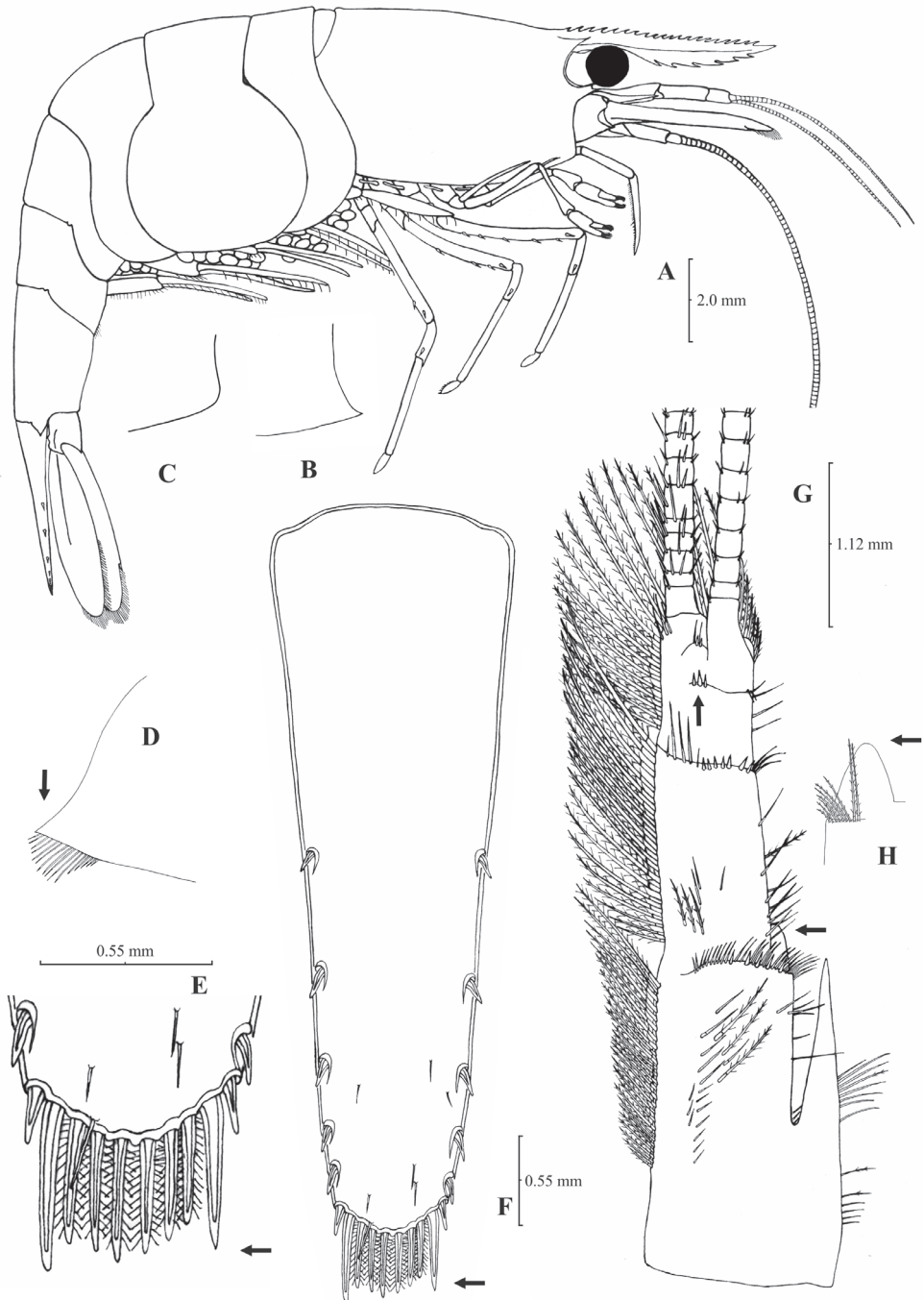


Figure 7. *Atyaephyra thymisensis* sp. n. Holotype, adult ovig. ♀ (NHM 2012.1476): **A** entire individual **B** detail of left pterygostomial boarder **C** detail of right pterygostomial boarder **D** right pleuron of fifth abdominal segment **E** telson **F** distal margin of telson **G** right antennular peduncle **H** right antennular lobe.

mm), ZMAUTH D-334, Epirus, Filipiada, Louros River (Fig. 1, stn 80), 20.10.1977, coll. P. Economides; 15 ♀♀ (CL 5.5–8.0) and 6 ♂♂ (CL 5.0–6.0), Louros River (Fig. 1, stn 80), 28.10.2001, coll. Ch. Anastasiadou; 8 ovig. ♀♀ (CL 6.4–8.0 mm) and 6 ♂♂ (CL 5.3–6.2 mm), NHMW 465, Lefkada Island, Kaligoni, Vardas River (Fig. 1, stn 81), Aug.1929, coll. Beier; 3 ovig. ♀♀ (CL 7.3–8.0 mm) and 3 ♂♂ (CL 5.0–5.9 mm), NHMW 466, Lefkada Island, Kaligoni, Vardas River (Fig. 1, stn 81), 2.10.1932, coll. Beier.

Description. Rostrum long, slender, dorsal margin straight or slightly curved in the middle and pointed upwards, shorter, equal to, or longer than scaphocerite, 6.0–9.50, most often (84% of the examined individuals) 6.33 to 8.76, \times as long as high. 18–27 (18–24 in 91% of the individuals) pre orbital teeth on dorsal margin arranged up to tip of rostrum. 0–2, predominantly (84%) 1–2, post-orbital teeth. 4–10 teeth, most often (87%) 5–8, arranged on ventral margin of rostrum (Fig. 7A). Carapace smooth with pterygostomial angle bluntly produced (Fig. 7B). Pleuron of fifth abdominal segment pointed with an acute posterior angle (Fig. 7D). Telson with 5–8, mostly (97%) 5–7, pairs of dorsal spines arranged in curved fashion (Fig. 7E). Distal border of telson with 8–12, mostly (86%) 8–10, spines (4–6 pairs) arranged in fork-like pattern. Outermost pair of spines shortest, similar to dorsal spines, adjacent pair stronger terminating beyond (or along with) the finely setulose inner pairs (Figs 7E–F). Basal segment of antennular peduncle with long stylocerite, with its tip reaching or overreaching the distal end of basal segment. Anterolateral lobe of basal segment short and round (Fig. 7H). Distal segment of antennular peduncle with 1–6, frequently (92%) 2–4, spines (Fig. 7G). Basal lower endite of maxilla densely covered with long simple setae arranged in 12–16 (13–15 in 80% of the individuals), oblique parallel rows. Endite of maxilla 1.84–2.24, mostly (93%) 1.89–2.05, \times as long as basal lower endite (Fig. 8G). Basal endite of first maxilliped failing or reaching to distal end of exopod (Fig. 8F). Distal third of terminal segment of third maxilliped bearing 13–38 (19–30 in 88% of the individuals) mesial spines and one subdistal lateral spine near the base of larger terminal spine (Fig. 8H). Armature along flexor margin of dactylus of third and fourth pereopod consisting of 6–9 (7–9 in 97% of the individuals) and 6–10 (7–9 in 97% of the individuals) spines respectively (Figs 8B, 8D). Merus of third and fourth pereopod with 3–7 (4–6 in 93% of the individuals) and 2–6 (4–5 in 96% of the individuals) spines respectively (Figs 8A, 8C). Dactylus of fifth pereopod with 28–43, usually (82%) 32–40, spines arranged in comb-like fashion on flexor margin (Fig. 8E). Endopod of first male pleopod expanded proximally and with a distal portion elongated (ribbon shaped) and tapering. Endopod with 14–21 spines arranged on a slightly or strongly curved inner margin and 12–18 setae arranged on outer margin (Fig. 8I). 172–465 eggs of 0.60–0.7 \times 0.40–0.45 mm in size.

Size. *Atyaephyra thymisensis* sp. n. is a large sized species with a maximum carapace length of 6.4 mm in ♂♂, 8.0 mm in ♀♀ and 8.1 mm in ovig. ♀♀.

Molecular characters. *A. thymisensis* sp. n. is different from all the other species of *Atyaephyra* by molecular characters, as shown by the phylogenetic analysis of mtDNA COI sequences. The one haplotype found was unique in the genus. Furthermore,

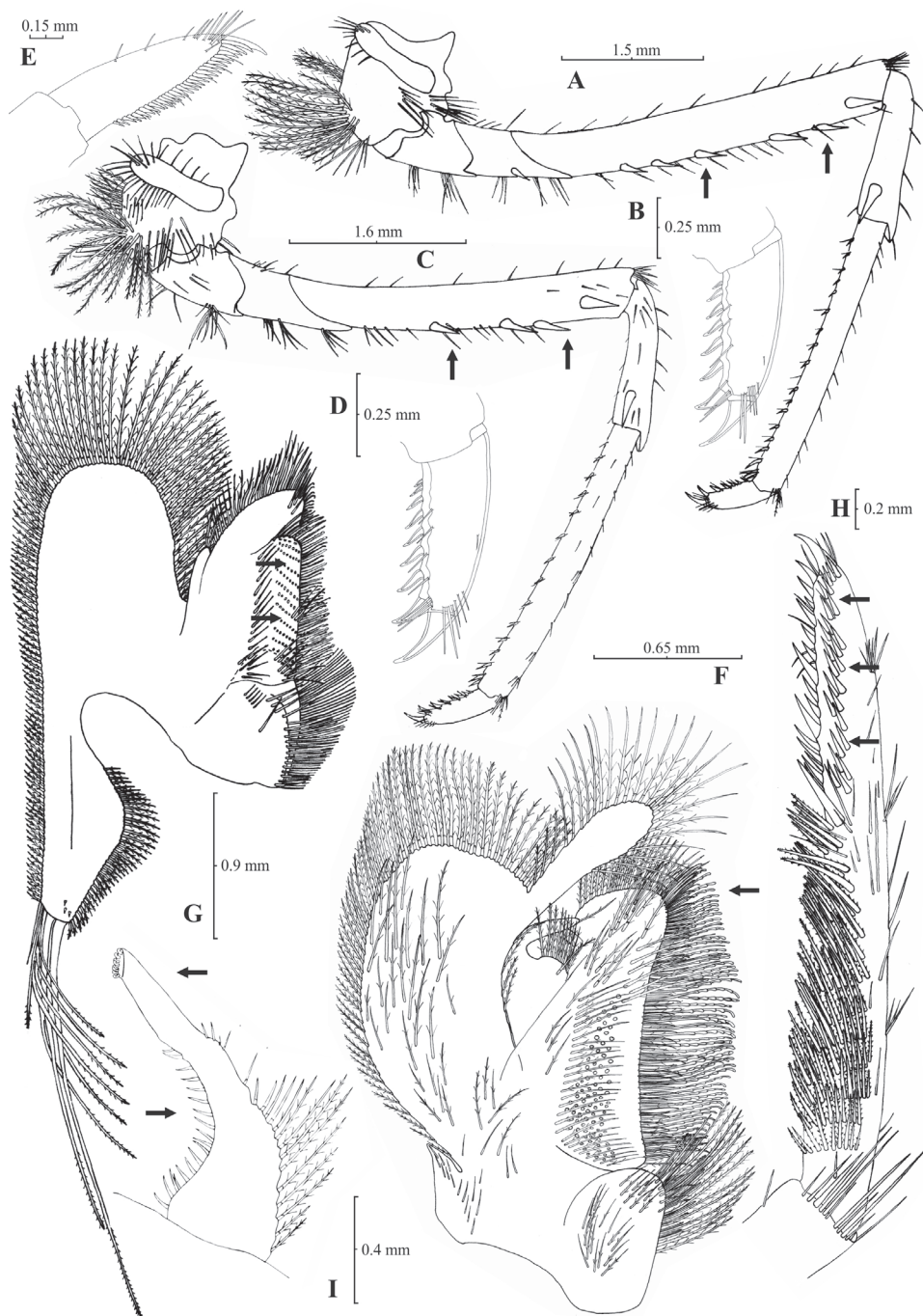


Figure 8. *Atyaephyra thymisensis* sp. n. Holotype, adult ovig. ♀ (NHM 2012.1476): **A** right third pereiopod **B** dactylus of third pereiopod **C** right fourth pereiopod **D** dactylus of fourth pereiopod **E** right dactylus of fifth pereiopod **F** right first maxilliped **G** right maxilla **H** right terminal segment of third maxilla **I** right endopod of first male pleopod. Allotype, adult ♂ (NHM 2012.1477): **I** right endopod of first male pleopod.

it differs from all the other species in the following nucleotide positions in the COI gene of *A. desmarestii* specimen Dour1, position 172: cytosine (C), position 207: cytosine (C), position 249: guanine (G), position 258: cytosine (C), position 324: guanine (G), position 348: guanine (G) and position 387: cytosine (C).

Etymology: *Atyaephyra thyamisensis* sp. n. is named after the Thyamis River, Greece, the type locality.

Distribution. *Atyaephyra thyamisensis* sp. n. is found in fresh water habitats of North-west Greece as well as in the islands Corfu and Lefkada (see material examined and Fig. 1).

Remarks: *A. thyamisensis* can be discriminated from *A. stankoi* by the presence of a sharply protruding pterygostomial angle (Fig. 7B). It should be noted that this character has been observed to be missing from one side (either the left or the right) in some very large sized individuals (Fig. 7C). This character is shared by *A. orientalis* (present in some populations) along with the presence of numerous spines (10–38) on terminal segment of third maxilliped (Figs 4H, 8H) and the presence of fewer rows of setae (12–16) on basal lower endite of maxilla (Figs 4G, 8G). The two species can be distinguished by the presence of a rounded antennular lobe in *A. thyamisensis* (Figs 7G–H) (vs. pointed in *A. orientalis*; Figs 3G–I). Further, *A. thyamisensis* can be distinguished by the slightly or strongly curved endopod of first male pleopod having its distal part always elongated and tapering (ribbon shaped; Fig. 8I) (vs. strongly curved and distally stout and not tapering in *A. orientalis*; Fig. 4I). *A. thyamisensis* can be separated easily from the remaining three species of *Atyaephyra* by the presence of numerous mesial spines (13–38; Fig. 8H) on terminal segment of third maxilliped (vs. 0–8 mesial spines in *A. desmarestii*, *A. strymonensis*, *A. acheronensis* and *A. tuerkayi*; Figs 10H, 12H, 14H).

***Atyaephyra strymonensis* sp. n.**

urn:lsid:zoobank.org:act:A0C25BDC-4FB3-4C41-A507-5FA0BF6BCFC7

http://species-id.net/wiki/Atyaephyra_strymonensis

Figs 9–10

Atyaephyra desmarestii. – Anastasiadou et al. 2004: 5–13, partim; Sket and Zaksek 2009: 786–818.

Atyaephyra sp. n. 3. – Christodoulou et al. 2008.

Atyaephyra sp. n. 4. – Christodoulou et al. 2010: Fig. 2.

Material examined. Type material. Holotype: NHM 2012.1486, adult ovig. ♀ (CL 7.0 mm), Greece, Macedonia, Mylopotamos Springs (Strymonas River), 41°08.90'N, 24°04.29'E (Fig. 1, stn 102), among aquatic plants, 23.5.2011, coll. M. Christodoulou and M.S. Kitsos. Allotype: NHM 2012.1487, adult ♂ (CL 5.0 mm), same data collection as holotype. Paratypes: NHM 2012.1488–1492, 4 ♀♀ (CL 5.2–7.0 mm) and 1 ♂ (CL 5.0 mm) same data collection as holotype. OUMNH.ZC 2012-08-002 4 ♀♀

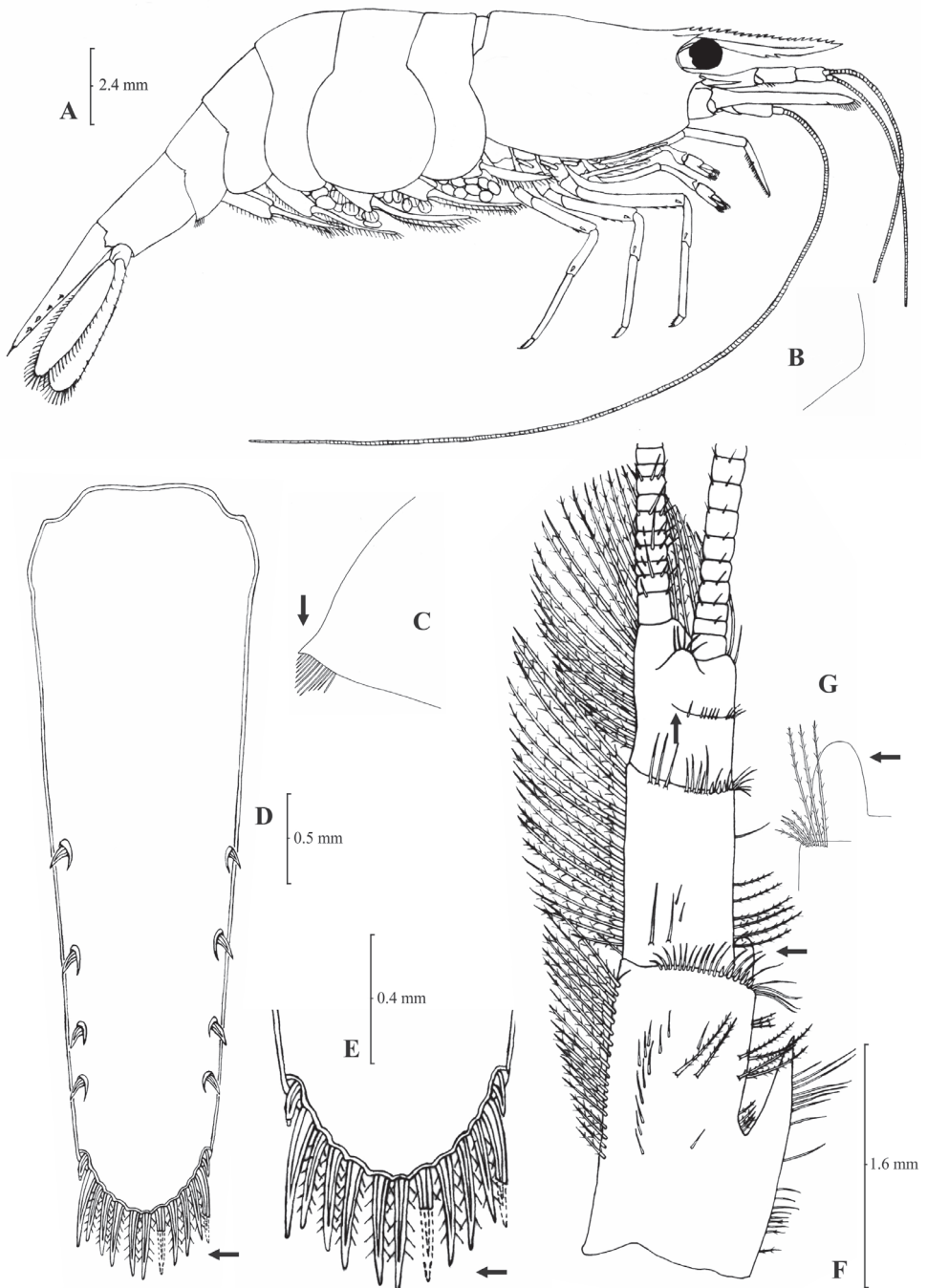


Figure 9. *Atyaephyra strymonensis* sp. n. Holotype, adult ovig. ♀ (NHM 2012.1486): **A** entire individual **B** detail of right pterygostomial boarder **C** right pleura of fifth abdominal segment **D** telson **E** distal margin of telson **F** right antennular peduncle **G** right antennular lobe.

(1 ovig.) (CL 5.2–7.0 mm) and 1 ♂ (CL 5.0 mm) same data collection as holotype; SMF 43023 2 ♀♀ (CL 6.7–7.2 mm) and 1 ♂ (CL 5.0 mm) same data collection as holotype; NHMW 25454, 2 ♀♀ (CL 6.1–7.3 mm) same data collection as holotype.

Non-type material. Greece: 3 ♀♀ (CL 5.4–6.0 mm) Macedonia, Strymonas River (Fig. 1, stn 101), 1.10.2001, coll. Ch. Anastasiadou; 20 ♀♀ (13 ovig.) (CL 6.3–7.9 mm), Macedonia, Mylopotamos Springs (Fig. 1, stn 102), 4.4.2001, coll. Ch. Anastasiadou; 9 ♀♀ (CL 5.5–7.1 mm) and 5 ♂♂ (CL 5.1–5.3 mm) Macedonia, Agias Varvaras Springs (Fig. 1, stn 103), 4.4.2001, coll. Ch. Anastasiadou; 11 ♀♀ (4 ovig.) (CL 6.0–7.4 mm) and 3 ♂♂ (CL 5.1–5.3 mm), Macedonia, Kefalariou Springs (Fig. 1, stn 104), 4.5.2001, coll. Ch. Anastasiadou; 2 ♀♀ (CL 6.3 mm) and 2 ♂♂ (CL 5.3–5.6 mm), Thrace, Paradeisos, Nestos River (Fig. 1, stn 105), ZMAUTH G1-1024, 6.7.1972, coll. P. Economides; 14 ♀♀ (CL 5.5–7.3 mm) and 6 ♂♂ (CL 5.1–5.5 mm) Thrace, Kyrnos, Nestos River (Fig. 1, stn 106), 30.9.2002, coll. Ch. Anastasiadou.

Description. Rostrum long, slender, dorsal margin straight or slightly curved in the middle and pointed upwards, 5.89–8.80, mostly (92% of the individuals examined) 6.75–8.80, × as long as high, shorter, equal to, or longer than scaphocerite. 10–29, frequently (92%) 14–23, pre orbital teeth on dorsal margin of rostrum arranged up to tip. Rostrum without post-orbital teeth, leaving a short unarmed proximal gap. With maximally five teeth, mostly (91%) up to three, arranged on ventral margin of rostrum (Fig. 9A). Carapace smooth with pterygostomial angle, not protruding, rounded (Fig. 9B). Pleuron of fifth abdominal segment pointed with an acute posterior angle (Fig. 9C). Telson with 2–7, predominantly (97%) 3–4, pairs of dorsal spines arranged in curved fashion (Fig. 9D). Distal border of telson with 11–15, usually (96%) 12–14, spines (6–8 pairs), arranged in fan-like way. Outermost pair of spines shortest, similar to dorsal spines, adjacent pair stronger terminating before the finely setulose inner pairs (Figs 9D–E). Basal segment of antennular peduncle with long stylocerite, with its tip failing to reach or reaching the distal end of basal segment. Anterolateral lobe of basal segment short and round (Fig. 9G). Distal segment of antennular peduncle with 0–1 but mostly (87%) with no spines (Fig. 9F). Basal lower endite of maxilla densely covered with long simple setae arranged in 12–17 (14–16 in 90% of the individuals), oblique parallel rows. Endite of maxilla 1.77–1.95, mostly (89%) 1.78–1.91, × as long as basal lower endite (Fig. 10G). Basal endite of first maxilliped failing, reaching or overreaching the distal end of exopod (reaching the end in 65% of the individuals) (Fig. 10F). Distal one-third of terminal segment of third maxilliped bearing 1–7 mesial spines and one subdistal lateral spine near the base of larger terminal spine (Fig. 10H). Armature along flexor margin of dactylus of third and fourth pereopod consisting of 6–8 (7–8 in 96% of the individuals) and 7–8 spines (including terminal spine) respectively (Figs 10B, 10D). Merus of third and fourth pereopod with 3–6 (3–5 in 90% of the individuals) and 3–5 spines respectively (Figs 10A, 10C). Dactylus of fifth pereopod with 25–37, mostly (87%) 30–35, spines arranged in comb-like fashion on flexor margin (Fig. 10E). Endopod of first male pleopod expanded proximally and with a distal portion elongated and tapering, often, with a small, protruding lobe in its outer subdistal part. Endopod with 14–23 spines arranged on a slightly curved

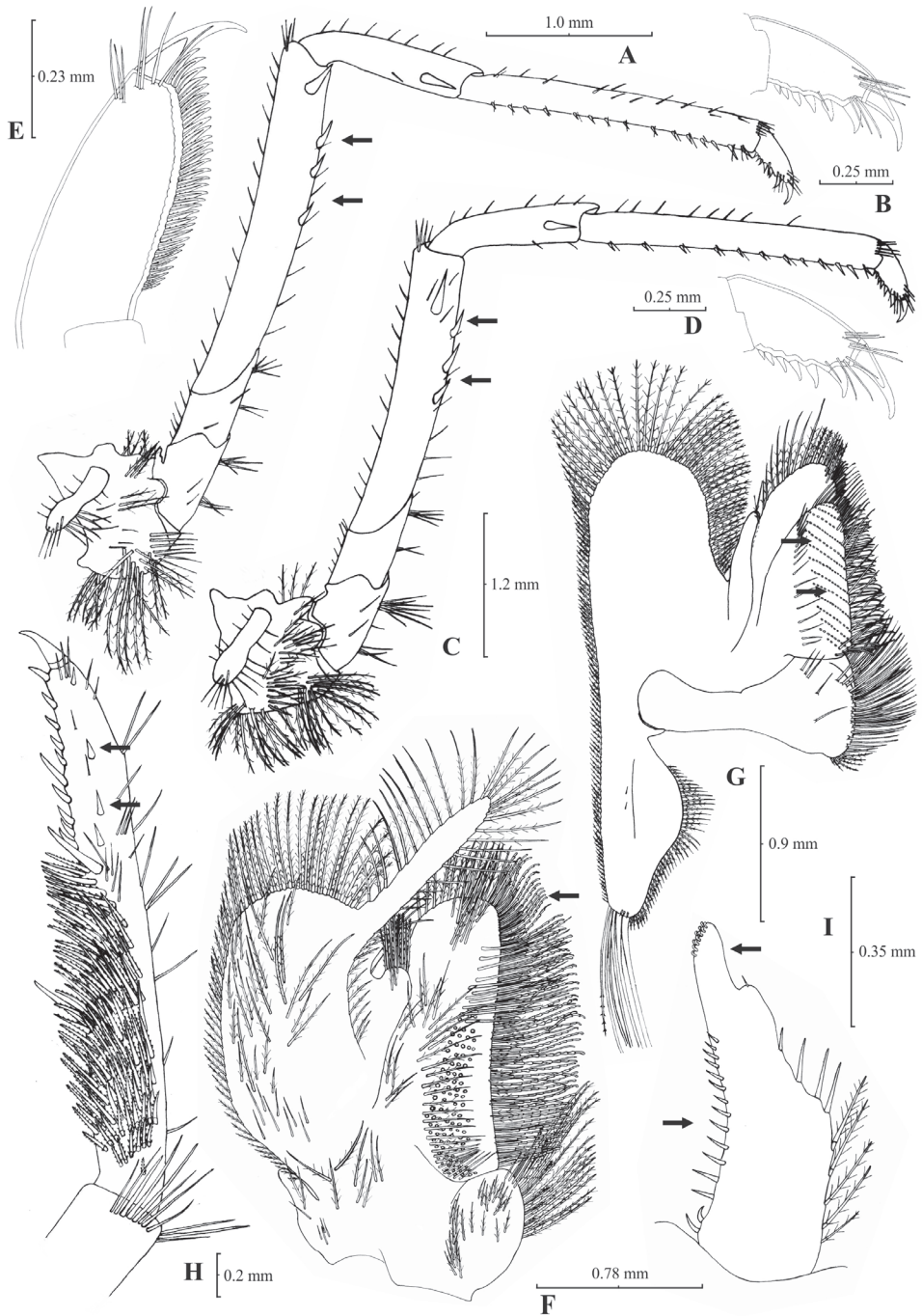


Figure 10. *Atyaephyra strymonensis* sp. n. Holotype, adult ovig. ♀ (NHM 2012.1486): **A** right third pereiopod **B** dactylus of third pereiopod **C** right fourth pereiopod **D** dactylus of fourth pereiopod **E** dactylus of fifth pereiopod **F** right first maxilliped **G** right maxilla **H** right terminal segment of third maxilliped. Allotype, adult ♂ (NHM 2012.1487): **I** right endopod of first male pleopod.

inner margin and 9–15 setae arranged on outer margin (Fig. 10I). 210–250 eggs of 0.50–0.70 × 0.40–0.50 mm in size.

Size. *Atyaephyra strymonensis* sp. n. is a large sized species with maximum carapace length to be 5.6 mm in ♂♂, 7.9 mm in ♀♀ and 7.5 mm in ovig. ♀♀.

Molecular characters. *Atyaephyra strymonensis* sp. n. is unique in the genus in having 2 haplotypes not found in any of the other species. Also, it differs from all the other species in the following nucleotide positions in the COI gene of *A. desmarestii* specimen Dour1, position 201: cytosine (C), position 252: guanine (G), position 303: cytosine (C), position 309: thymine (T), position 318: guanine (G), position 319: adenine (A), position 367: thymine (T), position 393: cytosine (C) and position 453: thymine (T).

Etymology: *Atyaephyra strymonensis* sp. n. is named after the Strymon (Strymonas) River, Greece, the type locality.

Distribution. *Atyaephyra strymonensis* sp. n. is found in North-western Greece in the Rivers Strymon and Nestos (see material examined and Fig. 1).

Remarks. *Atyaephyra strymonensis* sp. n. is unique in the combination of the following characters: (a) absence of post orbital teeth (Fig. 9A), (b) leaving a short unarmed proximal gap on dorsal surface of rostrum (Fig. 9A), (b) having a round anterolateral lobe on basal segment of antennular peduncle (Figs 9F–G), (c) having a not protruding, rounded pterygostomial angle (Fig. 9C), (d) endite of maxilla 1.77–1.95 × as long as basal lower endite (Fig. 10G) and having 1–7 mesial spines in the terminal segment of third maxilliped (Fig. 10H). *A. strymonensis* is similar to *A. desmarestii*, *A. acheronensis* and *A. tuerkayi* in having fewer spines in the terminal segment of third maxilliped. However *A. strymonensis* differs by the absence of post-orbital teeth, leaving a short unarmed proximal gap on dorsal surface of rostrum and by the endite of maxilla being 1.77–1.95 × as long as basal lower endite (vs. 1.49–1.71). *A. strymonensis* differs from *A. stankoi*, *A. thyamisensis* and *A. orientalis* in having fewer mesial spines in the terminal segment of third maxilliped.

Atyaephyra acheronensis sp. n.

urn:lsid:zoobank.org:act:EBF698A2-82F9-49E8-89DA-8C4EB7588939

http://species-id.net/wiki/Atyaephyra_acheronensis

Figs 11–12

Atyaephyra sp. n. 2. – Christodoulou et al. 2008: Fig. 4A.

Atyaephyra sp. n. 2. – Christodoulou et al. 2010: Fig. 2, partim.

Atyaephyra desmarestii. – Franjević et al. 2010: 159–166.

Material examined. Type material. Holotype: NHM 2012.1493, 1 ovig. ♀ (CL 5.9 mm), Greece, Epirus, Acherontas River, 39°13.96'N, 20°29.11'E (Fig. 1, stn 71), among aquatic plants, 15.4.2012, coll. Ch. Anastasiadou (Sequenced specimen: Ach1).

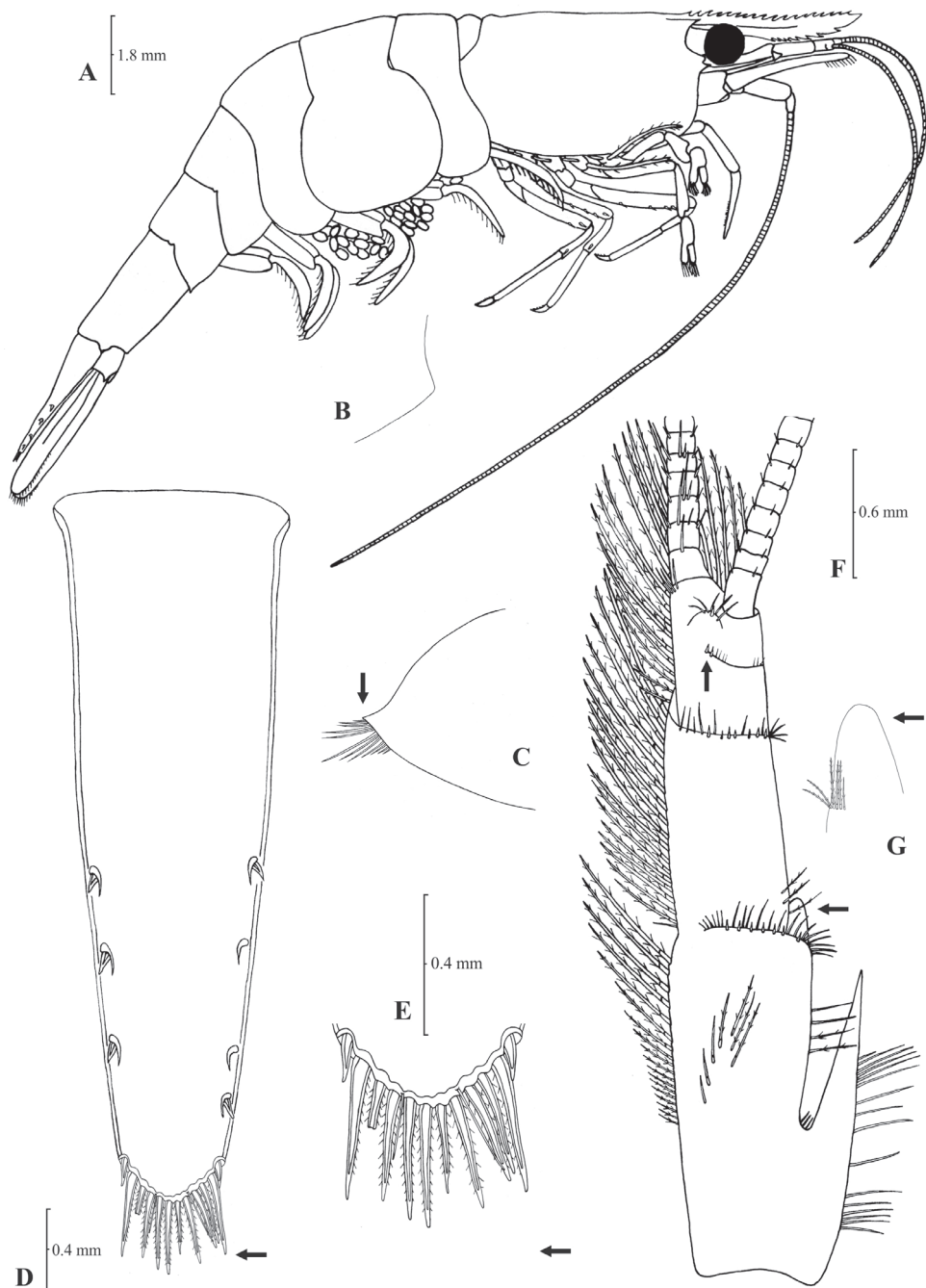


Figure 11. *Atyaephyra acheronensis* sp. n. Holotype, adult ovig. ♀ (NHM 2012.1493): **A** entire individual **B** detail of right pterygostomial border **C** right pleuron of fifth abdominal segment **D** telson **E** distal margin of telson **F** right antennular peduncle **G** right antennular lobe.

Non-type material. Greece: 1 ♀ (CL 7.6 mm) (Sequenced specimen: Lour1) and 1 ovig. ♀ (CL 7.0 mm) (Sequenced specimen: Lour2), Greece, Epirus, Louros River, 39°03.14'N, 20°46.26'E (Fig. 1, stn 72), 15.4.2012, coll. Ch. Anastasiadou; **Slovenia:** 1 ♂ (CL 5.1 mm), Dragonja River (Fig. 1, stn 66), Aug.1971 (Sequenced specimen: Drag1).

Description. Rostrum long, dorsal margin straight, 6.28–6.66 × as long as high, equal to or longer than scaphocerite. 19–26 pre orbital teeth on dorsal margin of rostrum arranged up to tip. With 1–3 post orbital teeth and 3–8 teeth on ventral margin of rostrum (Fig. 11A). Carapace smooth with pterygostomial angle not protruding, rounded (Fig. 11B). Pleuron of fifth abdominal segment pointed with an acute posterior angle (Fig. 11C). Telson with four pairs of dorsal spines arranged in curved fashion (Fig. 11D). Distal border of telson with 12–15 spines (6–8 pairs) arranged in a fan-like pattern. Outermost pair of spines shortest, similar to dorsal spines, adjacent pair stronger terminating before the finely setulose, inner pairs (Figs 11D–E). Antennular stylocerite with its tip failing to reach or reaching distal margin of basal peduncle segment. Anterolateral lobe of basal segment short and round (Fig 11G). Distal segment of antennular peduncle with 1–2 spines (Fig. 11F). Basal lower endite of maxilla densely covered with long simple setae arranged in 18–20 oblique parallel rows. Endite of maxilla 1.56–1.65 × as long as basal lower endite (Fig 12G). Basal endite of first maxilliped reaching clearly beyond distal end of exopod (Fig 12F). Distal one-third of terminal segment of third maxilliped bearing 1–5 mesial spines and one subdistal lateral spine near the base of larger terminal spine, interpretable as dactylus (Fig. 12H). Armature along flexor margin of dactylus of third and fourth pereopod consisting of 5–7 and 6–7 spines respectively (Figs 12B, 12D). Merus of third and fourth pereopod with 4–6 and 3–4 spines respectively (Figs 12A, 12C). Armature along flexor margin of dactylus of fifth pereopod consisting of 27–38 spines (Fig. 12E). Endopod of first male pleopod expanded proximally and with a distal portion elongated (ribbon shaped) and tapering. Endopod with 18 spines arranged on a slightly curved inner margin and 12 setae arranged on outer margin (Fig. 12I). 579–1117 eggs of 0.40–0.55 × 0.25–0.35 mm in size.

Size. *Atyaephyra acheronensis* sp. n. is a large sized species with maximum carapace length to be 5.1 mm in ♂♂, 7.6 mm in ♀♀ and 7.0 mm in ovig. ♀♀.

Molecular characters. Molecular information based on the COI sequences provides compelling evidence that is a well defined species. *Atyaephyra acheronensis* sp. n. is unique in *Atyaephyra* in having 2 haplotypes not shared by any other species. Furthermore, it differs from all its congeners in the following nucleotide positions in the COI gene of *A. desmarestii* specimen Dour1, position 255: adenine (A) and position 318: cytosine (C). Finally, the mean genetic distances between *A. acheronensis* and the remaining *Atyaephyra* species range from 8.3% to 23.8% (Table 2).

Etymology. *Atyaephyra acheronensis* sp. n. is named after the Acheron (Acherontas) River, Greece, the type locality.

Distribution. *Atyaephyra acheronensis* sp. n. is found in freshwater habitats of Croatia (Krka River), Slovenia (Dragonja River) and Greece (Acherontas River and Louros River) (see material examined and Fig. 1). Although this study was based on a limited

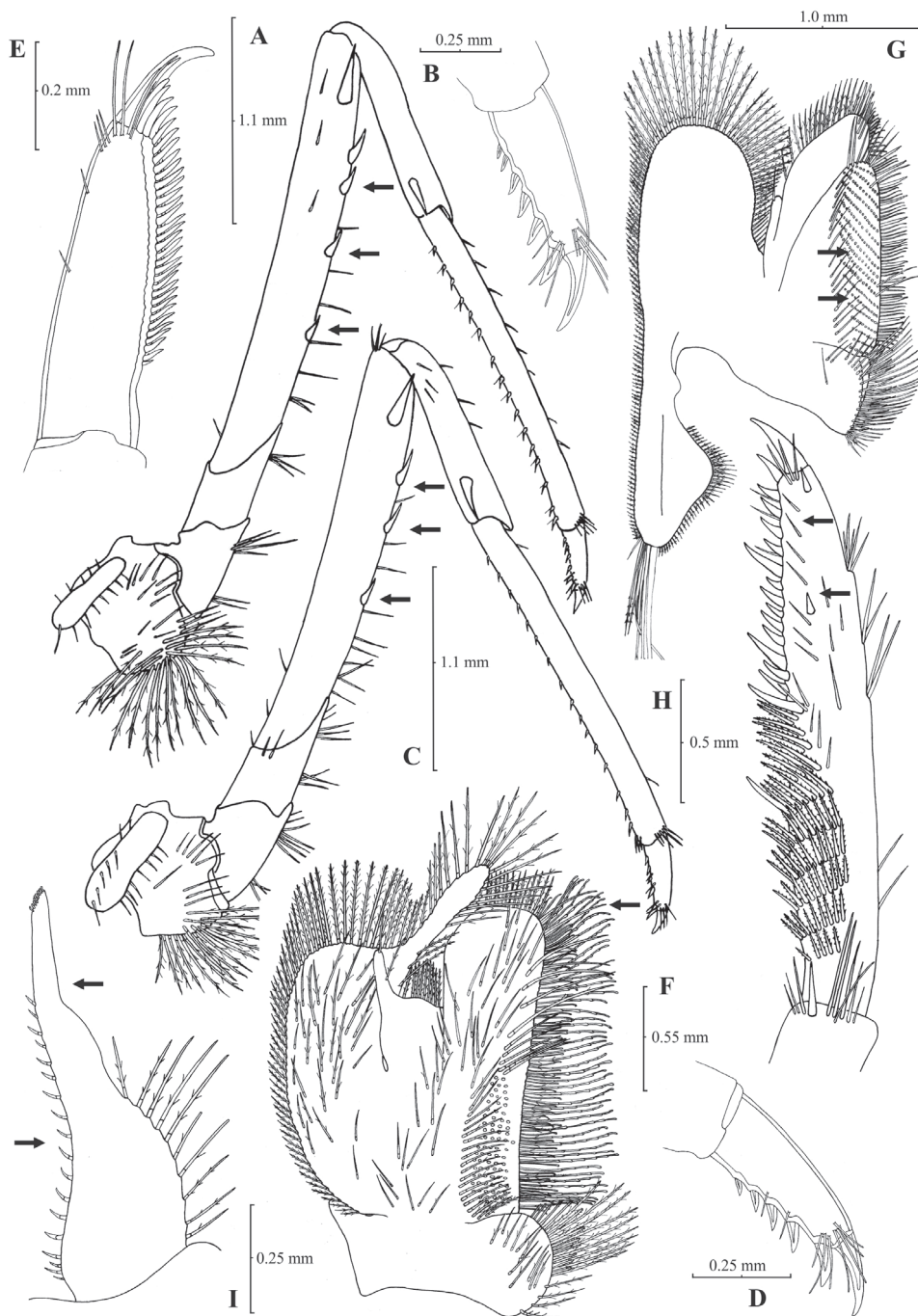


Figure 12. *Atyaephyra acheronensis* sp. n. Holotype, adult ovig. ♀ (NHM 2012.1493): **A** right third pereiopod **B** dactylus of third pereiopod **C** right fourth pereiopod **D** dactylus of fourth pereiopod **E** dactylus of fifth pereiopod **F** right first maxilliped **G** right maxilla **H** right terminal segment of third maxilliped. Adult ♂: **I** right endopod of first male pleopod.

number of specimens, it is postulated that *A. acheronensis* sp. n. occurs in more rivers covering an area ranging from Croatia to Greece.

Remarks. In addition to the type- and non type-material we investigated the morphology of the following specimens originating from the Balkan Peninsula: 6 ♀♀ collected from Dragonja River (Fig. 1, stn 66), Slovenia; 3 ♀♀ collected from Jadro River (Fig. 1, stn 67), NHMW 460 and 4 ♀♀ (3 ovig.) and 1 ♂ from Ombla River (Fig. 1, stn 69), NHMW 459, Croatia; 2 ♂♂ collected from Krupa River (Fig. 1, stn 68), NHMW 458, Bosnia and Herzegovina; 9 ♀♀ and 12 ♂♂ from Aaos River (Fig. 1, stn 70), Albania; 47 ♀♀ (13 ovig.) and 9 ♂♂ from Acherontas River (Fig. 1, stn 71), Greece, 10 ♀♀ and 2 ♂♂ collected from Louros River (Fig. 1, stn 72), Greece, 2 ♀♀ from Pamisos River (Fig. 1, stn 73), Greece, 4 ♀♀ and 1 ♂ sampled from Evrotas River (Fig. 1, stn 74), NHM 1987.93, Greece. However, without sequencing the individuals, their placement to *Atyaephyra acheronensis* sp. n. can't be made with certainty.

Out of the 135 characters examined (see Appendix: Table 1) there were no morphological features distinguishing *A. acheronensis* sp. n. from *A. desmarestii* and *A. tuerkayi* sp. n. Nevertheless, *A. acheronensis* sp. n. presents a more limited variability in the values of its morphological characters than *A. desmarestii*. *A. acheronensis* sp. n. can easily be distinguished from *A. orientalis*, *A. stankoi* and *A. thyamisensis* by the presence of fewer mesial spines (1–5) on terminal segment of third maxilliped (Fig. 12H) (vs. 10–38 in *A. orientalis*, *A. stankoi* and *A. thyamisensis*; Figs 4H, 6H, 8H) and by the basal endite of first maxilliped overreaching distal end of exopod (Fig. 12F) (vs. failing to reach or reaching distal end in *A. orientalis*, *A. stankoi* and *A. thyamisensis*; Figs 4F, 6F, 8F). *A. acheronensis* sp. n. can be separated from *A. strymonensis* by the presence of 1–3 post orbital rostral teeth (Fig. 11A) (vs. no post orbital teeth present leaving short unarmed proximal gap in *A. strymonensis*; Fig. 9A) and by the endite of maxilla being 1.56–1.65 × as long as basal lower endite (Fig. 12G) (vs. 1.77–1.95 in *A. strymonensis*; Fig. 10G).

***Atyaephyra tuerkayi* sp. n.**

urn:lsid:zoobank.org:act:94C1EC2A-1667-4456-8721-D10F03CDF4E6

http://species-id.net/wiki/Atyaephyra_tuerkayi

Figs 13–14

Atyaephyra desmarestii orientalis. – Kinzelbach and Koster 1985: 127–134, partim.

Atyaephyra n. sp. 2. – Christodoulou et al. 2010: Fig. 2, partim.

Material examined. Type material. Holotype: adult ♀ (CL 6.2 mm), SMF 43020, Syria, Nahr Al-Kabir River (Fig. 1, stn 122), at bridge near the coastal road, 5.3.1979, coll. R.K. Kinzelbach (Sequenced specimen: Nah1); Paratype: 1 ♀ (CL 7.1 mm), SMF 43021 same data as the holotype (Sequenced specimen: Nah2).

Description. Rostrum long, dorsal margin slightly curved in the middle and pointed upwards 6.43–6.66 × as long as high, shorter than or equal to scaphocerite.

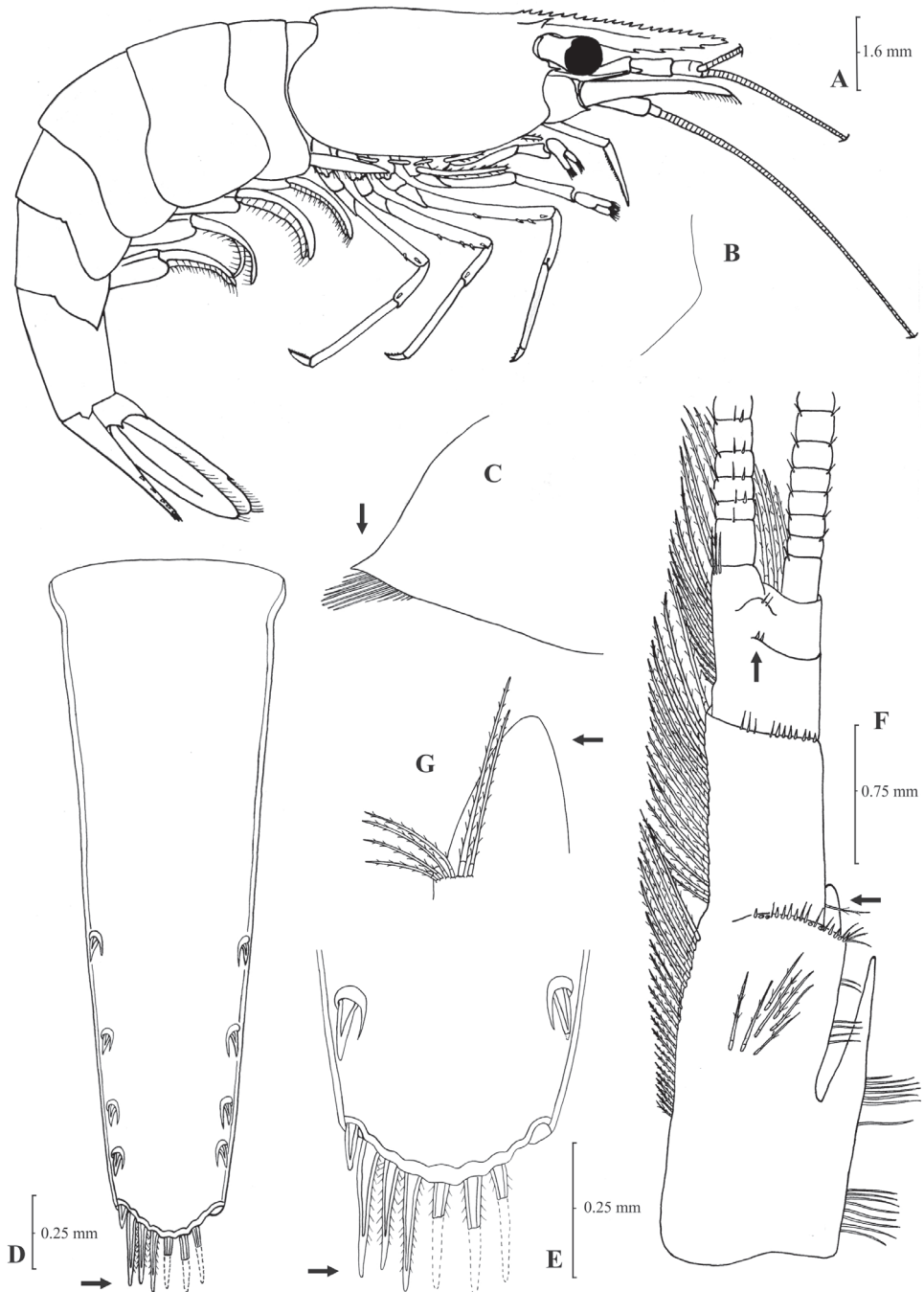


Figure 13. *Atyaephyra tuerkayi* sp. n. Holotype, adult ♀ (SMF 43020): **A** entire individual **B** detail of right pterygostomial boarder **C** right pleuron of fifth abdominal segment **D** telson **E** distal margin of telson **F** right antennular peduncle **G** right antennular lobe.

19–23 pre orbital teeth on dorsal margin of rostrum arranged up to tip. With two post orbital teeth and 4–7 teeth on ventral margin of rostrum (Fig. 13A). Carapace smooth with pterygostomial angle not protruding, rounded (Fig. 13B). Pleuron of fifth abdominal segment pointed with an acute posterior angle (Fig. 13C). Telson with four pairs of dorsal spines arranged in curved fashion (Fig. 13D). Distal border of telson with 9 spines (5 pairs) arranged in fan-like pattern. Outermost pair of spines shortest, similar to dorsal spines, adjacent pair stronger terminating before the finely setulose, inner pairs (Fig. 13E). Antennulary stylocerite with its tip failing to reach or reaching distal margin of basal peduncle segment. Anterolateral lobe of basal segment short and round (Fig. 13G). Distal segment of antennular peduncle with 1–2 spines (Fig. 13F). Basal lower endite of maxilla densely covered with long simple setae arranged in 18–20 oblique parallel rows. Endite of maxilla 1.58–1.59 × as long as basal lower endite (Fig. 14G). Basal endite of first maxilliped reaching clearly beyond distal end of exopod (Fig. 14F). Distal one-third of terminal segment of third maxilliped bearing 1–6 mesial spines and one subdistal lateral spine near the base of larger terminal spine (Fig. 14H). Armature along flexor margin of dactylus of third and fourth pereopod consisting of 6–7 and 6–7 spines respectively (Figs 14B, 14D). Merus of third and fourth pereopod with 4 and 3 spines respectively (Figs 14A, 14D). Armature along flexor margin of dactylus of fifth pereopod consisting of 28 spines (Fig. 14E).

Size. *Atyaephyra tuerkayi* is a large sized species with maximum carapace length to be 7.1 mm for ♀♀

Molecular characters. A haplotype found in *A. tuerkayi* sp. n. is not shared by any other species of *Atyaephyra*. Additionally, it differs from all the other species in the following nucleotide positions in the COI gene of *A. desmarestii* specimen Dour1, position 174: guanine (G), position 207: adenine (A), position 246: adenine (A), position 318: thymine (T), position 321: adenine (A), position 339: adenine (A), position 357: cytosine (C), position 372: thymine (T), position 399: thymine (T), position 417: adenine (A) and position 441: cytosine (C). Finally, the mean genetic distances between *A. tuerkayi* and the other species were ranging from 19.7% to 25.7% (Table 2).

Etymology. *Atyaephyra tuerkayi* sp. n. is named after Professor Michael Türkay, in appreciation of his contribution to the study of Decapoda.

Distribution. *Atyaephyra tuerkayi* sp. n. is found in the Nahr Al-Kabir River situated between Syria and Lebanon (see material examined and Fig. 1).

Remarks. In addition to the type-material we investigated the morphology of the 23 female individuals (6 ovig.) and 7 males originating from Nahr Al-Kabir River (Fig. 1, stn 122; SMF 12189, SMF 12191, SMF 12192). All the individuals examined (including the sequenced ones) were morphologically identical. However, their placement to *A. tuerkayi*, sp. n. has still to await sequencing. Since no male or ovigerous individual was sequenced observation regarding the form of the endopod of first male pleopod and number of eggs carried by the female were not included in the description. But observations were made in other individuals of the same sample and population and thus given here: endopod of first male pleopod expanded proximally and

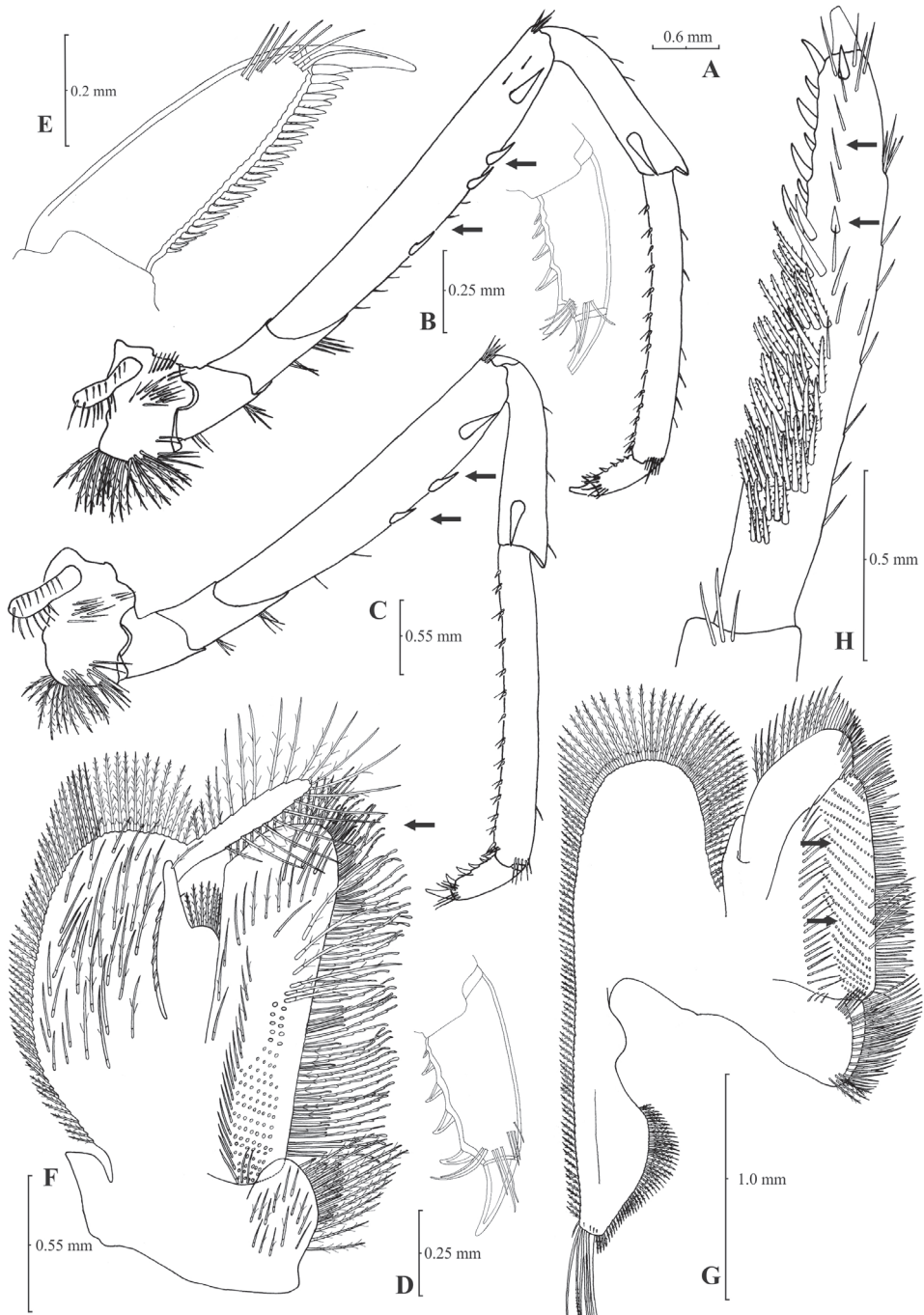


Figure 14. *Atyaephyra tuerkayi* sp. n. Holotype, adult ♀ (SMF 43020): **A** right third pereiopod **B** dactylus of third pereiopod **C** right fourth pereiopod **D** dactylus of fourth pereiopod **E** dactylus of fifth pereiopod **F** right first maxilliped **G** right maxilla **H** right terminal segment of third maxilliped.

with a distal portion elongated and tapering, endopod with 9–16 spines arranged on a slightly curved inner margin and 9–11 setae arranged on outer margin. 430–450 eggs of $0.45\text{--}0.50 \times 0.30\text{--}0.35$ mm in size. Maximum carapace length to be 5.7 mm for ♂♂, 7.9 mm for ♀♀ and 7.6 mm for ovig. ♀♀.

Out of the 135 characters examined (see Appendix: Table 1) there were no morphological features distinguishing *A. tuerkayi* sp. n. from *A. desmarestii* and *A. acheronensis* sp. n. However, *A. tuerkayi* sp. n. can easily be distinguished from *A. orientalis*, *A. stankoi* and *A. thyamisensis* by the presence of fewer mesial spines (Fig. 14H) (1–6) on terminal segment of third maxilliped (vs. 10–38 in *A. orientalis*, *A. stankoi* and *A. thyamisensis*; Figs 4H, 6H, 8H) and by the basal endite of first maxilliped overreaching distal end of exopod (Fig. 14F) (vs. failing to reach or reaching distal end in *A. orientalis*, *A. stankoi* and *A. thyamisensis*; Figs 4F, 6F, 8F). *A. tuerkayi* sp. n. can be separated from *A. strymonensis* by the presence of 1–3 post orbital rostral teeth (Fig. 13A) (vs. no post orbital teeth present leaving short unarmed proximal gap in *A. strymonensis*; Fig. 9A) and by the endite of maxilla being $1.58\text{--}1.59 \times$ as long as basal lower endite (Fig. 14G) (vs $1.77\text{--}1.95$ in *A. strymonensis*; Fig. 10G).

Discussion

Given the highly structured nature of freshwater habitats and the limited potential for dispersal of the freshwater species (mainly due to natural barriers) in combination with the wide distribution of *Atyaephyra* in the Mediterranean region, a hypothesis under which several species are expected to be harbored in the genus seemed highly possible.

However, until recently, *Atyaephyra* was considered as a monotypic genus. Over the last 100 years many authors (Bouvier 1913, Holthuis 1961, Karaman 1972, Kinzelbach and Koster 1985, Al-Adhub 1987) have attempted to challenge this perception. However, the high intra- and inter-population variability, which made even the previously proposed subspecies questionable (Gorgin 1996, Anastasiadou et al. 2004) along with the lack of a complete series of samples covering all the known distribution of *Atyaephyra*, proved to be far more challenging than many taxonomists would ever anticipate.

In the latest revision of the *Atyaephyra* (García Muñoz et al. 2009), which was based on the genetic information deriving from two mitochondrial genes (COI, 16S), two species were recognized while a third was proposed but without confirming it. In the current study seven species are defined, based both on morphological and molecular data. This difference in numbers is attributed to the limited geographical focus of the former study, which was primarily carried out on material collected from the Western Mediterranean area.

After an exhaustive study of a large number of specimens from 20 different countries and a thorough examination of more than 135 morphological characters, including somatometric distances, new characters were found which could differentiate species or groups of species within the *Atyaephyra*. One of these characters is the number of mesial spines on the terminal segment of the third maxilliped according to which

two main groups can be distinguished. The first group is characterized by 10–38 mesial spines and comprises three species, *A. thyamisensis* sp. n., *A. stankoi*, *A. orientalis* whereas the second by 1–8 mesial spines including the remaining four, namely *A. desmarestii*, *A. acheronensis* sp. n., *A. strymonensis* sp. n. and *A. tuerkayi* sp. n.

The species included in the first group can subsequently be distinguished by a series of features, e.g. presence-absence of a protruding pterygostomial angle, shape of antennular lobe and shape of endopod of first male pleopod. *Atyaephyra thyamisensis* sp. n., *A. stankoi* and *A. orientalis* are morphologically and phylogenetically well defined. In the phylogenetic tree they represent three well supported clades (16.7%–22.6% divergent from each other). In the second group, *A. strymonensis* sp. n. is also a well defined species morphologically and can be distinguished from the remaining members by a combination of characters such as the lack of post orbital teeth, presence of a short unarmed proximal gap on rostrum and ratio of basal lower endite of maxilla in relation to the whole maxilla endite. The genetic divergence observed between *A. strymonensis* sp. n. and its closest congeners by morphology is quite high (21.9%–25.4%). Thus, both morphological and molecular data show congruent patterns and jointly support its recognition as a distinct species within the genus. In addition, although *A. strymonensis* sp. n. seems to be morphologically closer to the members of the second group e.g. *A. desmarestii*, *A. acheronensis* sp. n., *A. tuerkayi* sp. n., genetically it is more closely related to the other two species of the first group from Greece (e.g. *A. thyamisensis* sp. n. and *A. stankoi*) with which it forms a strongly supported phylogroup (genetic divergence range: 11.9%–18.2%).

No diagnostic morphological characters were found to distinguish the species *A. desmarestii*, *A. acheronensis* sp. n. and *A. tuerkayi* sp. n. from each other, a fact which is mainly caused by the high morphological variability observed in *A. desmarestii*. However, their genetic distinctiveness coupled with their discrete geographical distribution provides enough evidence to distinguish the three species as distinct taxa.

The range of genetic divergence observed between the specimens of *A. desmarestii* and of *A. acheronensis* sp. n. (TrN distances: 5.9%–11.6%, Uncorrected p-distances: 5.3%–8.7%) is comparable to those found for other cryptic or sibling species of freshwater shrimps (e.g. Page et al. 2005a, Uncorrected p-distances: *Caridina* sp. A vs *Caridina* sp. B or C: 8.4–10.9%; *Caridina* sp. B vs *Caridina* sp. C: 6.7–8.8%), freshwater crabs (e.g. Jesse et al. 2011, Uncorrected p-distances: interspecific variability between 14 *Potamon* species range: 3.1%–11.2%) as well as for other decapod sibling or well defined species (e.g. Jones and Macpherson 2007, TrN distances: interspecific variability between 14 *Munidopsis* species range: 1.5%–19.6%). The mean genetic divergence observed between *A. desmarestii* and *A. acheronensis* (8.3 %) was the smallest among the *Atyaephyra* species (remaining genetic distances ranging from 11.9 to 25.7%). This level of divergence was also evident in morphology, indicating a more recent speciation event within the genus (compared to the ones that gave rise to the other species of *Atyaephyra*) and thus less time for these two species to diverge both morphologically and genetically.

Furthermore, the fact that no haplotypes were shared between *A. desmarestii* and *A. acheronensis* sp. n. would suggest that the populations of shrimps from both species,

although recently evolved, had independent evolutionary histories for a relatively long period of time. Additional support, although further research is still needed, comes from their geographical distribution since *A. desmarestii* and *A. acheronensis* sp. n. seems to be allopatric. *Atyaephyra acheronensis* is found in the western Balkan Peninsula, ranging from Croatia to Greece. In Greece, this species is found only on the west side of the mainland reaching most probably as far as South Peloponnese although with a remarkable fragmented distribution. In comparison *A. desmarestii* is distributed in West-central Europe and North Africa. It should be noted here that the native distribution of *A. desmarestii* is limited to Southern Europe and its presence in North-Central Europe up to the Danube River is believed to have been caused by its dispersal through the canals that were opened to connect the main rivers of Europe (Dhur and Massard 1995, Moog et al. 1999, Grabowski et al. 2005, Straka and Špaček 2009). Geographical barriers like the Alps and the Balkan mountains that isolated the Balkan drainages preventing faunal exchanges with the rest of Europe (Economou et al. 2007) could also account for this secluded population. Although, the current evidence deriving from mitochondrial data along with the geographic distribution supports the discrimination of *A. acheronensis* as a distinct species, further support could come from additional mitochondrial sequence data (especially from the Balkan peninsula) as well as by combining information provided by nuclear sequence data.

The monophyly of the species *A. desmarestii*, although supported by NJ, was poorly or not supported at all by BI and ML analyses, respectively. In the study of Garcia Muñoz et al. (2009) the monophyly of this species, based on the COI sequences, was strongly supported. This difference should be attributed to the larger number of sequences used in this study. *A. desmarestii* (Millet, 1831) does not comprise a strongly supported genetically distinct group and appears as a not well resolved part of the phylogeny. However, the genetic distances observed within this group are quite small in comparison with the other *Atyaephyra* species and this in combination with the morphological data supports the consideration of all the populations inside this group as one taxonomic entity. More sequence and morphological data, especially from the area of South Portugal and Morocco (the monophyly of the species is strongly supported once the sequences originating from Morocco and South Portugal material are removed), as well as other molecular markers are needed in order for the relationships within *A. desmarestii* to be clarified.

In the southwestern part of the Mediterranean area, only two species of *Atyaephyra* have been described to date: *A. desmarestii* and *A. rosiana*. These two species had been considered synonyms until Anastasiadou et al. (2008) resurrected *A. rosiana* after studying material from São Barnabé River (Odelouca River) in South Portugal. In their study Garcia Muñoz et al. (2009), stated that the hypothesis of the two distinct species could not be supported although they did note some genetic variability in the specimens originating from South Iberian Peninsula. Similar results are obtained in the current study. Sequences from North African and South Iberian individuals presented a noticeable mean genetic divergence (3.1% and 2.3% respectively) from the rest of west European and Tunisian sequences, but although noticeable is still weak to sup-

port the hypothesis of different species. A high variability in morphological characters, especially in the individuals from the South Iberia was also observed. Characters such as the length and height of the rostrum (the tendency is for rostra to be longer and narrower) and the number of rows in maxilla basal lower endite (usually 15–18) varied greatly from the typical form present in North Iberia and the rest of Europe as well as Tunisia (shorter and broader rostra, 17–21 rows on maxilla basal lower endite). Genetic diversity among the South and North-central Iberia populations is observed in many other freshwater species whereas only in a few of them is it robust enough to justify distinct species (Doadrio and Carmona 2003, Durand et al. 2003, Sanjur et al. 2003). An explanation for this should be sought in the eventful geological history as many basins of the Iberian Peninsula almost dried up and the southwestern part of the Peninsula became completely isolated during the Messinian period (Sanjur et al. 2003). In addition, the genetic diversity observed mainly between the Moroccan and remaining populations should be sought again to the geological history and the isolation of the North-west Africa from Europe and where dispersal between these land mass, across the Gibraltar strait ceased to be an option since Pliocene (Sanjur et al. 2003).

The Tunisian populations, on the other hand, are more closely related to the western European ones, probably due to the past connections through the Sicily Strait with European populations (Butler et al. 1999).

The second cryptic species *A. tuerkayi* sp. n. has been found only in the River Nahr Al-Kabir which is located along the borders of Lebanon with Syria. *A. tuerkayi* sp. n. is completely isolated geographically from the other two morphologically closest to it species, *A. desmarestii* and *A. acheronensis* sp. n. In fact *A. tuerkayi* sp. n. is surrounded by *A. orientalis* populations which show a wide distribution from Turkey to Iraq. *Atyaephyra tuerkayi* sp. n. is genetically well discriminated from *A. desmarestii* and *A. acheronensis* (genetic distances are 23.0% and 22.2% respectively) as well as from *A. orientalis* that is found in the adjacent areas (genetic distance is 19.7%). The genetic distances are among the highest observed between *Atyaephyra* species and by far exceed currently published records of intra-population variability of other fresh water decapods (e.g. Jesse et al. 2011). Furthermore, they are comparable with genetic distances of COI sequences described elsewhere for taxa recognized at the generic level (Avice 2000, Lefébure et al. 2006, Matzen da Silva et al. 2011). Therefore such an extensive differentiation should be attributed to speciation.

In the area of the Middle East, two subspecies were previously described, *A. desmarestii orientalis* Bouvier, 1913 and *A. desmarestii mesopotamica* Al-Adhub, 1987. However, no observable morphological characters were found that could differentiate them (see remarks of *A. orientalis*). Furthermore, although the genetic distances within the *A. orientalis* phylogroup were high (0.9%–10.2%) no firm conclusion could be drawn whether the hypothesis of multiple species is valid or not. Sequences from Orontes River (topotypical location of *A. d. orientalis*) and from Shatt Al-Arab River (topotypical location of *A. d. mesopotamica*) presented a noticeable mean genetic divergence (5.0%) but still not strong enough to support the hypothesis of different species. Detailed future studies on the morphological and genetic variability within

the samples of *Atyaephyra* distributed throughout the Middle East will help clarify the relationships between the populations in this region, however given the present data, only one species is considered to exist, *A. orientalis*.

Four species (*A. acheronensis* sp. n., *A. thyamisensis* sp. n., *A. stankoi*, and *A. strymonensis* sp. n.) were found to co-exist in Greece with well defined and clearly separated distributions. Only two species (*A. acheronensis* sp. n. and *A. thyamisensis* sp. n.) were found to co-exist in the same river (River Louros, Epirus). Multiple individuals collected from the Louros estuary and further upstream, dating back to 1977 until 2001 were examined. These specimens were all identified as *A. thyamisensis* sp. n. However, in a recent sample (2012) both species were found. Probably, this could be attributed to fish transfers or translocation where shrimps could have accidentally been introduced. Additionally, the distance between the estuaries of the Rivers Louros and Acherontas is less than 30 km making human mediated dispersal, between the two watersheds, highly possible. Furthermore, numerous translocations of fish were made within Greece over the last 70 years (Economidis et al. 2000) making this scenario even more justified. However, the natural co-existence of the two species cannot be entirely excluded.

It is surprising that four out of the seven *Atyaephyra* species examined for the present study are recorded from Greece and three of these are endemic. Greece is considered to be a faunal and floral biodiversity hot spot within the Mediterranean region where freshwater fauna is not an exception (Reyjol et al. 2007, Jesse et al. 2011). Jesse et al. (2011) after studying the diversity of the freshwater *Potamon* crabs, revealed the existence of 14 species within the greater Mediterranean region. Eight of these species (three endemic and five with limited distribution in adjacent countries) were found in Greece. High diversity and endemism is recorded in other freshwater groups too, such as fishes. Greece harbours the largest number of fish species of any region in the Mediterranean basin where the number of endemic species exceeds 45% of the total number of native species (130) recorded (Economou et al. 2007, Blondel et al. 2010). Freshwater endemism in Greece is considered as one of the highest in the Mediterranean region and has been ascribed to its eventful geological history combined with complex climatic events (Bobori et al. 2001, Economou et al. 2007).

The importance of morphology versus molecular data in order to resolve the phylogeny of a taxon still provides a forum for scientific debate (Tautz et al. 2003, Blaxter 2004, Page et al. 2005b). Although additional work is needed towards the exhibited morphological variability within the genus, the data provided by the present study demonstrate a case in which conventional and molecular taxonomy do not provide different patterns but, rather, complimentary. Finally, an additional step was taken by considering the molecular validation of the two cryptic species which couldn't be supported by morphological data alone. It seems, therefore, that when both molecular and morphological effort is combined towards a "total evidence" approach a whole greater than the sum of its parts emerges which is instrumental in our understanding the diversity of life (Page et al. 2005b).

Acknowledgements

We are very grateful to the following researchers who provided us with material either as loan or as a gift: Dr Chrysa Anastasiadou (University of Ioannina, Greece), Prof. Sonia Dhaouadi-Hassen (University of Carthage, Tunisia), Dr Cedric d' Udekem d' Acoz (Royal Belgian Institute of Natural Sciences, Belgium), Prof. Manuel Graça and Dr Veronica Ferreira (University of Coimbra, Portugal), Dr Carlo Froggia (Italy), Mr Ahmad Ghane (Inland Waters Aquaculture Research Centre, Iran), Dr Jure Jugovic (University of Ljubljana, Slovenia), Dr Christophe Lejeune (Doñana Biological Station, Spain), Prof. Mohammed Melhaoui (University of Oujda, Morocco), Prof. Jose Luis Moreno Alcaraz (University of Castilla-La Mancha, Spain), Mr Murtada D. Naser (University of Basrah, Iraq), Dr Javier Oscoz (University of Navarra, Spain), Ass. Prof. Murat Özbek (Ege University, Turkey), Dr Michael L. Zettler (Leibniz Institute for Baltic Sea Research, Germany), Mrs Niovi Christodoulou and Mr Andreas Savvides (Wageningen University, Netherlands). Also, we are very grateful to the following researchers that allowed us access to Museum collections: Dr Paul F. Clark (NHM), Dr Sammy De Grave (OUMNH), Dr Peter Dworschak (NMW), Dr Pier Noël (MNHN), Dr Svetozar Petkovski (MMNH) and Professor Michael Türkay (SMF). Furthermore, we will like to thank Dr Timothy J. Page (Griffith University, Australia) for offering us four COI sequences and Ass. Prof. Nikos Poulakakis (University of Crete, Greece) for supplying us with the DNA extraction protocol. The authors will like to thank Dr Sammy De Grave and Dr Arthur Anker for their help in finding Bouvier's material in NHMN. Specifically we will like to thank Dr Arthur Anker who went through the collection as well as for taking the photos of *A. desmarestii* and *A. rosiana* material. The senior author will like to thank Dr De Grave for his useful comments and help through some difficult issues dealing with the nomenclature code of zoology. For their helpful comments and critical reading we will like to thank Dr Paul Clark and Dr Christos Arvanitidis. We will also like to thank Mrs Kristin Pietratus (SMF), Mrs Miranda Lowe (NHM), Mrs Paula Martin-Lefevre and Dr Laure Corbari (MNHN) for their help with the loaned material from Museum collections. We also acknowledge the help of Stelios Derivianakis, Katerina Oikonomaki and Vaso Terzoglou in the genetic lab. The senior author will like to thank Synthesys: the European Union-funded Integrated Activities grant that supported her for a monthly visit to the NHM. Also the senior author will like to specially thank Dr Paul Clark for his supervision. Finally, the authors, gratefully acknowledge the three reviewers for their very useful comments and suggestions that improved significantly the manuscript. The senior author will like to acknowledge the State Scholarships Foundation for supporting partially her studies. This study was partially funded by MARBIGEN: "Supporting research potential for MARine BIodiversity and GENomics in the Eastern Mediterranean" and ViBRANT: "Virtual Biodiversity Research and Access Network for Taxonomy".

References

- Al-Adhub AHY (1987) On a new subspecies of a freshwater shrimp (Decapoda, Atyidae) from the Shatt Al-Arab River, Iraq. *Crustaceana* 53 (1): 1–4. doi: 10.1163/156854087X00565
- Anastasiadou Ch, Kitsos M-S, Koukouras A (2006) Redescription of *Atyaephyra desmarestii* (Millet, 1831) (Decapoda, Caridea, Atyidae) based on topotypical specimens. *Crustaceana* 79 (10): 1195–1207. doi: 10.1163/156854006778859597
- Anastasiadou Ch, Kitsos M-S, Koukouras A (2008) Redescription of *Atyaephyra rosiana* de Brito Capello, 1867 (Decapoda, Caridea, Atyidae) based on a population close to the topotypical area. *Crustaceana* 81 (2): 191–205. doi: 10.1163/156854008783476215
- Anastasiadou Ch, Koukouras A, Mavidis M, Chartosia N, Mostakim Md, Christodoulou M, Aslanoglou Ch (2004) Morphological variation in *Atyaephyra desmarestii* (Millet, 1831) within and among populations over its geographical range. *Mediterranean Marine Science* 5 (2): 5–13. <http://www.medit-mar-sc.net/files/200812/15-1703457.pdf>
- Anastasiadou Ch, Ntakos A, Leonardos ID (2011) Larval development of the freshwater shrimp *Atyaephyra desmarestii* (Millet, 1831) *sensu lato* (Decapoda, Caridea, Atyidae) and morphological maturation from juveniles to adults. *Zootaxa* 2877: 41–54. <http://www.mapress.com/zootaxa/2011/f/z02877p054f.pdf>
- Annandale N, Kemp S (1913) The Crustacea Decapoda of the Lake of Tiberias. *Journal and Proceedings of the Asiatic Society of Bengal, New Series* 9 (6): 241–258. <http://decapoda.nhm.org/pdfs/24601/24601.pdf>
- Avise JC (2000) *Phylogeography: the history and formation of species*. Harvard University Press, Cambridge, Massachusetts, 447 pp.
- Barrois T (1893) Liste des décapodes fluviatiles recueillis en Syrie suivie de quelques considérations sur le genre *Caridine*. *Revue Biologique du Nord de la France* 5 (4): 125–134. <http://ia700304.us.archive.org/22/items/revuebiologiqued05lill/revuebiologiqued05lill.pdf>
- Bjourson AJ, Cooper JE (1992) Band-stab PCR: a simple technique for the purification of individual PCR products. *Nucleic Acids Research* 20 (17): 4675. doi: 10.1093/nar/20.17.4675
- Blaxter ML (2004) The promise of a DNA taxonomy. *Philosophical Transactions of the Royal Society B: Biological Sciences* 359 (1444): 669–679. doi: 10.1098/rstb.2003.1447
- Blagoderov V, Brake I, Georgiev T, Penev L, Roberts D, Rycroft S, Scott B, Agosti D, Catapano T, Smith VS (2010) Streamlining taxonomic publication: a working example with Scratchpads and ZooKeys. *ZooKeys* 50: 17–28. doi: 10.3897/zookeys.50.539
- Blondel J, Aronson J, Bodiou J-Y, Boeuf G (2010) *The Mediterranean Region: biological diversity in space and time*, 2nd edn. Oxford University Press, Oxford, 392 pp.
- Bobori DC, Economidis PS, Maurakis EG (2001) Freshwater fish habitat science and management in Greece. *Aquatic Ecosystem Health and Management* 4 (4): 381–391. doi: 10.1080/146349801317276053
- Bolivar I (1892) Lista de la colección de crustáceos de España y Portugal del Museo de Historia Natural de Madrid. *Actas de la Sociedad Española de Historia Natural* 21: 124–141. <http://bibdigital.rjb.csic.es/spa/Libro.php?Libro=1163>

- Bouvier E-L (1912) *Dugastella marocana*, crevette primitive nouvelle de la famille des Atyidés. Comptes Rendus Hebdomadaires des Séances de l'Académie des Sciences 155 (21): 993–998. <http://archive.org/details/ComptesRendusAcademieDesSciences0155>
- Bouvier E-L (1913) Les variations d'une crevette de la famille des Atyidées, l'*Atyaephyra Desmaresti* Millet. Bulletin du Muséum National d'Histoire Naturelle 19 (2): 65–74. <http://www.biodiversitylibrary.org/item/27226>
- Bouvier E-L (1925) Recherches sur la morphologie, les variations et la distribution systématique des crevettes d'eau douce de la famille des Atyidés. Encyclopédie Entomologique 4: 1–365.
- Bradley RK, Roberts A, Smoot M, Juvekar S, Do J, Dewey C, Holmes I, Pachter L (2009) Fast Statistical Alignment. PLoS Computational Biology 5 (5): e1000392. doi: 10.1371/journal.pcbi.1000392
- Brito Capello F de (1867) Descrição de algumas especies novas ou pouco conhecidas de crustaceos e arachnidios de Portugal e possessões portuguezas do Ultramar. Memorias da Academia Real das Sciencias de Lisboa 4 (1): 1–17. <http://www.biodiversitylibrary.org/item/30746#page/5/mode/1up>
- Butler RWH, McClelland E, Jones RE (1999) Calibrating the duration and timing of the Messinian salinity crisis in the Mediterranean: linked tectonoclimatic signals in thrust-top basins of Sicily. Journal of the Geological Society, London 156: 827–835. <http://www.see.leeds.ac.uk/structure/tectonics/messinian/mescycles.pdf>, doi: 10.1144/gsjgs.156.4.0827
- Christodoulou M, Kitsos M-S, Chartosia N, Koukouras A (2008) The status of the genus *Atyaephyra*: comparison of *A. desmarestii* and *A. rosiana* with different populations from Greece. Ninth Colloquium Crustacea Decapoda Mediterranea, Torino (Italy), September 2008. Dipartimento di Biologia Animale e dell'Uomo, Torino University and Museo Regionale di Scienze Naturali of Torino, 41.
- Christodoulou M, Koukouras A, Thessalou-Legaki M (2010) Progress on the assessment of the taxonomic status of the circum-Mediterranean genus *Atyaephyra* de Brito Capello, 1867 (Decapoda, Atyidae). Twenty First International Senckenberg Conference: Freshwater Decapoda, Frankfurt am Main (Germany), December 2010. Senckenberg Research Institute and Natural History Museum, 33.
- Cook BD, Baker AM, Page TJ, Grant SC, Fawcett JH, Hurwood DA, Hughes JM (2006) Biogeographic history of an Australian freshwater shrimp, *Paratya australiensis* (Atyidae): the role life history transition in phylogeographic diversification. Molecular Ecology 15 (4): 1083–1093. doi: 10.1111/j.1365-294X.2006.02852.x
- Cook BD, Page TJ, Hughes JM (2008) Importance of cryptic species for identifying 'representative' units of biodiversity for freshwater conservation. Biological Conservation 141 (11): 2821–2831. doi: 10.1016/j.biocon.2008.08.018
- Creaser EP (1936) Crustaceans from Yucatan. In: Pearse AS, Creaser EP, Hall FG (Eds) The cenotes of Yucatan. A zoological and hydrographic survey. Carnegie Institution of Washington, Washington, 117–132. <http://decapoda.nhm.org/pdfs/25249/25249.pdf>
- De Grave S, Fransen CHJM (2011) Carideorum catalogus: the recent species of the dendrobranchiate, stenopodidean, procarididean and caridean shrimps (Crustacea, Decapoda). Zoologische Mededelingen, Leiden 85 (9): 195–588. <http://www.zoologischemededelingen.nl/85/nr02/a01>

- Dhur G, Massard JA (1995) Étude historique et faunistique des invertébrés immigrés ou introduits dans la Moselle luxembourgeoise et ses affluents. Bulletin de la Société des Naturalistes Luxembourgeois 96: 127–156. <http://www.vliz.be/imis/imis.php?module=ref&refid=208304>
- Doadrio I, Carmona JA (2003) Testing freshwater Lago Mare dispersal theory on the phylogeny relationships of Iberian cyprinid genera *Chondrostoma* and *Squalius* (Cypriniformes, Cyprinidae). Graellsia 59 (2–3): 457–473. <http://graellsia.revistas.csic.es/index.php/graellsia/article/view/260/260>
- Dormitzer M (1853) *Troglocaris Schmidtii*. Lotos 3: 85–88. <http://ia700306.us.archive.org/3/items/lotoszeitschrift03deut/lotoszeitschrift03deut.pdf>
- Drummond AJ, Suchard MA, Xie D, Rambaut A (2012) Bayesian phylogenetics with BEAUti and the BEAST 1.7. Molecular Biology and Evolution 29 (8): 1969–1973. doi: 10.1093/molbev/mss075
- Durand J-D, Bianco PG, Laroche J, Gilles A (2003) Insight into the origin of endemic Mediterranean ichthyofauna: phylogeography of *Chondrostoma* genus (Teleostei, Cyprinidae). Journal of Heredity 94 (4): 315–328. doi: 10.1093/jhered/esg074
- Economidis PS, Dimitriou E, Pagoni R, Michaloudi E, Natsis L (2000) Introduced and translocated fish species in the inland waters of Greece. Fisheries Management and Ecology 7 (3): 239–250. doi: 10.1046/j.1365-2400.2000.00197.x
- Economou AN, Giakoumi S, Vardakas L, Barbieri R, Stoumboudi M, Zogaris S (2007) The freshwater ichthyofauna of Greece – an update based on a hydrographic basin survey. Mediterranean Marine Science 8 (1): 91–166. <http://www.medit-mar-sc.net/files/200812/15-1813054.pdf>
- Excoffier L, Lischer HEL (2010) Arlequin suite ver 3.5: a new series of programs to perform population genetics analyses under Linux and Windows. Molecular Ecology Resources 10 (3): 564–567. doi: 10.1111/j.1755-0998.2010.02847.x
- Ferrer Galdiano M (1924) Una nueva especie del género *Atyaephyra* (Decap., Atyidae). Boletín de la Real Sociedad Española de Historia Natural 24: 210–213. <http://bibdigital.rjb.csic.es/ing/Libro.php?Libro=1232>
- Folmer O, Black M, Hoeh W, Lutz R, Vrijenhoek R (1994) DNA primers for amplification of mitochondrial cytochrome c oxidase subunit I from diverse metazoan invertebrates. Molecular Marine Biology and Biotechnology 3 (5): 294–299. http://www.mbari.org/staff/vrijen/PDFS/Folmer_94MMBB.pdf
- Franjević D, Kalafatić M, Kerovec M, Gottstein S (2010) Phylogeny of cave-dwelling atyid shrimp *Troglocaris* in the Dinaric Karst based on sequences of three mitochondrial genes. Periodicum Biologorum 112 (2): 159–166. http://hrcak.srce.hr/index.php?show=clanak&id_clanak_jezik=87840
- García Muñoz JE, Rodríguez A, García Raso JE, Cuesta JA (2009) Genetic evidence for cryptic speciation in the freshwater shrimp genus *Atyaephyra* de Brito Capello (Crustacea, Decapoda, Atyidae). Zootaxa 2025: 32–42. <http://www.mapress.com/zootaxa/2009/f/z02025p042f.pdf>
- Gorgin S (1996) The first record of two species of freshwater shrimps (Decapoda, Caridea, Atyidae) from Iran. Crustaceana 69 (5): 662–668. <http://www.jstor.org/discover/10.2307>

/20105244?uid=2129&uid=2134&uid=2&uid=70&uid=4&sid=21101302264147, doi: 10.1163/156854096X00664

- Grabowski M, Jazdżewski K, Konopacka A (2005) Alien Crustacea in Polish waters – Introduction and Decapoda. *Oceanological and Hydrobiological Studies* 34 (1): 43–61. http://153.19.140.20/obce/Baltic_Aliens/Grabowski.pdf
- Guindon S, Dufayard J-F, Lefort V, Anisimova M, Hordijk W, Gascuel O (2010) New algorithms and methods to estimate Maximum-Likelihood phylogenies: assessing the performance of PhyML 3.0. *Systematic Biology* 59 (3): 307–321. doi: 10.1093/sysbio/syq010
- Haan W de (1833–1850) Crustacea. In: von Siebold PF (Ed) *Fauna Japonica sive descriptio animalium, quae in itinere per Japoniam, jussu et auspiciis superiorum, qui summum in India Batava imperium tenent, suspecto, annis 1823–1830 collegit, notis, observationibus et adumbrationibus illustravit*. Lugduni-Batavorum, Arnz, 1–243. <http://decapoda.nhm.org/references/pdfpick.html?id=12488&pdfroot=http://decapoda.nhm.org/pdfs>
- Heller C (1862) Neue Crustaceen, gesammelt während der Weltumseglung der k.k. Fregatte Novara. Zweiter vorläufiger Bericht. *Verhandlungen der kaiserlich-königlichen zoologisch-botanischen Gesellschaft in Wien* 12: 519–528. <http://decapoda.nhm.org/pdfs/25686/25686.pdf>
- Heller C (1863) Die Crustaceen des südlichen Europa. Crustacea Podophthalmia. Mit einer Übersicht über die horizontale Verbreitung sämtlicher europäischer Arten. Wilhelm Braumüller, Wien, 336 pp. <http://archive.org/details/diecrustaceendes00hell>, doi: 10.5962/bhl.title.13110
- Holthuis LB (1961) Report on a collection of Crustacea Decapoda and Stomatopoda from Turkey and the Balkans. *Zoologische Verhandlungen* 47: 1–67. <http://www.repository.naturalis.nl/document/148913>.
- Holthuis LB (1993) The recent genera of the caridean and stenopodidean shrimps (Crustacea, Decapoda): with an appendix on the order Amphionidacea. *Nationaal Natuurhistorisch Museum, Leiden*, 328 pp.
- Jesse R, Schubart CD, Klaus S (2010) Identification of a cryptic lineage within *Potamon fluviatile* (Herbst) (Crustacea, Brachyura, Potamidae). *Invertebrate Systematics* 24 (4): 348–356. doi: 10.1071/IS10014
- Jesse R, Grudinski M, Klaus S, Streit B, Pfenninger M (2011) Evolution of freshwater crab diversity in the Aegean region (Crustacea, Brachyura, Potamidae). *Molecular Phylogenetics and Evolution* 59 (1): 23–33. doi: 10.1016/j.ympev.2010.12.011
- Joly M (1843) Études sur les mœurs, de développement et les métamorphoses d’une petite salicoque d’eau douce (*Caridina Desmarestii*), suivies de quelques réflexions sur les métamorphoses des crustacés décapodes en général. *Annales des Sciences Naturelles, Zoologie* 19: 34–86. <http://www.biodiversitylibrary.org/item/47973>
- Jones WJ, Macpherson E (2007) Molecular phylogeny of the East Pacific squat lobsters of the genus *Munidopsis* (Decapoda, Galatheididae) with the descriptions of seven new species. *Journal of Crustacean Biology* 27 (3): 477–501. doi: 10.1651/S-2791.1
- Karaman M (1972) Über eine neue Süßwassergarnelenunterart *Atyaephyra desmarestii stankoi* n. ssp. (Decapoda, Atyidae) aus Mazedonien. *Fragmenta Balcanica* 9 (8): 81–84.

- Kinzelbach RK, Koster B (1985) Die Süßwassergarnele *Atyaephyra desmaresti* (Millet 1832) in den Levante-Ländern (Crustacea, Decapoda, Atyidae). *Senckenbergiana Biologica* 66 (1/3): 127–134.
- Leach WE (1813–1814) Crustaceology. In: Brewster D (Ed) *The Edinburgh Encyclopædia*, Volume 7, A. Balfour, Edinburgh, 383–437.
- Lefébure T, Douady CJ, Gouy M, Gibert J (2006) Relationship between morphological taxonomy and molecular divergence within Crustacea: proposal of a molecular threshold to help species delimitation. *Molecular Phylogenetics and Evolution* 40 (2): 435–447. doi: 10.1016/j.ympev.2006.03.014
- Macpherson E, Machordom A (2005) Use of morphological and molecular data to identify three new sibling species of the genus *Munida* Leach, 1820 (Crustacea, Decapoda, Galatheidae) from New Caledonia. *Journal of Natural History* 39 (11): 819–834. doi: 10.1080/00222930400002473
- Matzen da Silva J, Creer S, dos Santos A, Costa AC, Cunha MR, Costa FO, Carvalho GR (2011) Systematic and evolutionary insights derived from mtDNA COI barcode diversity in the Decapoda (Crustacea, Malacostraca). *PLoS ONE* 6 (5): e19449. doi: 10.1371/journal.pone.0019449
- Millet PA (1831) Description d'une nouvelle espèce de crustacé, l'*Hippolyte* de Desmarests. *Mémoires de la Société d'Agriculture, Sciences et Arts d'Angers* 1: 55–57, Plate 1.
- Milne Edwards H (1837) *Histoire naturelle des crustacés, comprenant l'anatomie, la physiologie et la classification de ces animaux*. Volume 2. Librairie Encyclopédique de Roret, Paris, 532 pp. <http://www.biodiversitylibrary.org/bibliography/6234>
- Moog O, Neseemann H, Zitek A, Melcher A (1999) Erstnachweis der Süßwassergarnele *Atyaephyra desmaresti* (Millet 1831) (Decapoda) in Österreich. *Lauterbornia* 35: 67–70.
- Ortmann AE (1890) Die Decapoden-Krebse des Strassburger Museums, mit besonderer Berücksichtigung der von Herrn Dr. Döderlein bei Japan und bei den Liu-Kiu-Inseln gesammelten und z. Z. im Strassburger Museum aufbewahrten Formen. I. Die Unterordnung Natantia Boas. *Zoologische Jahrbücher. Abteilung für Systematik, Geographie und Biologie der Thiere* 5: 437–542. <http://biostor.org/reference/5004>
- Ortmann AE (1895) A study of the systematic and geographical distribution of the decapod family Atyidae Kingsley. *Proceedings of the Academy of Natural Sciences of Philadelphia* 1894: 397–416. <http://www.biodiversitylibrary.org/item/18073>
- Page TJ, Baker AM, Cook BD, Hughes JM (2005a) Historical transoceanic dispersal of a freshwater shrimp: the colonization of the South Pacific by the genus *Paratya* (Atyidae). *Journal of Biogeography* 32 (4): 581–593. doi: 10.1111/j.1365-2699.2004.01226.x
- Page TJ, Choy SC, Hughes JM (2005b) The taxonomic feedback loop: symbiosis of morphology and molecules. *Biology Letters* 1 (2): 139–142. doi: 10.1098/rsbl.2005.0298
- Page TJ, Hughes JM (2007) Radically different scales of phylogeographic structuring within cryptic species of freshwater shrimp (Atyidae, *Caridina*). *Limnology and Oceanography* 52 (3): 1055–1066. http://www.aslo.org/lo/toc/vol_52/issue_3/1055.pdf, doi: 10.4319/lo.2007.52.3.1055

- Page TJ, Humphreys WF, Hughes JM (2008) Shrimps down under: evolutionary relationships of subterranean crustaceans from Western Australia (Decapoda, Atyidae, *Stygiocaris*). PLoS ONE 3(2): e1618. doi: 10.1371/journal.pone.0001618
- Pelseener P (1886) Note sur la présence de *Caridina Desmaresti* dans les eaux de la Meuse. Bulletin du Musée Royal d'Histoire Naturelle de Belgique 4: 211–222. <http://www.biodiversitylibrary.org/item/120880>
- Posada D (2008) jModelTest: phylogenetic model averaging. Molecular Biology and Evolution 25 (7): 1253–1256. doi: 10.1093/molbev/msn083
- Rafinesque CS (1814) Précis des découvertes et travaux somiologiques de m.r. CS Rafinesque-Schmaltz entre 1800 et 1814 ou choix raisonné de ses principales découvertes en zoologie et en botanique, pour servir d'introduction à ses ouvrages futurs. Royal Typographie Militaire, Palerme, 56 pp. doi: 10.5962/bhl.title.6135
- Rafinesque CS (1815) Analyse de la nature, ou tableau de l'univers et des corps organisés. L'imprimerie de Jean Barravecchia, Palerme, 224 pp. <http://gallica.bnf.fr/ark:/12148/bpt6k98061z/>
- Reyjol Y, Huguency B, Pont D, Bianco PG, Beier U, Caiola N, Casals F, Cowx I, Economou A, Ferreira T, Haidvog G, Noble R, de Sostoa A, Vigneron T, Virbickas T (2007) Patterns in species richness and endemism of European freshwater fish. Global Ecology and Biogeography 16: 65–75. doi: 10.1111/j.1466-822x.2006.00264.x
- Richard J, De Grave S, Clark PF (2012) A new atyid genus and species from Madagascar (Crustacea, Decapoda, Caridea). Zootaxa 3162: 31–38. <http://www.mapress.com/zootaxa/2012/f/z03162p038f.pdf>
- Salman SD (1987) Larval development of *Atyaephyra desmaresti mesopotamica* Al-Adhub (Decapoda, Atyidae) reared in the laboratory. Investigacion Pesquera 51 (1): 27–42. doi: 10.1163/156854087X00484
- Sanjur OI, Carmona JA, Doadrio I (2003) Evolutionary and biogeographical patterns within Iberian populations of the genus *Squalius* inferred from molecular data. Molecular Phylogenetics and Evolution 29 (1): 20–30. doi: 10.1016/S1055-7903(03)00088-5
- Simon C, Frati F, Beckenbach A, Crespi B, Liu H, Flook P (1994) Evolution, weighting and phylogenetic utility of mitochondrial gene sequences and a compilation of conserved polymerase chain reaction primers. Annals of the Entomological Society of America 87 (6): 651–701. http://hydrodictyon.eeb.uconn.edu/projects/cicada/resources/reprints/Simon_ea_1994.pdf
- Sket B, Zakšek V (2009) European cave shrimp species (Decapoda, Caridea, Atyidae), redefined after a phylogenetic study; redefinition of some taxa, a new genus and four new *Troglocaris* species. Zoological Journal of the Linnean Society 155 (4): 786–818. doi: 10.1111/j.1096-3642.2008.00473.x
- Straka M, Špaček J (2009) First record of alien crustaceans *Atyaephyra desmarestii* (Millet, 1831) and *Jaera istri* Veuille, 1979 from the Czech Republic. Aquatic Invasions 4 (2): 397–399. doi: 10.3391/ai.2009.4.2.18
- Tamura K, Peterson D, Peterson N, Stecher G, Nei M, Kumar S (2011) MEGA5: Molecular Evolutionary Genetics Analysis using maximum likelihood, evolutionary distance, and

- maximum parsimony methods. *Molecular Biology and Evolution* 28 (10): 2731–2739. doi: 10.1093/molbev/msr121
- Taramelli T (1864) Sui crostacei di forme marine viventi nelle acque dolci e specialmente sul *Palaemon palustris* di Martens. Lettera del Signor Torquato Taramelli al Socio Prof. G. Balsamo Crivelli. *Atti della Società Italiana di Scienze Naturali*, Milano 6 (3): 363–371. <http://ia601209.us.archive.org/8/items/attidellasocieti6272soci/attidellasocieti6272soci.pdf>
- Tautz D, Arctander P, Minelli A, Thomas RH, Vogler AP (2003) A plea for DNA taxonomy. *Trends in Ecology and Evolution* 18 (2): 70–74. doi: 10.1016/S0169-5347(02)00041-1
- Udekem d' Acoz C d' (1999) Inventaire et distribution des crustacés décapodes de l'Atlantique nord-oriental, de la Méditerranée et des eaux continentales adjacentes au nord de 25°N. *Collection Patrimoines Naturels*, Volume 40, Muséum National d'Histoire Naturelle, Paris, 383 pp.
- Von Rintelen K, Page TJ, Cai Y, Roe K, Stelbrink B, Kuhajda BR, Iliffe TM, Hughes J, von Rintelen T (2012) Drawn to the dark side: a molecular phylogeny of freshwater shrimps (Crustacea, Decapoda, Caridea, Atyidae) reveals frequent cave invasions and challenges current taxonomic hypotheses. *Molecular Phylogenetics and Evolution* 63 (1): 82–96. doi: 10.1016/j.ympev.2011.12.015
- Zakšek V, Sket B, Trontelj P (2007) Phylogeny of the cave shrimp *Troglocaris*: evidence of a young connection between Balkans and Caucasus. *Molecular Phylogenetics and Evolution* 42 (1): 223–235. doi: 10.1016/j.ympev.2006.07.009

Appendix

List of morphological characters studied and photos of *A. desmarestii* and "*A. rosiana*" material examined by Bouvier (1913). (doi: 10.3897/zookeys.229.3919.app) File format: Microsoft Office Document (docx).

Explanation note: A list of 135 morphological characters (67 meristic and 68 somatometric distances) examined in *Atyaephyra* species is given. Schematic drawings of *Atyaephyra* appendages showing the studied somatometric characters are supplied. Furthermore, photos of *A. desmarestii* and *A. rosiana* material, collected from Maine et Loire (France) and Coimbra (Portugal) respectively, examined by Bouvier (1913) are given.

Copyright notice: This dataset is made available under the Open Database License (<http://opendatacommons.org/licenses/odbl/1.0/>). The Open Database License (ODbL) is a license agreement intended to allow users to freely share, modify, and use this Dataset while maintaining this same freedom for others, provided that the original source and author(s) are credited.

Citation: Christodoulou M, Antoniou A, Magoulas A, Koukouras A (2012) Revision of the freshwater genus *Atyaephyra* (Crustacea, Decapoda, Atyidae) based on morphological and molecular data. *ZooKeys* 229: @-@. doi: 10.3897/zookeys.229.3919.app

A new fossil cricket of the genus *Proanaxipha* in Miocene amber from the Dominican Republic (Orthoptera, Gryllidae, Pentacentrinae)

Sam W. Heads^{1,†}, David Penney^{2,‡}, David I. Green^{3,§}

1 Illinois Natural History Survey & Department of Entomology, University of Illinois at Urbana-Champaign, 1816 South Oak Street, Champaign, Illinois 61820, USA **2** Faculty of Life Sciences, University of Manchester, Manchester M13 9PT, UK **3** Department of Geology, Amgueddfa Cymru—National Museum Wales, Cathays Park, Cardiff CF10 3NP, UK

† [urn:lsid:zoobank.org:author:6AA1941C-335C-42E9-A542-CD2A01EE1F16](https://zoobank.org/urn:lsid:zoobank.org:author:6AA1941C-335C-42E9-A542-CD2A01EE1F16)

‡ [urn:lsid:zoobank.org:author:5D403689-0F2E-4AE5-AFC4-DA85ACA60257](https://zoobank.org/urn:lsid:zoobank.org:author:5D403689-0F2E-4AE5-AFC4-DA85ACA60257)

§ [urn:lsid:zoobank.org:author:3732D6E5-0173-4A59-8E29-4E6F6FF2FCF0](https://zoobank.org/urn:lsid:zoobank.org:author:3732D6E5-0173-4A59-8E29-4E6F6FF2FCF0)

Corresponding author: Sam W. Heads (swheads@illinois.edu)

Academic editor: Michael Engel | Received 12 July 2012 | Accepted 15 October 2012 | Published 22 October 2012

[urn:lsid:zoobank.org:pub:D8EC9B9D-9B68-4B8C-91F2-C17F44737DF1](https://zoobank.org/pub:D8EC9B9D-9B68-4B8C-91F2-C17F44737DF1)

Citation: Heads SW, Penney D, Green DI (2012) A new fossil cricket of the genus *Proanaxipha* in Miocene amber from the Dominican Republic (Orthoptera, Gryllidae, Pentacentrinae). ZooKeys 229: 111–118. doi: 10.3897/zookeys.229.3678

Abstract

A new species of the cricket genus *Proanaxipha* Vickery & Poinar (Orthoptera: Gryllidae: Pentacentrinae) from Early Miocene Dominican amber is described and illustrated. *Proanaxipha madgesuttonae* **sp. n.** is distinguished from congeners by: (1) head capsule bearing a distinctive posteriorly bilobed colour spot on the vertex; (2) presence of crossveins in the proximal part of the mediocubital area; (3) apical field of tegmen entirely dark; and (4) median process of epiphallus short. The poorly known *Proanaxipha bicolorata* Vickery & Poinar, of questionable affinity and status, is herein regarded as a *nomen inquirendum*.

Keywords

Orthoptera, Grylloidea, Gryllidae, Pentacentrinae, *Proanaxipha*, Dominican amber, Miocene

Introduction

The genus *Proanaxipha* was established by Vickery and Poinar (1994) to accommodate two fossil species from Early Miocene Dominican amber; namely *P. latoca* Vickery & Poinar, 1994 (the type species) and *P. bicolorata* Vickery & Poinar, 1994. Originally placed in the Trigonidiinae, the genus was recently moved to Pentacentrinae by Gorochov (2010) based on close similarities with modern Neotropical pentacentrines. The placement of *Proanaxipha* within Pentacentrinae is well supported by strong dorsoventral flattening of the head capsule, presence of small spines above the metatibial spurs (never present in Trigonidiinae or Nemobiinae) and all veins in the lateral tegminal field running parallel to the costal margin. Moreover, females tentatively identified as *P. latoca* by Gorochov (2010) clearly possess ovipositors typical of pentacentrines; i.e. slender and only very slightly curved with a narrow, sharply pointed apex. This differs markedly from the trigonidiine condition, in which the ovipositor is more strongly curved and has a broad, serrated apex. While the inclusion of *Proanaxipha* in Pentacentrinae is beyond doubt, its relationships to other pentacentrine genera have yet to be addressed. In this paper, we describe a new species of *Proanaxipha* from Early Miocene (Burdigalian) Dominican amber and briefly compare the genus with other Neotropical Pentacentrinae.

Material and methods

The specimen described here is deposited in the Department of Palaeontology, The Natural History Museum, London (NHM) with the accession number NHM II 3048. Photomicrographs were assembled by D.I.G. from a stacked series of digital images captured using a Nikon Coolpix 4500 digital camera mounted on a Leica M10 stereomicroscope with 0.63× and 1.6× planapochromatic objectives. The specimen was studied by S.W.H. using an Olympus SZX12 zoom stereomicroscope and drawings produced with the aid of a *camera lucida*. Morphological terminology generally follows that established by Otte and Alexander (1983) with minor modifications (see Heads 2010a). The age and origin of Dominican amber has been reviewed by Itturalde-Vinent and MacPhee (1996), Grimaldi and Engel (2005) and Penney (2010). The Orthoptera from Dominican amber have been reviewed by Heads (2009, 2010a, b).

Systematics

Genus *Proanaxipha* Vickery & Poinar, 1994

urn:lsid:orthoptera.speciesfile.org:TaxonName:30586

Proanaxipha Vickery & Poinar, 1994: 15. Type species: *Proanaxipha latoca* Vickery & Poinar, 1994 by original designation – Perez-Gelabert 2001: 72 – Arillo and Ortuño 2005: 8 – Otte and Perez-Gelabert 2009: 142 – Gorochov 2010: 78 [442]. – Penney and Green 2011: 108.

***Proanaxipha madgesuttonae* Heads & Penney, sp. n.**

urn:lsid:zoobank.org:act:2894AEE9-AD50-48FE-918C-46D86E4F9B0E

urn:lsid:orthoptera.speciesfile.org:TaxonName:76032

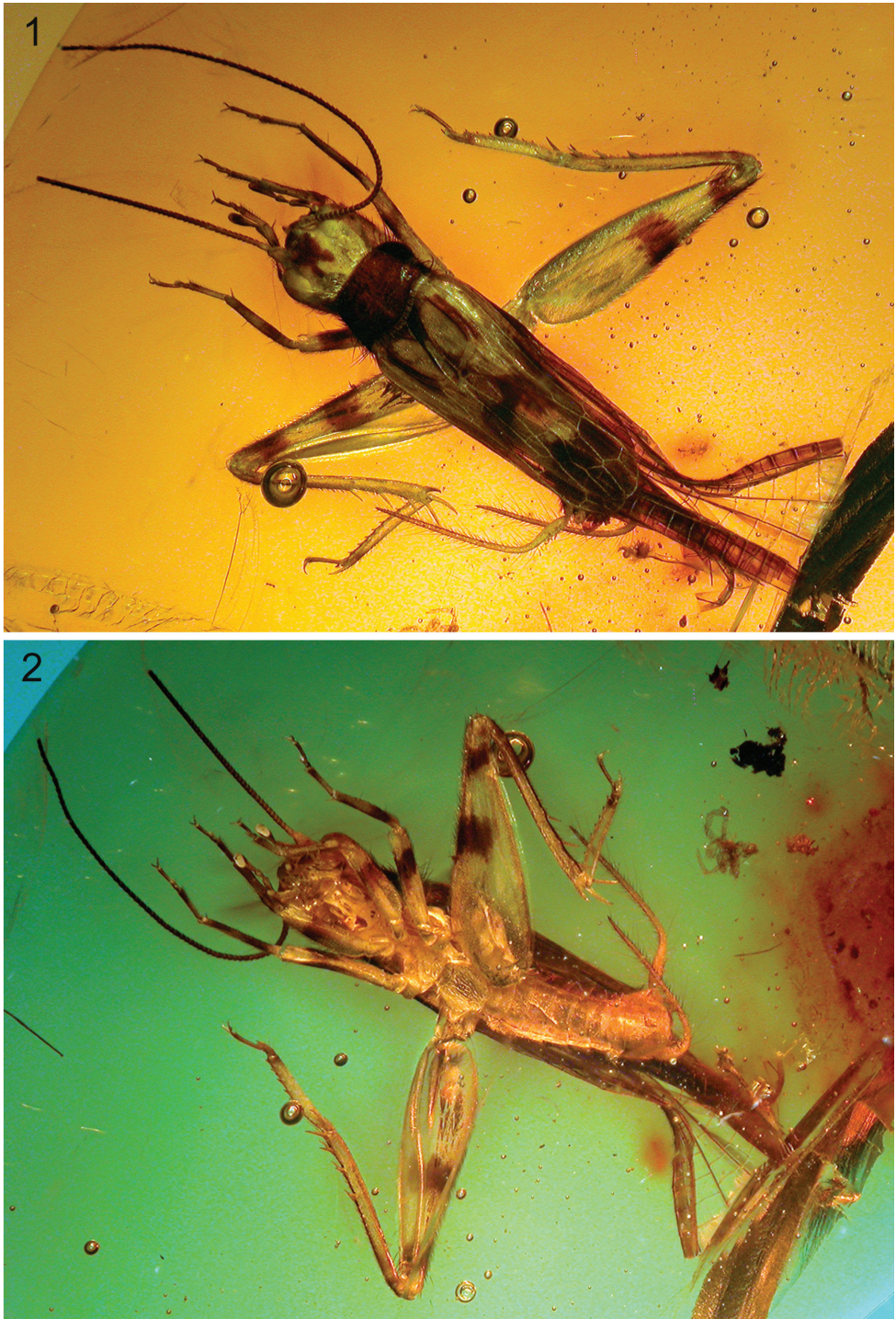
http://species-id.net/wiki/Proanaxipha_madgesuttonae

Figs 1–8

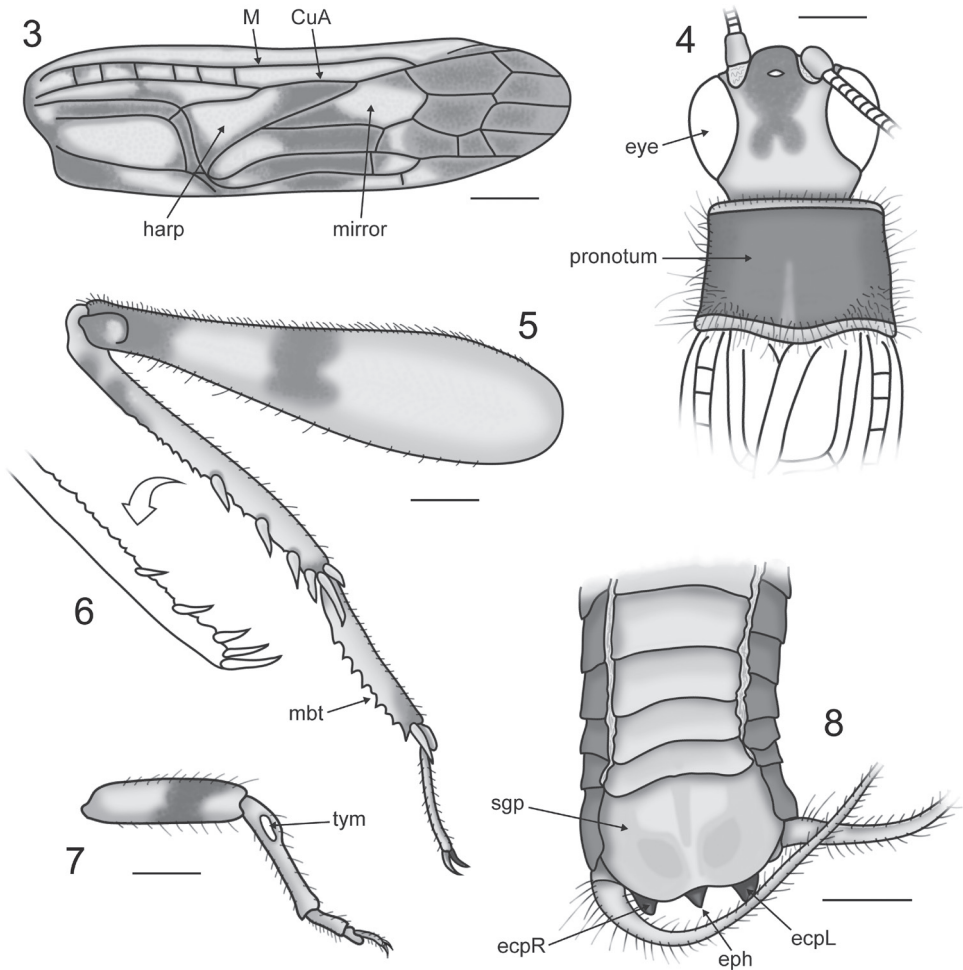
Diagnosis. Distinguished from congeners by the following characters: (1) head capsule with distinctive posteriorly bilobed colour spot on vertex; (2) presence of crossveins in the proximal part of the mediocubital area; (3) apical field of tegmen entirely dark; and (4) median process of epiphallus short.

Description. *Male:* Total body length measured from fastigium verticis to abdominal apex 5.97 mm (Figs 1–2). Head capsule (length 1.26 mm) compressed dorsoventrally; vertex with distinct posteriorly bilobed colour spot (Fig. 4); fastigium verticis broadly rounded; median ocellus situated dorsally, between antennal torulae; compound eyes large, interocular distance 0.64 mm; antennae filiform, scape approximately four times larger than pedicel; maxillary palpi long with apical palpomere triangular and distally concave (see Fig. 2). Pronotum (length 1.02 mm) wider than long, with lateral and marginal areas covered with long setae; disc largely dark with a pale median line not reaching anterior margin; posterior margin sinuous and slightly wider than anterior margin; marginal areas well-demarcated with prominent carinae (Fig. 4). Thoracic sternites polygonal, plate-like and densely pilose, increasing in size posteriorly (Fig. 2). Terminalia obscured dorsally by hind wings (see Fig. 1); subgenital plate pale, broadly rounded with an indistinct median ridge flanked by shallow depressions and the posterior margin shallowly emarginate (Fig. 8); cerci densely setose; epiphallus triangular with pointed apex directed dorsally; ectoparameres lobate.

Tegmen 3.78 mm long with distinct coloration and stridulatory apparatus only partially reduced (Fig. 3); harp elongate, without multiple harp veins; mirror small, lacking dividing vein; lateral field dark with veins running parallel to the costal margin; dorsal field with six crossveins in the basalmost part of the mediocubital area with dark patches running along the stridulatory and harp veins and merging with a large dark spot encompassing most of the proximal cells in the cubital system; apical field entirely dark (Fig. 3). Hind wing long and tightly folded, extending well beyond abdominal apex, with dark remigium and hyaline anal lobe. Prothoracic leg short and robust with a single dark band on the distal half of the profemur and ovoid tympana on both sides of the protibia (Fig. 7). Mesothoracic leg longer than prothoracic leg; mesofemur with single dark band and a prominent ventral sulcus distally; mesotibiae with two dark bands. Metafemur (length 3.54 mm) with a dense covering of setae and bearing two dark spots; one situated just distad of femoral midlength and the second situated apically, encompassing the genicula (Fig. 5). Metatibia (length 2.61 mm) approximately 25% shorter than metafemur and quadrate in cross section, with two small dark spots situated basally; dorsal longitudinal carinae armed with rows of small denticles interspersed distally with stout subapical spurs (3 inner and 3 outer); metatibial apex bearing 2 inner and 3 outer apical spurs (Figs 5–6); median outer apical spur twice as long as the



Figures 1–2. *Proanaxipha madgesuttonae* Heads & Penney, sp. n. Photomicrographs of holotype ♂. **1** dorsal view **2** ventral view.



Figures 3–8. *Proanaxipha madgesuttonae* Heads & Penney, sp. n. Drawings of holotype ♂. **3** dorsal field of right tegmen **4** head capsule and pronotum in dorsal view **5** outer view of right metathoracic leg **6** inner view of right metatibia **7** outer view of right prothoracic leg **8** terminalia in oblique ventral view. Abbreviations: **CuA** anterior cubitus; **ecpL** left ectoparamere; **ecpR** right ectoparamere; **eph** epiphallus; **M** media; **mbt** metabasitarsus; **sgp** subgenital plate; **tym** tympanum. All scale bars 0.5 mm.

other outer spurs. Metabasitarsus elongate with rows of sharp denticles along the dorsal longitudinal carinae and two apical spurs (1 inner and 1 outer); second metatarsomere much reduced; third metatarsomere long, slender and slightly curved (Fig. 5).

Holotype. ♂: Dominican Republic: Early Miocene (Burdigalian) amber (NHM II 3048).

Etymology. Named in honour of Madge Sutton at the request of Dr Susan Shawcross.

Remarks. *Proanaxipha madgesuttonae* is clearly congeneric with the type species *P. latoca*, sharing the partially reduced stridulatory apparatus, a long and straight metabasitarsus, similar metatibial armature and the presence of auditory tympana on both

faces of the protibia (see Gorochov 2010). Nevertheless, *P. madgesuttonae* differs markedly from *P. latoca* in its colouration. The new species is altogether darker than *P. latoca*, bearing a distinctive posteriorly bilobed colour spot on the vertex of the head capsule (Fig. 4) and a much darker tegmen. The apical field of the tegmen in *P. latoca* is either pale or bears a few diffuse dark patches (see Gorochov 2010, p. 443, fig. 6). In contrast, the apical field in *P. madgesuttonae* is entirely dark (Fig. 3). The holotype of *P. latoca* bears two dark spots on the vertex between the eyes but the rest of the head capsule is pale (see Vickery and Poinar 1994, p. 21, fig. 9). Gorochov (2010) briefly described a number of additional specimens that he tentatively assigned to *P. latoca*. However, all of these differ from the holotype in coloration and Gorochov (*op. cit.*, p. 444) remarked that they likely represent a complex of distinct species. While the original colouration of the specimen cannot be known with certainty, arthropod colour patterns are often extremely well preserved in amber (Poinar 1993; Grimaldi and Engel 2005; Penney 2010 and contributions therein). Given the remarkable preservation of the specimen as well as the obvious symmetry of the patterns, it is highly unlikely that they have been altered taphonomically. Morphologically, *P. madgesuttonae* is very similar to the holotype of *P. latoca* and to the specimens recently described by Gorochov (2010). However, the tegminal venation of *P. madgesuttonae* differs in the presence of six crossveins in the basal half of the mediocubital area (Fig. 3). The tegmina are not clearly illustrated in the original description of *P. latoca* making it impossible to determine whether or not these crossveins are present. However, the illustrations of *P. ?latoca* presented by Gorochov (2010) show no mediocubital crossveins. The distal parts of the phallic complex visible in the holotype of *P. madgesuttonae* (Fig. 8) are very similar to those illustrated by Gorochov (2010) though the median process of the epiphallus is shorter in *P. madgesuttonae*.

***Proanaxipha bicolorata* Vickery & Poinar, 1994, nomen inquirendum**

urn:lsid:orthoptera.speciesfile.org:TaxonName:30588

http://species-id.net/wiki/Proanaxipha_bicolorata

Proanaxipha bicolorata Vickery & Poinar, 1994: 16, fig. 4 – Perez-Gelabert 2001: 72 –
Otte and Perez-Gelabert 2009: 142 – Gorochov 2010: 80 [442].

Remarks. Based on Vickery and Poinar's (1994) photograph of the holotype (a nymph), it is clear that this species does not belong in *Proanaxipha* or even within Pentacentrinae. Unfortunately, neither the illustration nor the original description are sufficient to determine the subfamilial placement of this species, a situation that is further complicated by the nymphal condition of the specimen. Gorochov (2010) suggested a possible affinity with Nemobiinae or Eneopterinae and while both seem possible, neither can be confirmed. Therefore, the species is herein regarded as a *nomen inquirendum* until the type can be redescribed.

Discussion

The relationships of *Proanaxipha* with other Neotropical Pentacentrinae have yet to be adequately investigated and in the absence of a formal analysis, remain largely unknown. Four extant pentacentrine genera are known from the Neotropical region, namely *Aphemogryllus* Rehn, 1918, *Nemobiopsis* Bolívar, 1890, *Trigonidomimus* Caudell, 1912 and *Velapia* Otte & Perez-Gelabert, 2009. Of these, *Proanaxipha* is most similar to *Nemobiopsis*, sharing with the latter an almost identical arrangement of the metatibial spurs. In particular, Gorochov (2010) drew comparisons between *Proanaxipha* spp. and *N. eugethes* Otte, 2006 from Costa Rica and suggested that the latter species may in fact belong within *Proanaxipha*. *Nemobiopsis eugethes* shares with *Proanaxipha* the presence of tympana on both sides of the protibia, the metabasitarsus elongate and almost completely straight, the male stridulatory apparatus only partially reduced and the somewhat shortened median epiphallic process (Otte 2006; Gorochov 2010). Moreover, while the presence of tympana on both faces of the protibia appears to be unique to *Proanaxipha* and *N. eugethes*, a long and straight metabasitarsus and partially reduced stridulatory apparatus are present in a number of *Nemobiopsis* species (e.g. *N. cavicola* Bonfils, 1981, *N. cortico* Otte & Perez-Gelabert, 2009, *N. decui* Bonfils, 1981, *N. diadromos* Otte & Perez-Gelabert, 2009 and *N. metanasticos* Otte & Perez-Gelabert, 2009). Whether or not these species are more closely allied to *Proanaxipha* than *Nemobiopsis* remains unclear. Indeed, the status of *Nemobiopsis*, *Proanaxipha* and *Grossoxipha* Vickery & Poinar, 1994 (also from Dominican amber) as separate, monophyletic genera is itself questionable and careful revision of the Neotropical Pentacentrinae will undoubtedly shed much-needed light on these problems.

Acknowledgements

S.W.H. acknowledges support from the Illinois Natural History Survey (University of Illinois at Urbana-Champaign) and the Herbert H. Ross Foundation. D.P. acknowledges support from the Systematic Research Fund (jointly administered by the Linnean Society of London and the Systematics Association) and Dr Susan Shawcross (University of Manchester).

References

- Arillo A, Ortuño VM (2005) Catalogue of fossil insect species described from Dominican amber (Miocene). *Stuttgarter Beiträge zur Naturkunde Serie B* 352: 1–68.
- Bolívar I (1890) Diagnóstico de ortópteros nuevos. *Anales de la Sociedad Española de Historia Natural* 19: 299–333.

- Bonfils J (1981) Orthoptères récoltés par les expéditions biospéologiques cubano-roumaines à Cuba 1969 à 1973. Resultats des expéditions biospéologiques cubano-roumaines à Cuba 3: 103–112.
- Caudell AN (1912) A new genus and species of Gryllidae from Texas. Proceedings of the Entomological Society of Washington 14: 187–188.
- Gorochov AV (2010) New and little known orthopteroid insects (Polyneoptera) from fossil resins: communication 3. Paleontologicheskii Zhurnal 2010: 70–87 [in Russian; English translation published separately in Paleontological Journal 44: 434–450].
- Grimaldi D, Engel MS (2005) Evolution of the Insects. Cambridge University Press, Cambridge, London & New York, xv + 755 pp.
- Heads SW (2009) New pygmy grasshoppers in Miocene amber from the Dominican Republic (Orthoptera: Tetrigidae). Denisia 26: 69–74.
- Heads SW (2010a) The first fossil spider cricket (Orthoptera: Gryllidae: Phalangopsinae): 20 million years of troglobiomorphosis or exaptation in the dark? Zoological Journal of the Linnean Society 158: 56–65. doi: 10.1111/j.1096-3642.2009.00587.x
- Heads SW (2010b) New Tridactyloidea in Miocene amber from the Dominican Republic (Orthoptera: Caelifera). Annales de la Société Entomologique de France 46: 204–210.
- Itturalde-Vinent MA, MacPhee RDE (1996) Age and paleogeographical origin of Dominican amber. Science 273: 1850–1852. doi: 10.1126/science.273.5283.1850
- Otte D (2006) Eighty-four new cricket species (Orthoptera: Grylloidea) from La Selva, Costa Rica. Transactions of the American Entomological Society 132: 299–418.
- Otte D, Alexander RD (1983) The Australian crickets (Orthoptera: Gryllidae). Monographs of the Academy of Natural Sciences of Philadelphia 22: 1–477.
- Otte D, Perez-Gelabert DE (2009) Caribbean Crickets. Publications on Orthopteran Diversity, The Orthopterists' Society, Philadelphia, 792 pp.
- Penney D (Ed) (2010) Biodiversity of fossils in amber from the major world deposits. Siri Scientific Press, Manchester, 304 pp.
- Penney D, Green DI (2011) Fossils in amber: snapshots of prehistoric forest life. Siri Scientific Press, Manchester, 226 pp.
- Perez-Gelabert DE (2001) Preliminary checklist of the Orthoptera (Saltatoria) of Hispaniola. Journal of Orthoptera Research 10: 63–74. doi: 10.1665/1082-6467(2001)010[0063:PC OTOS]2.0.CO;2
- Poinar GO (1993) Insects in amber. Annual Review of Entomology 46: 145–159. doi: 10.1146/annurev.en.38.010193.001045
- Rehn JAG (1918) On a collection of Orthoptera from the state of Pará, Brazil. Proceedings of the Academy of Natural Sciences, Philadelphia 70: 144–236.
- Vickery VR, Poinar GO (1994) Crickets (Grylloptera: Grylloidea) in Dominican amber. Canadian Entomologist 126: 13–22. doi: 10.4039/Ent12613-1